

**Calibration of Traffic Simulation Models Using Simultaneous
Perturbation Stochastic Approximation (SPSA) Method
extended through Bayesian Sampling Methodology**

By

JUNG-BEOM LEE

A dissertation submitted to the

Graduate School-New Brunswick

Rutgers, The State University of New Jersey

in partial fulfillment of the requirements

for the degree of

Doctor of Philosophy

Graduate Program in Civil and Environmental Engineering

written under the direction of

Dr. Kaan Ozbay

and approved by

New Brunswick, New Jersey

October 2008

ABSTRACT OF THE DISSERTATION

Calibration of Traffic Simulation Models Using Simultaneous Perturbation Stochastic Approximation (SPSA) Method extended through Bayesian Sampling Methodology

By JUNG-BEOM LEE

Dissertation Director:

Dr. Kaan Ozbay

The main goal of this dissertation is to propose a new methodology for the calibration of traffic simulation models. Simulation is useful in representing complex real-world systems, and many alternatives can be compared via different system designs. However, to evaluate road conditions accurately, the selection of model parameters to be calibrated and the calibration methodology are very important aspects of the overall simulation modeling process.

One of the key elements of this dissertation is the application of the Simultaneous Perturbation Stochastic Approximation (SPSA) algorithm (Spall (1992))—one of the well-known stochastic approximation (SA) algorithms, to determine optimal model parameters. The SPSA algorithm has an inherent advantage that can be exploited in both stochastic gradient and gradient-free settings; it can also be applied to solve optimization problems that have a large number of variables.

One of the main distinctions between this study and previous studies is with regards to calibration while considering a wide range of all likely demand conditions. Previous studies on calibration have focused on minimizing a deterministic objective function, which is the sum of the relative error between the observed data and the simulation output from a certain time period in a typical day. Even though this approach can be considered a calibration that uses data obtained at one point in time, this type of calibration approach cannot capture a realistic distribution of all possible traffic conditions. Thus, a more general calibration methodology needs to be implemented—one that enables use with any traffic condition. In this dissertation, we propose the Bayesian sampling approach, in conjunction with the application of the SPSA stochastic optimization method, which enables the modeler to enhance the theoretic application to consider statistical data distribution. Thus, this proposed new and advanced methodology makes it possible to overcome the limitations of previous calibration studies.

Testing the methodology for larger networks, as well as for other microscopic traffic simulation tools such as CORSIM or VISSIM, are future research tasks. In the future, other simulation parameters and more extensive data sets can be used to test the strengths and weaknesses of the proposed calibration methodology.

Acknowledgement

I would like to express my deep gratitude and appreciation to Dr. Kaan Ozbay. His support, supervision, and inspiration encouraged me to finish this dissertation during my graduate studies at Rutgers University.

My sincere thanks are extended to the members of my committee—Dr. Hani H. Nassif, Dr. Maria P. Boile, and Dr. Richard K. Brail—for their valuable suggestions for improving this research.

I am also indebted to Baik Hoh and Sandeep Mudigonda, for their assistance in writing this dissertation.

I would like to express my appreciation to Junghoon Kim, for his kindness and friendship. Thank you for being a great listener.

Above all, infinite thanks go to my parents and my family. Without your loving support, encouragement, and motivation, I would never have completed my degree. Every accomplishment in my life, including this dissertation, is dedicated to my parents ImJae Lee and SunSoon Choi, my wife YoungJoo Lee, and my daughter Hannah D. Lee.

Table of Contents

Abstract of the Dissertation	ii
Acknowledgement	iv
Table of Contents	v
List of Tables	ix
List of Illustrations	xi
Chapter 1. Introduction	1
1.1 Introduction	1
1.2 Motivation and Background	2
1.3 Organization	4
Chapter 2. Literature Review	6
2.1 Review of Traffic Simulation Packages	6
2.1.1 Microscopic Simulation Tools	7
2.1.2 Macroscopic Simulation Tools	10
2.1.3 Mesoscopic Simulation Tool	10
2.2 Comprehensive Review of Previous Calibration Studies	11
2.3 Review of Optimization Methods for Parameter Calibration	23
Chapter 3. Overall Calibration Framework Using the SPSA Algorithm	24
3.1 Introduction	24
3.2 Proposed Research Methodology	24
3.3 The Simultaneous Perturbation Stochastic Approximation (SPSA) Algorithm	28
3.3.1 Description for Standard SPSA Algorithm	29

3.3.2 Convergence of the Stochastic Approximation (SA) Algorithm	31
3.3.3 The Effect of Random Seed on the Results	33
Chapter 4. Calibration of a Macroscopic Simulation Model Using the Simultaneous Perturbation Stochastic Approximation Method	35
4.1 Introduction	35
4.2 Cell Transmission Model (CTM)	35
4.3 Input Variables of Cell Transmission Model (CTM)	36
4.4 Goodness-of-Fit Test	37
4.5 Simulation Results and Summary	40
Chapter 5. Calibration of a Microscopic Simulation Model Using the Simultaneous Perturbation Stochastic Approximation Method	42
5.1 Introduction	42
5.2 Key Calibration Parameters	43
5.3 Data Collection and Extraction	47
5.3.1 Data Collection	47
5.3.2 Data Extraction	48
5.4 The PARAMICS Programmer API Code	51
5.5 Measures of Effectiveness for Calibration Study	52
5.6 Calibration Process (Under-Congested Traffic Flow Condition)	53
5.6.1 Calibration of Headway and Reaction Time	53
5.6.2 The SPSA Iteration Process	56
5.6.3 Results of the Calibration Study	58
5.6.4 Goodness-of-Fit Test	60

5.6.5 Sensitivity Analysis	63
5.6.6 Validation of the Calibrated PARAMICS Simulation Model	72
5.7 Simulation Results and Summary	74
Chapter 6. Calibration of a Macroscopic Traffic Simulation Model Using	
Enhanced SPSA Methodology	76
6.1 Introduction	76
6.2 Proposed Enhanced Methodology for Calibrating Cell Transmission Model	77
6.3 Description of Sampling Methodology	83
6.4 Implementation Details of E-SPSA Calibration Methodology for a Freeway Segment	84
6.4.1 Demand Matrix Generation from Observed Distribution of Demands	84
6.4.2 Determination of Optimal Parameters That Minimize the Error Using the Enhanced SPSA Algorithm	86
6.4.3 Perform Kolmogorov-Smirnov (K-S) Test	87
6.5 Case Study	89
6.5.1 Data Collection	89
6.5.2 CTM and Selection of Input Parameters	90
6.5.3 Demand Matrix Generation from Observed Distribution of Demands	91
6.5.4 Determination of Optimal Parameters That Minimize Error Using the Enhanced SPSA Algorithm	93
6.5.5 Description of the Kolmogorov-Smirnov Test	95
6.5.6 Verification and Validation Tests	101
6.6 Simulation Results and Summary	112

Chapter 7. Calibration of a Microscopic Simulation Model Using Extended-SPSA Methodology	116
7.1 Introduction	116
7.2 Proposed Methodology for the Calibration of a Microscopic Simulation Model	117
7.3 Implementation Details of the Proposed Ex-SPSA Calibration Methodology	120
7.3.1 Data Collection	120
7.3.2 Demand Matrix Generation from the Observed Distribution of Demands	121
7.3.3 Determination of the Optimal Parameters that Minimize the Error using the Extended SPSA Algorithm	123
7.3.4 Verification Test	130
7.3.5 Analysis of the Simulation Output for the Optimized Input Parameters	130
7.3.6 Statistical Comparison of the Distributions Obtained Using Simulated and Observed Data	132
7.3.7 Validation Test	135
7.4 Simulation Results and Summary	137
Chapter 8. Conclusions and Recommendation for Future Research	140
References	144
Appendix A. PARAMICS Programmer API Code	149
Curriculum Vita	157

List of Tables

Table 2.1 Summary of previous calibration studies	11
Table 2.2 Calibration parameters and effective ranges	20
Table 2.3 Validation guidelines	21
Table 4.1 Results of the calibration study	39
Table 5.1 Perception Reaction Time comparisons	46
Table 5.2 Average flow, speed, and density of morning peak data (three-minute intervals)	54
Table 5.3 Relative errors, depending on mean headway and mean reaction time	55
Table 5.4 The result of calibration study	59
Table 5.5 Results of the chi-square test for goodness-of-fit	63
Table 5.6 Sensitivity analysis depending on the headway	64
Table 5.7 Chi-square test with different mean target headway values	71
Table 6.1 Possible demand sampling method	85
Table 6.2 Optimal calibration parameters and other statistics	94
Table 6.3 Kolmogorov-Smirnov values for each time period (Intermediate ramp case)	95
Table 6.4 Kolmogorov-Smirnov values for each time period	105
Table 6.5 Sum of relative errors for the validation test for three randomly selected days	110
Table 7.1 Results of the K-S test	123
Table 7.2 Simulated data, mean target headway, and mean reaction time given flow	131
Table 7.3 Results of the Kolmogorov-Smirnov test	133
Table 7.4 Results of the Kolmogorov-Smirnov test	134

List of Illustrations

Figure 3.1 Overall procedure proposed for the calibration and validation of a simulation model	27
Figure 3.2 Comparison between poorly designed and well-designed SPSA algorithms	33
Figure 4.1 Flow-density relationship for the basic CTM	36
Figure 4.2 I-880 freeway segment	37
Figure 5.1 Headway for each lane	45
Figure 5.2 The Freeway Service Patrol study section	51
Figure 5.3 The example of the SPSA algorithm procedure	56
Figure 5.4 Change in the objective function	60
Figure 5.5 Histogram of the headway distribution of the observed data	61
Figure 5.6 Histogram of the headway distribution of the simulated data (PARAMICS)	62
Figure 5.7 Sensitivity analysis of mean target headway (flow comparison)	66
Figure 5.8 Sensitivity analysis of mean target headway (density comparison)	68
Figure 5.9 Sensitivity analysis with upper and lower bounds of the parameters (flow and density comparison)	70
Figure 5.10 Flow comparison using the observed and simulated data	73
Figure 5.11 Density comparison using the observed and the simulated data	73
Figure 6.1 Proposed combined enhanced SPSA simulation calibration methodology	83
Figure 6.2 The network geometry	91
Figure 6.3 Histogram based on the distribution of 17 days of observed demand matrix: no intermediate ramp	92

Figure 6.4 Histogram based on the distribution of 17 days of observed demand	
matrix: intermediate ramp	93
Figure 6.5 Comparison of simulated and observed flow and density distributions: no intermediate ramp	96
Figure 6.6 Comparison of simulated and observed flow distributions: intermediate ramp	98
Figure 6.7 Comparison of simulated and observed density distributions: intermediate ramp	100
Figure 6.8 Comparison of simulated and observed flow distributions	103
Figure 6.9 Comparison of simulated and observed density distributions	104
Figure 6.10 Comparison of simulated and observed flow distributions	107
Figure 6.11 Comparison of simulated and observed density distributions	109
Figure 7.1 Proposed extended SPSA calibration methodology and validation methodology	119
Figure 7.2 Histogram based on the distribution of 16 days of observed demand	120
Figure 7.3 The layout of the study segment modeled using PARAMICS	121
Figure 7.4 Histogram and the best fit distribution of the observed data	122
Figure 7.5 A conceptual representation of traditional calibration methods	124
Figure 7.6 A conceptual representation of calibration method of complete range of possible traffic conditions	125
Figure 7.7 The conceptual representation of the proposed methodology for finding the distribution of h_i and r_i given I_i ($h_i, r_i I_i$)	126
Figure 7.8 Mean target headway distribution	126

Figure 7.9 Mean reaction time distribution	127
Figure 7.10 Comparison between observed and simulated flow and speed (October 28, 1993)	128
Figure 7.11 Comparison between observed and simulated flow and speed (October 29, 1993)	129
Figure 7.12 The estimated distribution of sampled flow data	131
Figure 7.13 Comparison of the observed and simulated probabilities of flow	133
Figure 7.14 Comparison of the observed and simulated values of traffic flow	135
Figure 7.15 Comparison of the observed and simulated probabilities of flow (For the range of 1200~1400)	136

Chapter 1

Introduction

1.1 Introduction

The need for a robust and realistic modeling tool for evaluating various intelligent transportation system (ITS) technologies—such as ramp-metering, traffic diversion, and others—is clear. Traffic simulation models can be helpful in estimating current conditions, such as delays, travel times, queues, and flows. In addition, these models can predict future conditions and be used to optimize network operations for current and future real-world conditions. However, it is important to validate and calibrate a traffic simulation model accurately.

The focus of this dissertation is to propose a new methodology for calibrating previously developed microscopic simulation models, by using one of the popular simulation tools—namely, PARAMICS. PARAMICS is a traffic simulation tool widely used for modeling traffic networks and various traffic management and control strategies. In general, the modeler starts by using its default parameters, which might not always represent the observed conditions of the modeled network. The next step commonly employed is to change the default parameters manually until various observations, such as flows or travel times, match observed values. This is a trial-and-

error approach that depends on the judgment of the modeler; however, the size of the modeled network and the number of variables to be modified dictate the extent and effectiveness of this manual calibration process. The manual calibration does not have a theoretical basis to assure the modeler about the optimality (or approximate optimality) of the new parameters with respect to the outputs they generate. Thus, a theoretically sound calibration methodology that takes into account the stochastic nature of microscopic simulation is needed to improve this widely used manual calibration process.

1.2 Motivation and Background

Simulation, a popular and widely used method for studying stochastic and complex real-world systems, can accurately represent those conditions when parameters are effectively calibrated. Simulation is useful in evaluating the performance of a current system, and many alternatives can be compared via the system designs. The input parameters of the simulation can be modified to match a particular experimental condition.

Estimating real-world traffic conditions is very complex when used to evaluate actual traffic conditions and predict future traffic conditions. The costs of performing field studies to measure traffic conditions in large networks can be prohibitive; moreover, in the real world, it is impossible to evaluate strategies that are not yet implemented. For example, one cannot change the geometry of an intersection to investigate changed network conditions and its impact on traffic, in terms of delays and traffic flows. Simulation effectively addresses these kinds of difficulties.

Many papers about traffic simulation models have been published; for example, Ding (2003), Gardes et al. (2002), and Lee et al. (2001) simulated various freeway sections using the PARAMICS simulation tool, and Toledo et al. (2004) and Jha et al. (2004) used MITSIM as a simulation tool. Kim and Rilett (2003) used both CORSIM and TRANSIMS and Schultz and Rilett (2004) used CORSIM. AIMSUN, DynaMIT-P, VISSIM, and DYNASMART-X were used as simulation tools by Hourdakis et al. (2003), Kundé (2002), Park and Qi (2005), and Qin and Mahmassani (2004), respectively.

However, to estimate traffic conditions accurately, an effective calibration of the simulation model is required. Ding (2003), Gardes et al. (2002), Ma and Abdulhai (2002), and Lee et al. (2001) used mean target headway and mean reaction time as the parameters to be calibrated. Hourdakis et al. (2003) and Mahut et al. (2004) calibrated global and local parameters, and Toledo et al. (2004) and Jha et al. (2004) used origin-destination (O-D) flows and driver behavior parameters as calibration parameters. Various methodologies have also been used to calibrate these parameters. Lee et al. (2001), Schultz and Rilett (2004), Park and Qi (2005), and Ma and Abdulhai (2002) used genetic algorithms (GAs) to calibrate microscopic simulation tools. Kim and Rilett (2003) used the simplex algorithm as the calibration methodology, while Kundé (2002) used the Simultaneous Perturbation Stochastic Approximation (SPSA) algorithm to calibrate a model developed in DynaMIT-P, a mesoscopic simulation tool. Ding (2003) calibrated a network model using PARAMICS, while employing the SPSA algorithm. Nonetheless, Kundé (2002) and

Ding's (2003) calibration work was incomplete, because they did not consider random perturbation vector Δ_k .

These previous calibration studies focused on minimizing the sum of the relative error between the observed data during a certain period of time in a typical day and the simulation output for the same time period. This static approach can be explained as a calibration process that uses data obtained at one point in time. However, this type of calibration approach cannot capture a realistic distribution of all possible traffic conditions and may produce inaccurate calibration results; thus, a more general calibration methodology needs to be implemented—one that can be used for any road condition or with any uncertainties in flow data. Molina et al. (2005) used a Bayesian approach to overcome these problems and predicted behavior of traffic at a signalized intersection in Chicago; however, they did not use a stochastic optimization method to find the “best” values for their calibration parameters. This dissertation proposes a new calibration methodology—namely, the Bayesian sampling approach, in conjunction with the application of the SPSA stochastic optimization method (Ex-SPSA)—that considers a wide range of all likely demand conditions.

1.3 Organization

This dissertation is organized as follows.

Chapter 1 presents the motivation behind the research work and provides an overview of the issue of simulation model calibration. Chapter 2 provides a literature review. Also, an explanation of the simulation package and a review of

comprehensive previous studies with regards to calibration and the validation of simulation models are summarized in this chapter.

Chapter 3 introduces the algorithm that is used in this dissertation. This chapter describes the standard SPSA algorithm and the random numbers that affect the results. Chapter 4 provides a preliminary test to ensure the effectiveness of the algorithm explained in this research work. Rather than apply it to a microscopic model, a macroscopic simulation model is used for the test, because the simulation of a macroscopic model is quicker and easier to run than a complex microscopic model. Chapter 5 presents the methodology behind our calibration work, which uses the SPSA algorithm with a microscopic simulation model. In addition, the validation and sensitivity analysis, as a verification test, is presented in the latter part of that chapter.

Chapter 6 describes the concept of calibration, considering input distribution. Instead of calibrating with a single demand, input values from randomly generated demand matrices are used in the new calibration methodology. Using the enhanced SPSA algorithm, the calibration using input data distribution is performed for the macroscopic simulation model.

Chapter 7 explains the advanced calibration methodology, which takes an extended SPSA approach and enables one to enhance the theoretic application to consider data distribution. In addition, this approach makes it possible to represent accurately a wide range of all the likely demand conditions observed at the facility that will ultimately benefit from the calibration. This new and advanced methodology enables one to overcome the limitations of previous calibration studies.

Chapter 2

Literature Review

Many traffic simulation models have been used to analyze road conditions and collect vehicle travel times, delays, and flows. This chapter introduces the commercial software packages widely used in these analyses and reviews studies wherein traffic simulation tools are calibrated and validated.

2.1 Review of Traffic Simulation Packages

Simulation models can be classified into three types: microscopic, macroscopic, or mesoscopic. Some of the most widely used microscopic simulation tools are PARAMICS (Ding (2003), Gardes et al. (2002), Lee et al. (2001), Ma and Abdulhai (2002), Abdulhai et al. (1999)), CORSIM (Kim and Rilett (2003), Schultz and Rilett (2004), Milam (2005), Sacks et al. (2002)), FRESIM (Cheu et al. (1998)), MITSIM (Toledo et al. (2004), Jha et al. (2004)), VISSIM (Park and Qi (2005), Gomes et al. (2004)), TRANSIMS (Kim and Rilett (2003)), and AIMSUN(Hourdakis et al. (2003)). Microscopic simulation models represent an individual vehicle's behaviors and measures each vehicle's movements. In the past, Ding (2003), Gardes et al. (2002), Lee et al. (2001), and Ma and Abdulhai (2002) calibrated PARAMICS

simulation models. Toledo et al. (2004) and Jha et al. (2004) calibrated models through the use of MITSIM, while Kim and Rilett (2003), Schultz and Rilett (2004), and Milam (2005) calibrated CORSIM-based models.

Among the most popular macroscopic traffic simulation tools are AUTOS (Boxill and Yu (2000)), FREQ (Boxill and Yu (2000)), PASSER- II (Boxill and Yu (2000)), TRANSYT-7F (TRANSYT-7F Users Guide (1998)), and TRANSYT/10 (Boxill and Yu (2000)). The measures of effectiveness for the calibration of macroscopic models are flow, speed, and density.

DYNAMIT (Kundé (2002), Bottom et al. (1999)), DYNEMO (Boxill and Yu (2000)), and DYNASMART (Qin and Mahmassani (2004)) are mesoscopic traffic simulation tools. Kundé (2002) calibrated a supply simulator that is part of DYNAMIT-P, and Qin and Mahmassani (2004) calibrated the DYNASMART-X simulation tool using a transfer function model.

2.1.1 Microscopic Simulation Tools

PARAMICS (PARAllel MICroscopic Simulation) (PARAMICS programmer users guide (2000))

PARAMICS, a micro stochastic simulation model, is developed by Quadstone Limited and includes five software modules: Modeller, Processor, Analyzer, Programmer, and Monitor. PARAMICS can simulate individual vehicle movements based on a microscopic car-following and lane-changing model on freeways, arterial networks, advanced signal controls, roundabouts, incidents, high occupancy vehicle (HOV) lanes, etc. A Graphical User Interface (GUI) with graphical windows provides

a three-dimensional animation of car movements through a simulated network. An Application Programming Interface (API) can customize car-following, gap acceptance, lane-changing, and route choice simulations, and the simulation results can be matched with real-world conditions. The API also uses signal optimization, adaptive ramp-metering, and incident detection as control strategies.

Input parameters can be categorized into four different types: network characteristics, demand data, assignment, and general configuration. The output parameters are travel time, flows, queue length, delay, speed, and density.

CORSIM (CORridor SIMulation) (Boxill and Yu (2000))

CORSIM, a microscopic stochastic simulation model, was developed by the U.S. Federal Highway Administration (FHWA), and it consists of the NETSIM and FRESIM models. The NETSIM model is used for surface street design, while the FRESIM model is used for freeway design. In the case of a multiple-model network, an urban sub-network is built using NETSIM and freeway sections are modeled using FRESIM, both at the same time. Each vehicle in NETSIM can be classified into one of nine different types, and driver behavioral characteristics are assigned. Speed, acceleration, and status of vehicle can also be specified. Each vehicle's movement and position on the link responds to control devices and demands, and calculations are based on car-following logic. Traffic operations are affected by fleet components, load factor, turn movement bus operations, HOV lanes, and queue discharge distribution, among others.

The FRESIM model, a microscopic freeway simulation model, is capable of simulating more complex geometric calculations. This model represents more detailed freeway situations, with such operational features as a lane-changing model, clock-time and traffic-responsive ramp-metering, representations of nine different vehicle types, heavy-vehicle movements, 10 different driver habits, and driver reactions to upcoming geometric changes.

MITSIM (Microscopic Traffic SIMulator) (Boxill and Yu (2000))

MITSIM was developed by Ben-Akiva at the MIT ITS program and evaluates advanced traffic management systems (ATMS) and route guidance systems. MITSIMLab consists of three modules: a Microscopic Traffic Simulator (MITSIM), a Traffic Management System (TMS), and a GUI.

By modifying driver behavior factors—such as desired speed, aggressiveness, etc.—MITSIM can specify each vehicle's characteristics. Individual vehicle movements are simulated based on a car-following model and a lane-changing model. Real-time information is provided for drivers by route guidance systems, so they can make route-choice decisions.

Control and routing strategies—such as ramp control, freeway mainline control, intersection control, variable message sign, and in-vehicle route guidance—are evaluated through the traffic management simulator. A visualization of vehicle movements is available through the GUI, to monitor traffic impact.

2.1.2 Macroscopic Simulation Tools

TRANSYT-7F (TRAffic Network Study Tool) (TRANSYT-7F Users Guide (1998))

TRANSYT-7F, a macroscopic simulation model, was developed by the FHWA. It is used to analyze existent traffic signal timing and optimize it to reduce delays, stops, and fuel consumption for a two-dimensional network.

PASSER (Progression Analysis and Signal System Evaluation Routine) (Boxill and Yu (2000))

PASSER, a macroscopic simulation model, was developed by researchers at the Texas Transportation Institute (TTI). The PASSER model includes traffic signal timing optimization software programs. PASSER-II is used to optimize a single signalized roadway, while PASSER-III is used for diamond interchanges and PASSER-IV for single, multiple roadway, and diamond interchanges.

2.1.3 Mesoscopic Simulation Tool

DYNAMIT (Boxill and Yu (2000))

DynaMIT, a mesoscopic traffic simulation tool, was developed by Ben-Akiva et al. (www.ivhs.mit.edu/products/simlab) It is a Dynamic Traffic Assignment (DTA) system developed for route guidance and traffic prediction and estimation. This tool can control real-time operations and accept real-time surveillance data. In addition, time-dependent O-D flows are estimated and predicted based on DynaMIT. This system also has self-calibration and route-guidance generation capabilities.

2.2 Comprehensive Review of Previous Calibration Studies

This calibration study considers various simulation models. The selection of parameters to be calibrated and the methodology followed are very important aspects of the overall calibration process. Ding (2003), Gardes et al. (2002), Lee et al. (2001), Toledo et al. (2004), Jha et al. (2004), Kim and Rilett (2003), Schultz and Rilett (2004), Hourdakis et al. (2003), Park and Qi (2005), and Ma and Abdulhai (2002) used microscopic simulation tools. In each study, model parameters were selected and various methodologies adopted for calibration, such as the SPSA algorithm (Ding (2003), Kundé (2002), Balakrishna et al. (2007), Ma et al. (2007)), GA (Lee et al. (2001), Schultz and Rilett (2004), Park and Qi (2005), Ma and Abdulhai (2002), Cheu et al. (1998), Kim et al. (2005)), and simplex algorithm (Kim and Rilett (2003)). Ding (2003), Kim and Rilett (2003), and Ma and Abdulhai (2002) used mean absolute error (MAE) as a validation process. Hourdakis et al. (2003) used the sum of squared errors to validate calibrated parameters. Kundé (2002) and Qin and Mahmassani (2004) used mesoscopic simulation tools, and the root-mean-square error (RMSE) was used in the validation process. In this chapter, comprehensive reviews of previous calibration studies are summarized in Table 2.1.

Table 2.1 Summary of previous calibration studies

Authors	Simulation Tool	Calibrated Parameters	Optimization Methodology	Type of Roadway Section	Objective Function	Validation Measure
Ding (2003)	PARAMICS	Mean target headway, mean reaction time	SPSA algorithm	Freeway	Flow, density	MAE
Gardes et al. (2002)	PARAMICS	Mean target headway, mean reaction time	N/A	Freeway	Speed, Volume	N/A
Lee et al. (2001)	PARAMICS	Mean target headway, mean reaction time	Genetic algorithm	Freeway	Occupancy, Flow	N/A
Ma and Abdulhai	PARAMICS	Mean headway, mean reaction time, feedback,	Genetic algorithm	Roadway	Traffic counts	MAE

(2002) Kundé (2002)	DynaMIT-P	perturbation, familiarity Speed–density relationship, Capacity	Box complex, SPSA algorithm	Network	Free-flow, Minimum speed Volume	RMSE
Kim and Rilett (2003)	CORSIM, TRANSIMS	CORSIM: Car- following factors, driver's aggressiveness factor TRANSIMS: O-D matrix, PT1 parameters	Simplex algorithm	Freeway		MAER
Schultz and Rilett (2004)	CORSIM	Driver behavior parameters, vehicle performance parameters	Automated Genetic algorithm	Freeway	Volume, Travel time	MAE
Jha et al. (2004)	MITSIMLab	Parameters of the driving behavior models and route choice model, O-D flows, habitual travel times	Iterative approach	Urban Network	Travel time	N/A
Balakrishna et al. (2007)	MITSIMLab	Driver behavior model parameters	SPSA algorithm	Freeway, Parkway	Traffic Counts	RMSN, RMSPE, MPE
Toledo et al. (2004)	MITSIMLab	O-D flow, behavioral parameters	Complex algorithm	Freeway and arterial	Speed, Density	RMSE, RMSP, MAE, MAPE RMSP
Hourdakis et al. (2003)	AIMSUN	Global, local parameters	Trial and error	Freeway	Volume	
Park and Qi (2005)	VISSIM	Eight parameters	Genetic algorithm	Intersecti on	Average travel time	N/A
Ma et al. (2007)	Microscopic simulation	Global parameters (Mean target head, mean reaction time etc) Local parameters (link headway factor, link reaction factor, etc.)	SPSA algorithm	Freeway	Capacity	N/A
Kim et al. (2005)	Microscopic Simulation	Various microscopic simulation parameters in VISSIM	Genetic Algorithm with Non- parametric statistical test Dynamic	Freeway	Travel Time Distributio n	N/A
Mahut et al. (2004)	EMME/2	Local parameters, global parameters	MSA equilibration algorithm	Network	Travel time, Counts	N/A
Qin and Mahmassani (2004)	DYNASMA RT-X	N/A	Transfer function model	Network	Speed	RMSE

RMSP: Root-Mean-Square Percent error

$$RMSP = \sqrt{\frac{1}{n} \sum_{i=1}^n \left(\frac{x_i - y_i}{y_i} \right)^2}$$

RMSE: Root-Mean-Square Error

$$RMSE = \sqrt{\frac{\sum_i (y_i - \hat{y}_i)^2}{N}}$$

MAPE: Mean-Absolute-Percent-Error
$$MAPE = \sum_{t=1}^T \left| \frac{(x_t - f_t)}{x_t} \times 100 \right|$$

MAE: Mean Absolute Error
$$MAE = \frac{\sum |AVI_{-OD_g} - C_{-OD_g}|}{N}$$

MAER: Mean Absolute Error Ratio
$$MAER_i = \frac{\sum_{j=1}^N \left(\frac{|V_j^o - V_j^d|}{V_j^o} \right)}{C}$$

RMSN: Root mean square error

$$RMSN = \sqrt{\frac{\sum_{n=1}^N (Y_n^o - Y_n^s)^2}{\sum_{n=1}^N Y_n^o}}$$

RMSPE: Root mean square percent error

$$RMSPE = \sqrt{\frac{1}{N} \sum_{n=1}^N \left[\frac{Y_n^o - Y_n^s}{Y_n^o} \right]^2}$$

MPE: Mean percent error

$$MPE = \frac{1}{N} \sum_{n=1}^N \left[\frac{Y_n^o - Y_n^s}{Y_n^o} \right]$$

MSA: Method of Successive Averages (Mahut (2004))

Ding (2003) performed a calibration study of a microscopic simulation model developed using PARAMICS. She used mean target headway and mean reaction time as the key parameters to be calibrated, since these two parameters affect the car-following and lane-changing models. SPSA was used as the optimization algorithm, and the relative error of density and flow was used as the objective function. The selection of these parameters was based on the previous work of Sanwal et al. (1996).

Ma and Abdulhai (2002) performed a calibration study of microscopic simulation models based on combinatorial parametric optimization using a GA. They used GENOSIM (a GA-based simulation-optimization system) to solve a combinatorial parametric optimization problem; it minimized the relative error between field data and simulation output by searching for an optimal value of micro-simulation parameters.

Ma and Abdulhai (2002) employed four types of GAs—namely, simple GA, steady-state GA, crowding GA, and an incremental GA. In the case of the simple GA,

the population was displaced with new individuals; on the other hand, in the steady-state GA, some parts of the population overlapped with new individuals. The crowding-based GA was the same as the simple GA type in selection and reproduction, but replacement was discriminated. As the objective function, the MAE of the difference between real-world and simulated traffic was used.

Gardes et al. (2002) performed a calibration and application study of a PARAMICS model of Interstate 680, located in the San Francisco Bay Area. In order to calibrate input parameter values, significant checks and changes were performed for four major categories: network (network geometry, signposting, link speeds), demand (vehicle proportions, vehicle mean top speed), overall simulation configuration (time steps per seconds, speed memory), and driver behavior factors (mean target headway, mean reaction time). Gardes et al. (2002) then included a new ramp-metering strategy, in addition to auxiliary lanes and an HOV lane, to evaluate a range of operational strategies applicable to the modeled network.

Lee et al. (2001) calibrated the parameters of a PARAMICS model of a Southern California network using a GA. Mean target headway and mean reaction time were employed as key parameters. Mean target headway affects the acceleration and deceleration times of each vehicle and mean reaction time affects the acceptable gap of the lane-changing model. Using a GA, a number of input parameters were repeatedly generated until the parameters were optimized. As a fit test, the differences between occupancy and volume, as obtained from the PARAMICS model and field data, were used.

Kundé (2002) conducted a calibration study of a supply simulator that is a part of DynaMIT-P, a mesoscopic traffic simulator. He studied various methodologies classified into three categories—namely, path search methods, pattern search methods, and random methods. Path search methods estimate a direction to move, from an initial vector to an improved point. Response Surface Methodology (RMS) and SA are major path search methods, and pattern search methods—such as the Hooke and Jeeves method, the Nelder and Mead (simplex search) method, and the Box Complex method—search for a characteristic or pattern from the observations. Random search methods look for an improved point, without the aid of previous information. The stochastic ruler algorithm, stochastic comparison method, and simulated annealing are random search methods.

The calibration methodology used by Kundé (2002) involves three stages, at the disaggregate level, the sub-network level, and the entire network level. The first stage of the methodology is used to calibrate a study of speed-density relationships and the capacities of each segment. The second stage is performed when an accurate O-D can be collected from the sensors. In the last step, the stochastic optimization problem is carried out, which is the calibration at the entire network level. At this stage, the Box Complex method and the SPSA algorithm are employed.

Kim and Rilett (2003) performed a calibration study of micro-simulation modeling using the simplex algorithm. Two micro-simulation models—namely CORSIM and TRANSIMS—were tested using the simplex algorithm. The CORSIM O-D matrix—which uses the CORSIM O-D estimation model and the automatic vehicle identification (AVI) O-D matrix—is the information maximization estimation

model they used. In this calibration study, the parameters used in TRANSIMS were the O-D matrix and the PT parameters, described as the deceleration probability (PT_1), the lane-change probability (PT_2), and the plan look-ahead distance (PT_3). CORSIM calibration parameters were car-following factors, acceleration/deceleration factors, and lane-changing factors. Both CORSIM and TRANSIMS were calibrated when parameter sets were default values. Preliminary calibrations for the AM, PM, or off-peak time periods were conducted using the simplex algorithm mean absolute error ratio (MAER) was used to compare observed CORSIM and TRANSIMS volumes. Models calibrated via the simplex approach were found to have a lower MAER than the models that used default values.

Schultz and Rilett (2004) conducted the calibration of a microscopic simulation model using the FHWA's corridor simulation model (CORSIM), and also used the distribution of car-following sensitivity factors as the main calibration parameter. Car-following sensitivity factors included driver behavior characteristics that depended on the car ahead, with specified sensitivity. The author classified 10 different car-following sensitivity factors and identified them to explain variability among driver types. A GA was used for the calibration methodology and the new distribution was examined to fit the data. For the car-following sensitivity analysis, the author outlined two alternatives that were lognormal and normal car-following sensitivity analyses, and compared those with initial distributions.

Jha et al. (2004) performed a calibration of a large-scale network using MITSIMLab, a micro traffic simulation model. They calibrated driving behavior parameters with a single freeway section without considering route choice. After

driving behavior parameters were calibrated, the values were fixed; the calibration work of route-choice parameters, an estimation of O-D flows, and habitual travel times was then jointly performed for a large-scale network, using an iterative solution approach. As the function of the validation process, the travel times of field data were compared with the output of the simulation model.

Toledo et al. (2004) performed a calibration study of microscopic traffic simulation models. They focused on the interactions of O-D flow estimations and calibrations of behavior parameters. He proposed an iterative solution approach that starts with habitual travel times, because O-D flow estimation needs to generate an assignment matrix based on route-choice behavior and experienced travel times. Habitual travel times are important variables in solving a driver's route-choice problems. The assignment matrix was generated based on these travel times, and an O-D flow estimation was performed using a generalized least squares (GLS) formulation. The new O-D matrix is used to recalibrate route choice and driving behavior parameters, and this iterative procedure was repeated to minimize the least square error. To demonstrate the efficiency of this approach, it was applied to two different case studies developed with the use of MITSIMLab, a microscopic traffic simulation model (Toledo et al. (2004), Jha et al. (2004)). In the first case study, O-D flows were known and route choice was not present in the network. In this case, driving behavior was the only parameter to calibrate. As a function of the fit test, the RMSE, the root-mean-square percent error (RMSP), the MAE, and the mean absolute percent error (MAPE) of the difference between observed and simulated speed measurements were used. For the other case study, O-D flow estimations and

calibration work with regard to the travel time coefficient of the route choice were performed. As a function of the fit test, Toledo et al. (2004) used RMSE and MAE to compare the observed and simulated counts. Both of the case studies were good fits.

Hourdakis et al. (2003) proposed a calibration procedure for microscopic traffic simulation models for a 20-km freeway section in Minneapolis. For this calibration study, they divided the simulator parameters into global parameters such as length, width, desired speed, maximum acceleration/deceleration, and minimum headway, as well as local parameters like the speed limits along individual sections of the freeway model. Global parameters were closely related to the performance of the entire model, and local parameters affected specific parts of the network.

Hourdakis et al. (2003) divided the calibration process into volume-based calibrations and speed-based calibrations. The objective of volume-based calibrations was to obtain the volumes from simulation that were as close to the real-world counts as possible; the objective of the speed-based calibrations was to obtain the speeds from simulation that were as close to the real-world speeds as possible. The sum of the squared errors was used as the optimization technique to calibrate the simulator parameters, and traffic volumes were used as an objective function to be minimized.

Park and Qi (2005) performed a calibration of a microscopic and stochastic simulation model developed in VISSIM, based on a parameter optimization using a GA. The traffic simulator included car-following and lane-changing logic, as well as the signal state generator that can decide signal control logic. The location was the intersection of U.S. Route 15 and U.S. Route 250 in Virginia, and the average travel time was used as the measure of effectiveness. In order to acquire an accurate

simulation result, the acceptable ranges of eight parameters were determined and multiple simulation runs performed to reduce the stochastic variance with default parameter values. A GA approach was applied to calibrate parameter values. In order to verify whether the calibrated parameters were statistically significant, a t-test and visualization check were also performed.

Cheu et al. (1998) performed a calibration of a FRESIM-based model of a Singapore expressway, using GAs. The existing representative optimization algorithms used a gradient approach that lacks robustness. This algorithm has only one solution, and this may lead only to a local solution; therefore, a GA was applied to reduce this problem and find a global solution. The calibration work was performed for a 5.8-km section of the Ayer Rajar Expressway in Singapore. The parameters calibrated for FRESIM are free-flow speed and driver behavior parameters. As a fit test, Average Absolute Error (AAE) was used between FRESIM simulation output and field data from the loop detector.

Milam (2005) recommends guidelines for the calibration and validation of traffic simulation models. The calibration requires modifying traffic control operations, traffic flow characteristics, and driver behavior. He summarizes the default values of the parameters to be calibrated in CORSIM, as well as their effective range. The parameters presented in the validation guidelines were traffic volume, average travel time, average travel speed, freeway density, and average and maximum vehicle queue lengths. The author recommends each parameter's acceptable range of error between CORSIM simulation results and field data. Tables 2.2 and 2.3 show the calibrations and their effective range and validation guidelines.

For a greater understanding of the validation guideline in Table 2.3, CORSIM output was compared with observed data from the town of Lafayette, California, until all the ranges of the validation parameters were acceptable. CORSIM is based on stochastic algorithms, i.e., the results of each run change, depending on the random seed. For more accurate results, the average simulation result of multiple runs with many different random numbers was used.

Table 2.2 Calibration parameters and effective ranges (Milam (2005))

Parameters	Calibration Parameters (Milam (2005))		
	Effect	Default Value	Calibration Range
Start-up Lost Time (Arterials)	Link Specific	2.0 Seconds	0.5 to 9.9 Seconds
Start-up Lost Time (Freeways)	Link Specific	1.0 Second	0.5 to 6.0 Seconds
Queue Discharge Rate (Arterials)	Link Specific	1.8 Seconds (2,000 vphpl)	1.4 to 2.4 Seconds (1,500 - 2,270 vphpl)
Pedestrian Demand	Link Specific	0 (If left blank) No pedestrians	Demand 0 to 4 0 – 500 pedestrians
Car-Following Sensitivity Factor (Freeways)	Network-wide	Driver Type 1 (0.6 Seconds) to Driver Type 10 (1.5 Seconds)	0.6 to 1.5 Seconds for Driver Types 1 to 10
Time to complete a lane change (Freeways)	Network-wide	3.0 Seconds	2.0 to 5.0 Seconds
Acceptable gap in oncoming traffic for permissive left-turners (Arterials)	Network-wide	Driver Type 1 (7.8 Seconds) to Driver Type 10 (2.7 Seconds)	2.7 to 7.8 Seconds for Driver Types 1 to 10
Acceptable gap in oncoming traffic for right-turns-on-red or right-turn at stop sign (Arterials)	Network-wide	Driver Type 1 (10.0 Seconds) to Driver Type 10 (3.6 Seconds)	3.6 to 10.0 Seconds for Driver Types 1 to 10

Driver's Familiarity with Network (Arterials)	Network-wide	10 Percent Recreational 90 Percent Commuter	Sum of recreational and commuter must equal 100
--	--------------	---	---

Table 2.3 Validation guidelines (Milam (2005))

Validation Guidelines		
Parameters	Description	Validation Criteria
Volume Served	Percent difference between input volume and CORSIM output or assigned volume	95 to 105 % of observed value
Average Travel Time	Standard Deviation between floating car average travel times and CORSIM simulated average travel time for a series of links	1 Standard Deviation
Average Travel Speed	Standard Deviation between floating car average travel speed and CORSIM simulated average travel speed for individual links	1 Standard Deviation
Freeway Density	Percent difference between observed freeway density (from volume counts and floating car travel speed) and CORSIM simulated density	90 to 110 % of observed value
Average and Maximum Vehicle Queue Length	Percent difference between observed queue lengths and CORSIM simulated queue lengths	80 to 120 % of observed value

Dowling et al. (2004) recommend the calibration/validation of micro-simulation models in three steps. The simulation model is first calibrated for capacity and then traffic flow, both at a bottleneck section. Finally, the model is calibrated for system performance at the entire network level. According to the author, for the capacity calibration procedure, the capacity of the given model was estimated by counting the maximum possible flow rate of the target section, and parameters that directly affect the capacity were selected. The mean squared error (MSE) was used for the objective function, and the optimal parameter values were obtained at the

point where the MSE was minimized. In the case of matching observed traffic flow, the route choice algorithm parameters were adjusted until predicted volumes fit field counts. Finally, overall traffic performance was compared with various field data, including travel time, queue lengths, and duration of queuing. As an example of satisfying the three-step application, Dowling et al. (2004) used the sample problem offered by Bloomberg et al. (2003), which compared six simulation models with the *Highway Capacity Manual (HCM)*.

Mahut et al. (2004) performed calibration work based on the dynamic traffic assignment (DTA) model. DTA is a procedure where network users choose the best route, to minimize overall travel cost. The DTA model used in this study is based on an iterative approach, where flows are updated with successive iterations that are based on travel times from the simulation model. The EMME/2 software package was used to calibrate a DTA trip table that was modified through a matrix adjustment. As part of the verification process, three consecutive 15-minute counts were compared with calibrated model results.

Qin and Mahmassani (2004) performed a calibration study of dynamic speed-density relationships by using data collected from Interstate Freeways I-5 and I-405 in California. They estimated the parameters to find the minimum discrepancy between observed and simulated speed, using transfer function, one-regime modified Greenshields, and two-regime modified Greenshields models. The RMSE of speed was used as a goodness-of-fit test. As a result of the comparison, the transfer function approach was found to be more accurate than static modified Greenshields models in estimating dynamic traffic speed.

2.3 Review of Optimization Methods for Parameter Calibration

Optimization methods can be classified into the random search, pattern search, and path search methods.

1. The random search method, one of the simplest methods, is used to find the optimal value where the feasible region (Θ) is discrete. Each iteration is performed, with no input from the previous situation. The new selected value is based on loss function, and it is selected if the loss function is lower than the previous value. This method is very slow in converging to the optimal value. The simple random search, the localized random search, and the enhanced localized random search methods are representative random search methods (Spall (2003)).
2. The Hooke and Jeeves method is a well-known example of the pattern search method. This method tests multivariate directions from the initial parameters, and the improved value becomes the new value Kundé (2002). The nonlinear simplex algorithm by Nelder and Mead (Spall (2003)) is also a pattern search method.
3. The path search method estimates the direction of the best vector in finding an improved estimate from the current value. The SA, one of the path search methods, is the selected value; it is updated until the gradient equals zero, to solve the optimization problem Kundé (2002), (Spall (2003)). RSM (Spall (2003)) is another path search method; it uses the path of steepest descent method, repeating until it finds the final best vector.

Chapter 3

Overall Calibration Framework Using the SPSA Algorithm

3.1 Introduction

The main reason for performing simulation is to test future scenarios under conditions similar to real-world conditions. However, since this representation may not be accurate if the model parameters are not carefully calibrated, calibrating model parameters is a very important task. Selecting appropriate model parameters for calibration, as well as the calibration methodology, are both crucial tasks. This chapter provides a description of the standard SPSA algorithm and the overall calibration process. In this dissertation, the study area is a section of the I-880 freeway in Hayward, California. For the calibration of the PARAMICS model, the mean target headway and mean reaction time—which affect the car-following model and lane-changing model—were selected as the key parameters.

3.2 Proposed Research Methodology

Optimization algorithms can be classified into deterministic and stochastic approximation (SA) algorithms; in the latter case, objective function is probabilistic.

Each algorithm can be further divided into two general categories: gradient and gradient-free settings. The steepest descent method (Spall (2003)) and Newton-Raphson method (Spall (2003)) use deterministic optimization algorithms. Nelder and Mead (1965) proposed the nonlinear simplex algorithm, a deterministic method that is based on a gradient-free multivariate optimization method. The steepest descent method is a very simple deterministic technique, wherein given value θ changes to the best gradient vector until the solution to $\min_{a \geq 0} \left[L(\hat{\theta}_k - ag(\hat{\theta}_k)) \right]$ is derived.

Newton-Raphson iterated the algorithm based on the inverse Hessian matrix; this method examines worst direction, rather than steepest descent. The nonlinear simplex algorithm is based on the gradient-free multivariate optimization method.

Stochastic objective function of the stochastic approximation (SA) algorithms (usually termed as loss function L) can be used in the presence or absence of the gradient function $g(\theta)$. The stochastic root-finding algorithm by Robbins and Monro (1951) is generally used for nonlinear problems when the gradient function is available. When measuring the gradient is impossible, such as in the case of simulation, a gradient-free approach is applied. The finite-difference (FD) approximation is the most well-known gradient approximation method; however, the FD approximation is performed only when the noise measurements of the loss function are available. SPSA, one of the well-known Stochastic Approximation (SA) algorithms, can be applied in both stochastic gradient and gradient-free settings; it can also be applied to solve optimization problems that have a large number of variables. The SPSA algorithm is proposed as the main calibration mechanism for PARAMICS.

The validation process is performed to minimize the relative error of flow and density between the real world and the output of a PARAMICS simulation. For the independent verification process, a chi-square test is performed on the headway distribution; this is the most commonly used method for determining the level of statistical significance of certain variables. The chi-square test is used to check whether the headway distribution from the simulation is consistent with the observed data. Finally, a sensitivity analysis is carried out for the headway distribution, for each value of mean target headway.

Figure 3.1 shows the overall procedure for the calibration and validation methodology.

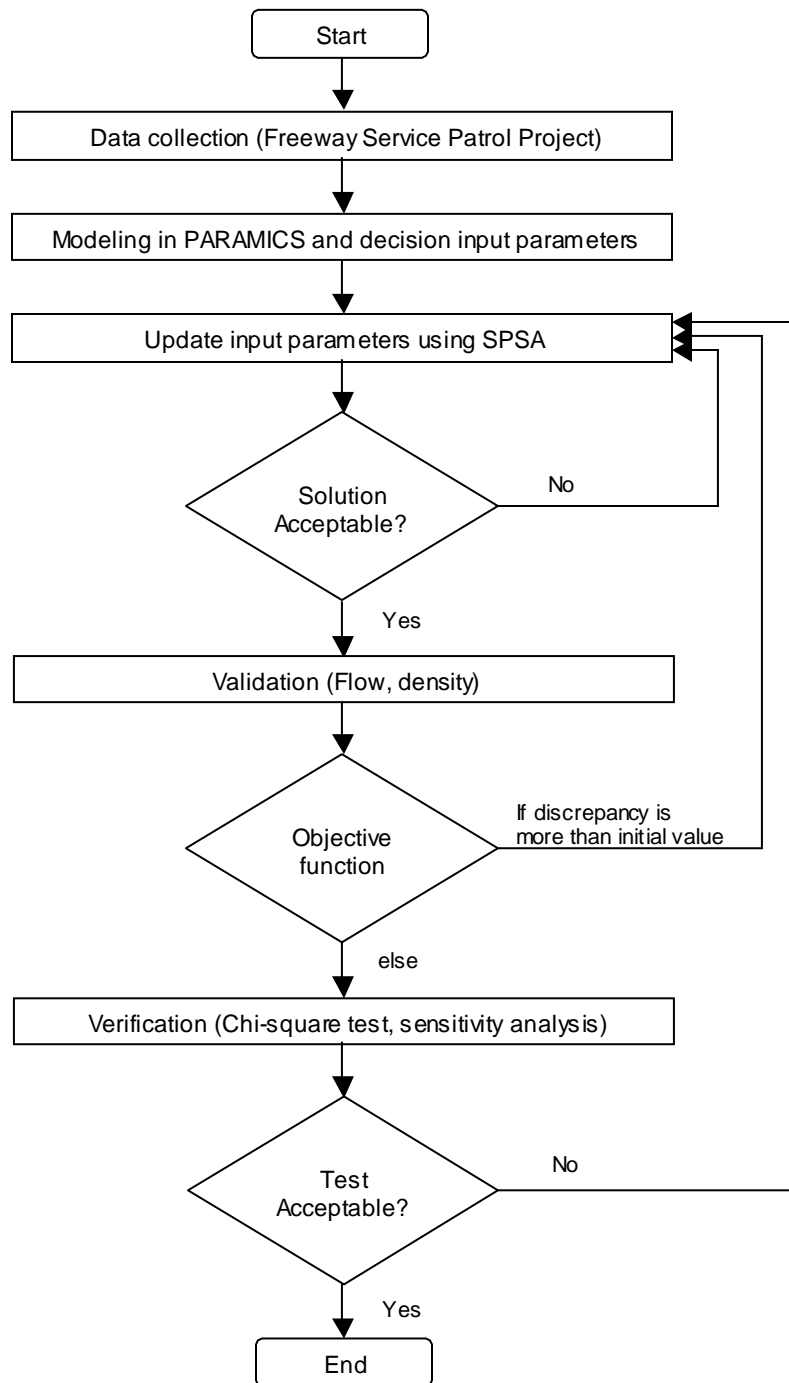


Figure 3.1 Overall procedure proposed for the calibration and validation of a simulation model

The first step is data collection. In this thesis, data was obtained from a section of the I-880 freeway in Hayward, California. The data was classified as incident data, probe vehicle data, and loop data. Loop data is used for our calibration study. The second step is to accurately model the network using PARAMICS. In addition, the input parameters to be calibrated—namely, mean target headway and mean reaction time—are determined. The next step is to update the simulation input parameters using SPSA and repeat the iteration process until the solution is acceptable. Differences between simulated and observed flow and density values are compared in the next step. If this difference exceeds a pre-determined value, then the input parameters are updated again. If the value of the objective function is acceptable, i.e., smaller than the pre-determined value, then the verification process is performed to test whether or not new parameters are statistically significant. If all these above steps are acceptable, then the calibration process is terminated.

3.3 The Simultaneous Perturbation Stochastic Approximation (SPSA) Algorithm

Stochastic approximation (SA) optimization methods are used in a number of areas relevant to statistical modeling and control, e.g., sequential parameter estimation, adaptive control, experimental design, and stochastic optimization and neural network weight estimation (Spall (1992)).

The SA algorithm is based on a simultaneous perturbation gradient approximation introduced by Spall (1992). It is used to find a root of the multivariate gradient equation.

A dynamic multi-ramp-metering control using the SPSA algorithm was performed by Luo (2003), and the effectiveness of SPSA therein was shown for freeway operations. Spall (1997) performed the optimization work to control signal timing using the SPSA algorithm, and its effectiveness was proved. The calibration study using the SPSA algorithm can be also found in Ding's (2003) and Kundé's (2002) respective papers.

Using this SPSA algorithm, the present calibration study is performed to determine how well the PARAMICS model represents reality. To minimize the relative error between the real world and the model, two key parameters (i.e., the mean headway and the mean reaction time) are modified to fit U.S. conditions. In addition, the seed value, used by the random number generator, also affects the simulation result, and so the simulation is run with several seed values, to determine the influence of the random number generator on the PARAMICS output.

3.3.1 Description for Standard SPSA Algorithm (Spall (2003))

The SA algorithm normally focuses on finding the vector value $\theta \in \Theta$, which either minimizes the loss function $L(\theta)$ or makes the gradient equation $g(\theta)$ equal to zero. The SPSA is an applicable stochastic optimization method for multivariable equations, and the standard SPSA algorithm has the following form (Spall (2003)):

$$\hat{\theta}_{k+1} = \hat{\theta}_k - a_k \hat{g}_k(\hat{\theta}_k) \quad [3.1]$$

Here, $\hat{g}_k(\hat{\theta}_k)$ is the SP of the gradient $g(\theta) = \frac{\partial L(\theta)}{\partial \theta}$ estimated, based on the loss function measurements, at $\theta = \hat{\theta}_k$ at the k^{th} iteration. a_k indicates the step size and is a nonnegative scalar coefficient. The basic solution to an optimization problem is to minimize the loss function $L(\hat{\theta}_k - a_k g(\hat{\theta}_k))$ at the k^{th} iteration. The new value of θ , obtained for every iteration, is calculated by subtracting the product of step size and the gradient at the present value from the previous value of θ .

The gradient approximation $\hat{g}_k(\hat{\theta}_k)$ is the most important part of the SPSA algorithm. With Stochastic Perturbation (SP), loss measurements are obtained by randomly perturbing the elements of $\hat{\theta}_k$. Assuming that θ is p -dimensional, the Stochastic Perturbation (SP) gradient approximation can be shown in the following form:

$$\hat{g}_k(\hat{\theta}_k) = \begin{bmatrix} \frac{\hat{L}(\theta + c_k \Delta_k) - \hat{L}(\theta - c_k \Delta_k)}{2c_k \Delta_{k1}} \\ \bullet \\ \bullet \\ \bullet \\ \frac{\hat{L}(\theta + c_k \Delta_k) - \hat{L}(\theta - c_k \Delta_k)}{2c_k \Delta_{pk1}} \end{bmatrix}$$

$$= \frac{\hat{L}(\theta + c_k \Delta_k) - \hat{L}(\theta - c_k \Delta_k)}{2c_k} [\Delta_{k1}^{-1}, \Delta_{k2}^{-1}, \dots, \Delta_{kp}^{-1}]^T \quad [3.2]$$

Here, the, p -dimensional random perturbation vector, $\Delta_k = [\Delta_{k1}, \Delta_{k2}, \dots, \Delta_{kp}^{-1}]^T$ is a user-specified vector for which the components of Δ_k are normally distributed ± 1 Bernoulli variables. Here, c_k is a positive scalar.

The problem of minimizing $L = L(\theta)$ for a differentiable loss function is equivalent to finding a solution of the gradient approximation $g(\theta) = \frac{\partial L(\theta)}{\partial \theta} = 0$. The loss function for this study is a standard quadratic measure, as shown below:

$$L(\theta) = E[x^T x | \theta], \quad [3.3]$$

where $E[\bullet | \theta]$ denotes an expected value that is conditional on the set of controls with weights θ (Spall (1997)).

3.3.2 Convergence of the Stochastic Approximation (SA) Algorithm (Spall (1992))

The convergence theory of SA has been studied for many years, and it is used to determine if at the k^{th} iteration $\hat{\theta}_k$ converges to a minimizing point $\theta^* \in \Theta^*$. Most of the convergence results for SA are in the almost sure (a.s.) sense. Over many years, several conditions have been added for the almost sure (a.s.) convergence of the SA recursions in $\hat{\theta}_{k+1} = \hat{\theta}_k - a_k Y_k(\hat{\theta}_k)$. (Here, Y_k replaces the exact root-finding function $\hat{g}_k(\hat{\theta}_k)$.)

Some of the conditions used to determine the almost sure (a.s.) convergence are represented below.

$$a_k > 0, c_k > 0, a_k \rightarrow 0, c_k \rightarrow 0, \sum_{k=0}^{\infty} a_k = \infty, \\ \sum_{k=0}^{\infty} a_k c_k = \infty, \text{ and } \sum_{k=0}^{\infty} a_k^2 / c_k^2 < \infty.$$

The gain sequence is used to balance the algorithm stability; the desired form of the gain sequence is shown below.

$$a_k = \frac{a}{(k+1+A)^\alpha}, c_k = \frac{c}{(k+1)^\gamma} \quad [3.4]$$

The recommended value for A in the gain sequence is zero. If the numerator a is small, the calculations are initially stable. However, this may result in slug performance for large calculations. On the other hand, a large numerator $a_k > 0$, which is used to produce nonnegligible step sizes, leads to instability early in the calculation. It is most effective to set the numerator c to a small positive number. Ding (2002) suggests that the values for α and γ should be set to 0.602 and 0.01 respectively; these values are used in this dissertation.

For the iteration process to be successful, a large number of individual iterations must be performed until the differential distance between the k^{th} iteration

$\hat{\theta}_k$ and the optimal value θ^* decreases. If the starting point $\hat{\theta}_0$ is set near θ^* , the calculation fluctuates around θ^* and the calculation proceeds slowly.

Figure 3.2 compares calculations with poor convergence (Figure (a)) and good convergence (Figure (b)). Graph (a) shows that $\hat{\theta}_k$ reaches the circled area without bouncing. On the other hand, graph (b) shows that the value of $\hat{\theta}_k$ bounces around θ^* when it reaches the circled area.

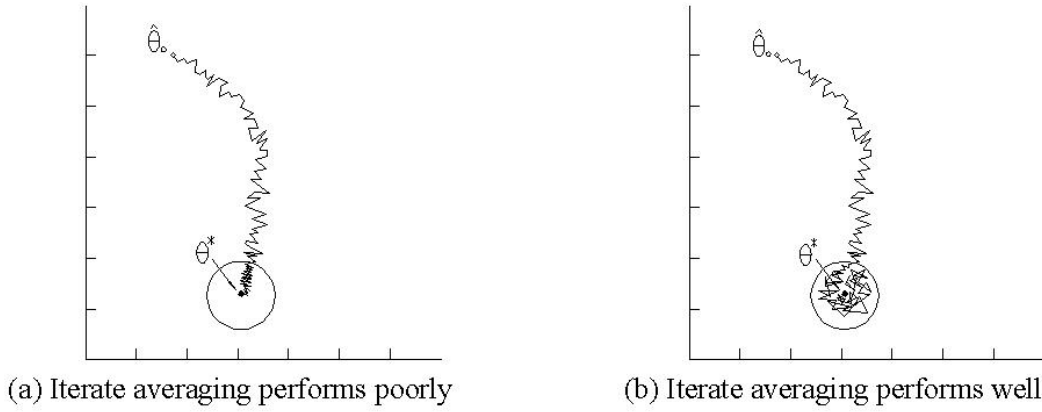


Figure 3.2 Comparison between poorly designed and well-designed SPSA algorithms
(Spall (2003))

3.3.3 The Effect of Random Seed on the Results

The random seed is another factor that is studied, to determine its effect on simulation results. In a stochastic analysis, a random number is used to represent measurement noise; to obtain more accurate results, it is necessary to consider the effects of random numbers. Spall (2003) compares the variance of the error

$$y_k^{(+)} - y_k^{(-)} = Q(\theta_k + c_k \hat{\Delta}_k, V_k^{(+)}) - Q(\theta_k - c_k \hat{\Delta}_k, V_k^{(-)})$$

for the gradient estimate from the SPSA algorithm, between the common random number (CRN) and non-common

random number (non-CRN); the results of the loss values for CRN were lower than those for non-CRN. Here, $V_k^{(\pm)}$ are random variables that affect noise measurement. Thus, it is necessary to perform a simulation with many different random numbers, to minimize the variance of the error.

Chapter 4

Calibration of a Macroscopic Simulation Model Using the Simultaneous Perturbation Stochastic Approximation Method

4.1 Introduction

Before performing the calibration of the PARAMICS microscopic simulation tool by applying the SPSA optimization method, it is necessary to test the effectiveness of the SPSA algorithm when applied to simpler traffic simulation models.

In this chapter, the cell transmission model (CTM) developed by Daganzo (1994) is used to prove the effectiveness of the SPSA algorithm when various random numbers are used, because this model is much faster to run compared to PARAMICS. Free-flow speed and jam density were selected as the input parameters, and the average gradient with multiple runs from SPSA algorithm was used.

4.2 Cell Transmission Model (CTM)

To test whether the SPSA algorithm works as intended when applied to traffic simulations, the CTM was used. The CTM can be used to represent complex traffic

situations such as acceleration/deceleration, stop and go, or shock waves. This model defines flow as the minimum value of the upstream capacity of the cell and downstream capacity of the cell (Daganzo (1994)). When demand is low, the upstream flow is very low (minimum value); on the other hand, when demand is high, downstream capacity becomes very low (minimum value).

The basic shape of the flow density relationship used by the CTM is a trapezoid, as shown in Figure 4.1. There, V_f indicates free-flow speed and K_j is the jam density.

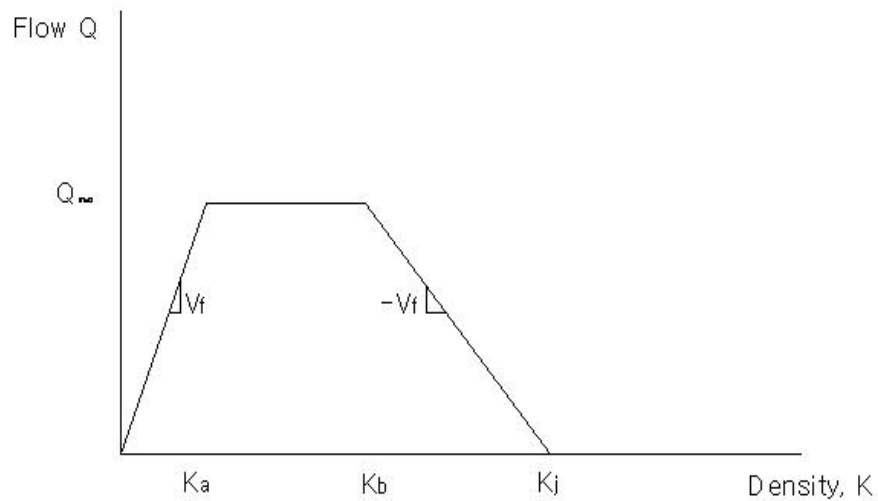


Figure 4.1 Flow-density relationship for the basic CTM (Daganzo (1994))

4.3 Input Variables of Cell Transmission Model (CTM)

Demand

Demand is one of the major input variables. This relation supposes free-flow speed V_f under low density and the shock wave speed W under high density. The

maximum number of vehicles in the under-congested condition is the product of the jam density and cell length at the cell i ; the maximum number of vehicles in the over-congested condition is the capacity of the cell $i - 1$.

Geometry

The network geometries in the CTM are the length of the network and number of lanes. The number of cells is defined by the length of the network.

4.4 Goodness-of-Fit Test

The CTM is used to model a section of the I-880 freeway section in California. The selected freeway section is two lanes of one-way road where there are no intermediate ramps. The length of the section is one mile and this section is divided into 20 cells.

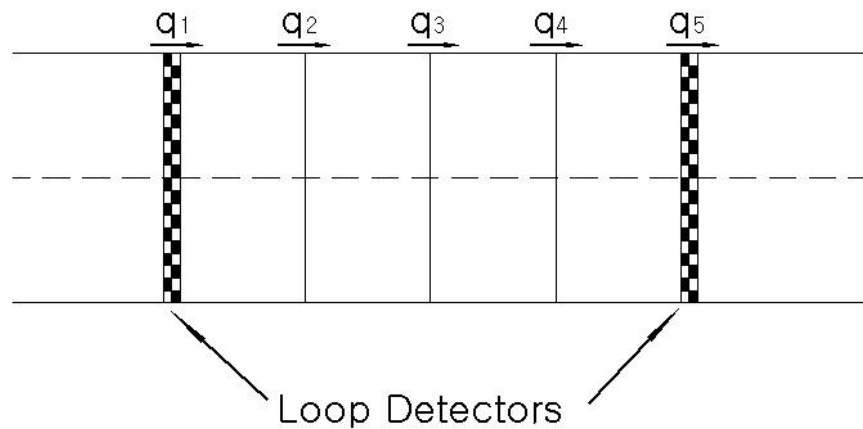


Figure 4.2 I-880 freeway segment

The calibration procedure for the model is as follows.

The density is used as a criterion to measure performance in the calibration study. The relative error—i.e., the sum of the square error between field data and cell transmission results of density for every 3 min, for two lanes—is used as the objective function. The objective function is the minimum relative error that optimizes the free-flow speed and jam density, which are the parameters to be calibrated. Because there is no on-off ramp in the network and the number of vehicles does not change much, the flow is not included in the objective function. The objective function is of the form shown below:

$$F = \sum_{INTERVAL} \sum_{DETECTOR} \sum_{LANE} \frac{\|K_{real} - K_{sim}\|^2}{K_{real}}, \quad [4.1]$$

where

K_{real} : Density for each lane and each detector on the freeway during each time interval (veh/mile)

K_{sim} : Density for each lane and each detector in simulation during each time interval (veh/mile)

The initial value of the parameters were 55 miles per hour for free flow speed (V_f) and 110 vehicles per mile for jam density (K_j); each iteration process was performed with three different seed values. The values of the two variables are shown to converge, where there is a small difference in density between real-world data and

cell transmission simulation results, reducing the error from 35.72 to 12.37 percent. The difference between the two values decreased from $(-8.59, 8.59)$ when $k=0$ to $(-0.99, 0.99)$ when $k=23$. The results of this calibration study are summarized in Table 4.1.

Each iteration process was performed multiple times with different random numbers. The difference between observed and simulated density was reduced from 35.72 to 12.37 percent. As the gradient approaches zero, the objective function is minimized—i.e. the SPSA algorithm is found to be an effective stochastic optimization approach.

Table 4.1 Results of the calibration study

k	c_k	a_k	$\hat{\theta}_k$	Δ_k	$\hat{\theta}_k + c_k \Delta_k$	$\hat{L}(\hat{\theta}_k + c_k \Delta_k)$	$\hat{\theta}_k - c_k \Delta_k$	$\hat{L}(\hat{\theta}_k - c_k \Delta_k)$	$\hat{g}_k(\theta)$	$\hat{\theta}_{k+1}$
0	0.500	0.200	(55.00, 110.00)	(1, -1)	(55.50, 109.5)	35.22	(54.50, 110.5)	43.81	(-8.59, 8.59)	(56.72, 108.28)
1	0.467	0.132	(56.72, 108.28)	(-1, 1)	(56.25, 108.7)	30.19	(57.18, 107.8)	25.23	(-5.32, 5.32)	(57.42, 107.58)
2	0.448	0.103	(57.42, 107.58)	(-1, -1)	(56.97, 107.1)	25.43	(57.87, 108.0)	21.63	(-4.24, -4.24)	(57.86, 108.02)
3	0.435	0.087	(57.86, 108.02)	(1, -1)	(58.29, 107.6)	20.41	(57.42, 108.5)	23.71	(-3.79, 3.79)	(58.19, 107.69)
4	0.426	0.076	(58.19, 107.69)	(1, 1)	(58.61, 108.1)	19.25	(57.76, 107.3)	23.17	(-4.60, -4.60)	(58.53, 108.04)
5	0.418	0.068	(58.53, 108.04)	(1, -1)	(58.95, 107.6)	18.79	(58.12, 108.5)	20.85	(-2.46, 2.46)	(58.70, 107.87)
6	0.412	0.062	(58.70, 107.87)	(1, 1)	(59.11, 108.3)	16.78	(58.29, 107.5)	20.44	(-4.45, -4.45)	(58.98, 108.15)
7	0.406	0.057	(58.98, 108.15)	(-1, -1)	(58.57, 107.7)	19.37	(59.38, 108.6)	16.38	(-3.68, -3.68)	(59.19, 108.36)
8	0.401	0.053	(59.19, 108.36)	(1, -1)	(59.59, 108.0)	15.22	(58.79, 108.8)	18.93	(-4.62, 4.62)	(59.43, 108.11)
9	0.397	0.050	(59.43, 108.11)	(-1, 1)	(59.04, 108.5)	17.66	(59.83, 107.7)	15.09	(-3.24, 3.24)	(59.60, 107.95)
10	0.393	0.047	(59.60, 107.95)	(1, 1)	(59.99, 108.3)	14.64	(59.20, 107.6)	17.11	(-3.14, -3.14)	(59.74, 108.10)

11	0.390	0.045	(59.74, 108.10)	(-1, 1)	(59.35, 108.5)	16.57	(60.13, 107.7)	14.27	(-2.94, 2.94)	(59.88, 107.97)
12	0.387	0.043	(59.88, 107.97)	(1, - 1)	(60.26, 107.6)	13.32	(59.49, 108.4)	16.13	(-3.63, 3.63)	(60.03, 107.81)
13	0.384	0.041	(60.03, 107.81)	(1, - 1)	(60.42, 107.4)	13.28	(59.65, 108.2)	16.22	(-3.83, 3.83)	(60.19, 107.66)
14	0.381	0.039	(60.19, 107.66)	(-1, 1)	(59.81, 108.0)	15.51	(60.57, 107.3)	12.93	(-3.37, 3.37)	(60.32, 107.52)
15	0.379	0.038	(60.32, 107.52)	(1, 1)	(60.70, 107.9)	12.78	(59.94, 107.1)	15.85	(-4.05, - 4.05)	(60.47, 107.68)
16	0.377	0.036	(60.47, 107.68)	(1, - 1)	(60.85, 107.3)	12.64	(60.10, 108.1)	14.43	(-2.39, 2.39)	(60.56, 107.59)
17	0.374	0.035	(60.56, 107.59)	(-1, 1)	(60.18, 108.0)	14.04	(60.93, 107.2)	12.17	(-2.51, 2.51)	(60.65, 107.50)
18	0.372	0.034	(60.65, 107.50)	(-1, - 1)	(60.27, 107.1)	14.12	(61.02, 107.9)	12.25	(-2.51, - 2.51)	(60.73, 107.59)
19	0.371	0.033	(60.73, 107.59)	(1, - 1)	(61.10, 107.2)	12.21	(60.36, 108.0)	13.80	(-2.15, 2.15)	(60.80, 107.52)
20	0.369	0.032	(60.80, 107.52)	(1, - 1)	(61.17, 107.1)	12.32	(60.43, 107.9)	13.92	(-2.17, 2.17)	(60.87, 107.45)
21	0.367	0.031	(60.87, 107.45)	(1, 1)	(61.24, 107.8)	12.26	(60.51, 107.1)	13.81	(-2.11, - 2.11)	(60.94, 107.51)
22	0.365	0.030	(60.94, 107.51)	(1, - 1)	(61.30, 107.1)	12.41	(60.57, 107.9)	13.17	(-1.04, 1.04)	(60.97, 107.48)
23	0.364	0.029	(60.97, 107.48)	(-1, 1)	(60.61, 107.8)	13.36	(61.33, 107.1)	12.63	(-0.99, 0.99)	(61.00, 107.45)
24	0.362	0.028	(61.00, 107.45)	(1, - 1)	(61.36, 107.1)	12.63	(60.64, 107.8)	13.82	(-1.64, 1.64)	

4.5 Simulation Results and Summary

Before the calibration of the microscopic PARAMICS based simulation model, a cell transmission-based macroscopic model was used to test the effectiveness of the SPSA algorithm when various seeds were used. Two parameters—namely, free-flow speed and jam density—were selected and the average gradient with multiple runs from the SPSA algorithm was used. The initial points were 55 miles per hour for free-flow speed and 110 vehicles per mile for jam density. The relative error between the simulated density and observed data was

reduced from 35.72 to 12.37 percent. Thus, the convergence process using the SPSA algorithm was found to be acceptable.

Chapter 5

Calibration of a Microscopic Simulation Model Using the Simultaneous Perturbation Stochastic Approximation Method

5.1 Introduction

This chapter presents the implementation of the proposed calibration procedure for the model developed using the PARAMICS simulation tool. PARAMICS software is beneficial, as it has an application programming interface (API) which customization of various features of the simulation model, such as car-following, gap acceptance, and signal optimization. PARAMICS graphical user interface (GUI) that is capable of animating vehicle movement through a simulated network is also a useful capability.

Selecting input parameters and finding optimal values for those parameters is crucial to ensure the accuracy of the simulation results. In this dissertation, driver behavior factors—namely, mean target headway and mean reaction time—were selected as input parameters, because those values affect the outcome of the microscopic simulation model. In addition, the evaluation of the performance is

studied, if PARAMICS has the ability to replicate real-world conditions; this necessarily validates and verifies the model.

5.2 Key Calibration Parameters

The PARAMICS model developed by Quadstone Limited is a microscopic stochastic simulation model that is very comprehensive and has the potential for application to a wide set of freeway arterial and network situations (Gardes (2002)).

PARAMICS is capable of controlling individual vehicle movements that address model input parameters, such as car-following parameters, seed value, signpost distance, lane-changing, and time step of simulation per second.

Network geometry

For the calibration procedure, the first step is to accurately represent real-world conditions in the simulation model. For example, nodes or the stop-line position will affect vehicle movement and vehicle speed to a great extent; they can suddenly reduce traffic speed or result in unexpected shockwaves.

Signposting

Signposting is about giving information to drivers about a hazard: traffic signals, lane additions, on-ramps or off-ramps, etc. Awareness distance to the hazard and reaction time to the hazard can be modified separately.

Time steps per second

The initial value of time steps is set to 2 s; this means that every 0.5 s, the simulation is calculated. Simulation results change, depending on time step value.

Driver behavior factors

Driver behavior factors—namely, the mean target headway and mean reaction time—directly influence the car-following model and the lane-changing model. Many studies of microscopic calibration work have been performed with these two parameters, to modify simulation results. In this dissertation, these two factors were used for the calibration process.

Mean target headway

Headway is the time between two consecutive vehicles that pass a specific point. The time interval is calculated from the front (or the rear) bumper of the front vehicle to the front (or the rear) bumper of the rear vehicle.

The average headway in a lane is the reciprocal of the flow rate; thus, at a flow of 1,200 vehicles per hour per lane (veh/h/ln), the average headway is $3,600/1,200$ or 3 s. Vehicles do not, however, travel at constant headways; vehicles tend to travel in groups, or platoons, with varying headways between successive vehicles (*HCM* (2000)). The *HCM* (2000) shows the headway distribution that is observed on the Long Island Expressway, which has three lanes; this information is provided in Figure 5.1. The headway of the third lane is the most uniformly distributed. The headway of the second lane is a little more scattered than the

headway of the third lane (0.5~0.9 s), and the first lane has a more scattered distribution than that of either of the other two lanes (0.5~12 s). Few vehicles have a headway of less than 1.0 s. If the headway is 1.0 s, a vehicle driving at 95 km/h would have a 26 m gap between its front bumper and the next car's rear bumper.

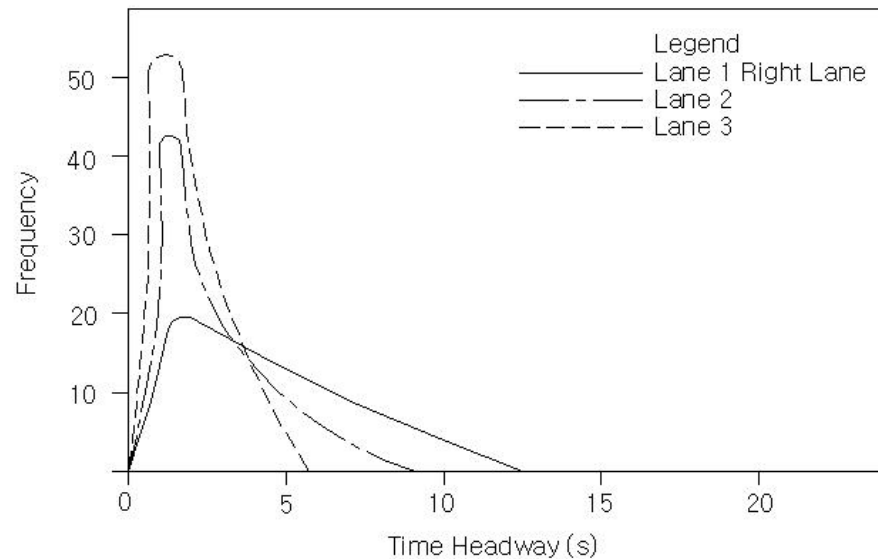


Figure 5.1 Headway for each lane (Highway Capacity Manual (2000))

Mean reaction time

The reaction time is the physical response to an unexpected condition, which is an important safety factor. A driver reacts in the following sequence of events: perception or detection, identification, emotion, and reaction. These events account for the time that a driver takes to recognize an unexpected situation and determine and enact the appropriate behavior. Reaction time is shorter when a vehicle's speed is high, because the driver is more alert and thus concentrates more on traffic situations

at increased speeds. At high speeds, one has less time to react to an unexpected situation.

Koppa et al. (1996) performed a reaction time test with expected and surprise conditions. The reaction time under surprise conditions was determined by suddenly moving a barrel onto the road from a hidden area and measuring the time the driver took to brake. Under expected conditions, the reaction time was measured from the time it took a driver to brake after seeing a LED illuminate. The result is that the driver's reaction time was shorter for the expected condition than for the surprise condition. Table 5.1 shows driver Perception Reaction Time (PRT).

Table 5.1 Perception Reaction Time comparisons (Koppa et al. (1996))

Condition	Car	Number	Mean	STD	25th	95th	99th
Expected	TTI	38	0.60	0.18	0.42	1.05	1.22
Surprise	TTI	38	0.82	0.18	0.64	1.23	1.39
Expected	Own	12	0.62	0.21	0.29	1.36	1.63
Surprise	Own	10	1.04	0.27	0.64	1.83	2.12
On Road	Own	11	1.10	0.21	0.80	1.69	1.91

Rodger J. Koppa, Daniel B. Fambro, and Richard A. Zimmer, Measuring Driver Performance in Braking Maneuvers, TRB 1550.

Green (2000) also performed a brake reaction time study for three different situations: expected, unexpected, and surprise events. The time taken by drivers made aware of the signal to apply the brakes was about 0.70 to 0.75 sec. For unexpected stops, the time was about 1.25 s, and it took about 1.50 s for surprise events.

5.3 Data Collection and Extraction

5.3.1 Data Collection

The data for this calibration study was acquired from the Freeway Service Patrol study conducted by the University of California at Berkeley (Skabardonis et al. (1998)). The purpose of that project was to evaluate the effectiveness of the Freeway Service Patrol and reduce congestion-related delays. This delay pertained to the time needed to detect, respond to, and clear a road incident. The data was collected from February 16 to March 19, 1993 and from September 27 to October 29, 1993. The collection times for each day in the case of loop data were between 5:00 AM and 10:00 AM and between 2:00 PM and 8:00 PM. This data was classified as incident data, probe vehicle data, and loop data; this data is available from the website <http://ipa.eecs.berkeley.edu/~pettyk/FSP/>, which contains raw data as well as processed data.

The calibration study in this dissertation uses loop data to determine the values of key calibration values. The loop detectors sense each vehicle and calculate the number of vehicles, their occupancy, and their speeds. On the other hand, data collected by probe vehicles may contain errors: Because the drivers therein press a sequence of keys when they pass expected points along the roadway, the driver might accidentally press the wrong key or forget to press the keys at all. Basically, each loop detector obtains flow, speed, and occupancy data. This data is then recorded in an individual file.

The basic file name is shown in the following format.

{f, g, h}loopXX.{n, s}{s, c, o}Y

The “f” character means that there has been no fix applied, and the “g” means that the holes in the loop data were fixed; the “h” means that the holes were fixed and the consistency errors were corrected. “XX” is the number of each detector. For example, if the file name is gloop7, this means is that the loop data is from loop7 and that the holes have been corrected.

The terms {n, s} correspond to the direction, wherein an “n” indicates northbound and “s” indicates southbound detectors. The next set of terms, {s, c, o}, indicates the type of data: The “s” character stands for speed, “c” stands for the counts or flow, and “o” stands for occupancy. Therefore, if the file name is “floop3.sc,” the file contains flow data from the southbound direction of loop number 3 and the data has not been fixed. We can determine the file type by its name.

The “Y” character is a number from 1 to 5 or the character “d.” The numbers indicate either a lane number or an on- or off-ramp. The “d” character stands for the average of all lanes.

5.3.2 Data Extraction

The program consists of fsp and xfsp. fsp is a software tool used to interrogate data collected during the Freeway Service Patrol evaluation project; this program performs diagnostics on the data, generates error reports, and makes plots of various pieces of data. The program takes as its input arguments a file that contains the commands that the fsp program needs to run. This fsp program takes as input a runfile, an incident filter file, various configuration files, and data. It generates various error reports, graphs, and tables as output (Petty (1995)).

The procedure of generating the fsp code and running it is as follows:

1. Download software.
2. Compile the program using the included makefile. (Set the location of the directory from Makefile.)
3. Install the configuration files using the included makefile.
4. Input data.
5. Make a runfile.
6. Make an incident filter.
7. Run the fsp program.

This fsp program was originally created for the Unix environment and allows users to modify the road environment by changing various options with a makefile. Linux is based on the Unix environment, and this program is also compatible with the Linux environment. Thus “Red Hat” (version 6.1), which is a Linux system, is used to run this fsp program. The downloaded files are in a compressed tar file; these files can be unpacked by using “uncompress” commands and should be set to the path of the directory from makefile, named “Makefile.”

The xfsp program is a GUI to the fsp program. It allows the user to generate the runfile and the incident filter that the fsp program requires by pointing and clicking on various buttons with the mouse (Petty (1995)). The lists of the xfsp program consist of Tcl7.3, Tk3.6, and Expect 5. These files must be compiled and installed. In addition, they must also be set to the location of the directory from makefile, named “Makefile.”

When the fsp program runs, it takes as one of its arguments the name of a file that is called the runfile. The runfile contains the commands that tell the program what to do: what data to analyze, what tests to run, what output to generate, etc. (Petty (1995)). The output contains speed and occupancy, and counts data in each direction (southbound and northbound). Each of the speed, occupancy, and counts outputs is produced every minute. By changing the “LOOP_OUTPUT_PERIOD” parameter, different time intervals for the output can be obtained.

Fsp program was run with data from September 30, 1993 (093093) and the northbound direction of the network. The network was created in the PARAMICS model according to the data from the Freeway Service Patrol study. The layout of that study section is shown in Figure 5.2. The infrastructure includes six traffic zones, as well as lamps and loop detectors. The O-D demand matrix, based on the average value of traffic flow, is generated from the fsp program’s output; it is controlled by the API code when the PARAMICS simulation package runs. The PARAMICS programmer is used to get the optimal calibration results by changing the vehicle release rate. In the O-D demand matrix, the default value of the vehicle release rate is set to 5 min. This value is too large to achieve more accurate calibration results. Therefore, the vehicle release rate was set in the API to 1 min for the O-D demand matrix.

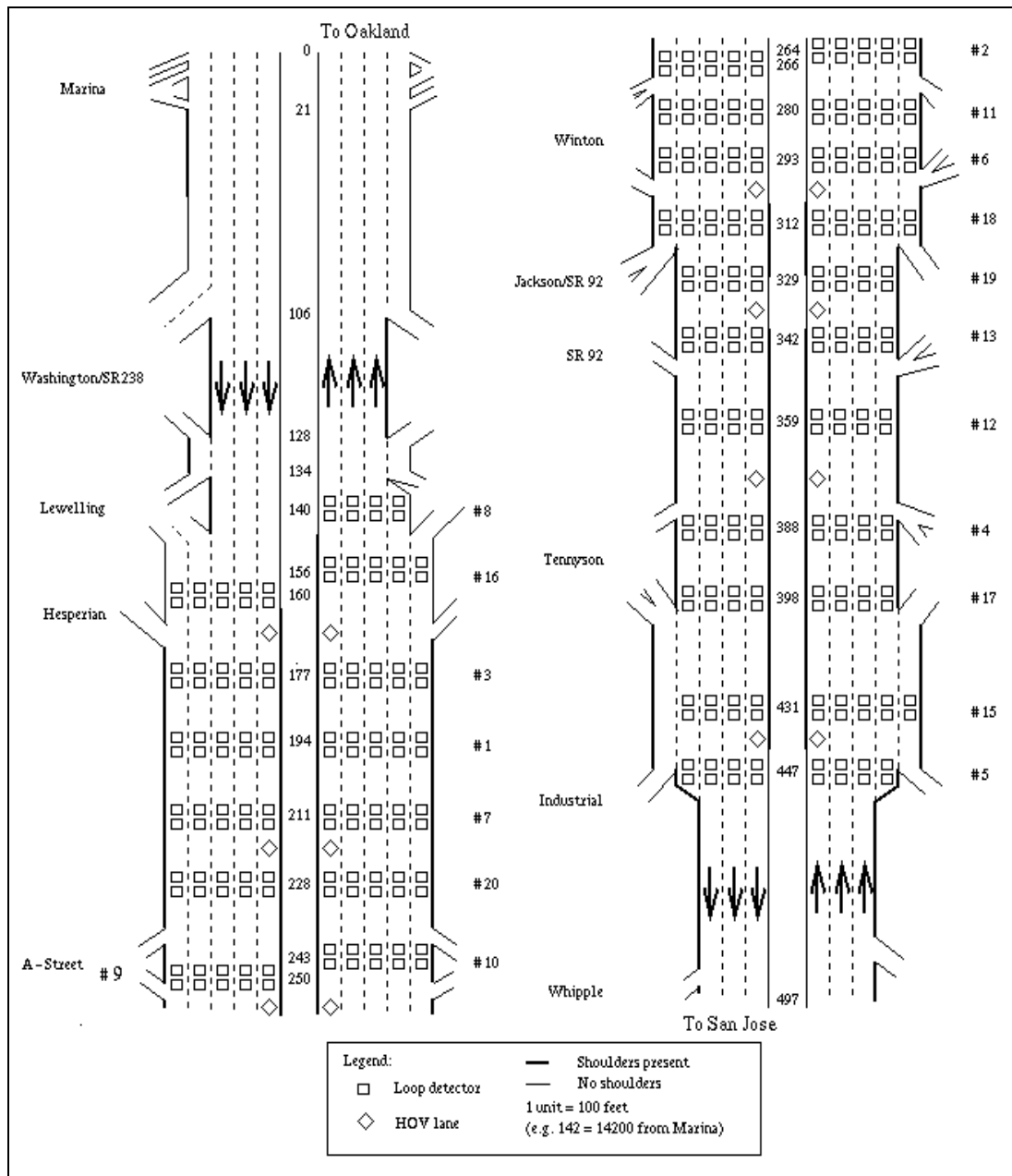


Figure 5.2 The Freeway Service Patrol study section (Petty (1995))

5.4 The PARAMICS Programmer API Code

PARAMICS Programmer is a framework that is used to customize many of the features of the underlying simulation model. Access is provided through a functional interface or API. The functional interface allows the user to develop

additional modules referred to as “plug-ins” (*PARAMICS Programmer User Guide* (2000)). The PARAMICS Programmer consists of C source files and is implemented from a “dll” file (dynamic linked libraries).

In our calibration study, one file called “plugin.c” is used, which is modified from the tutorial example file in the *PARAMICS Programmer User Guide* (2000). This plug-in uses the Programmer API to provide an interface for specifying vehicle release rates between O-D pairs. It uses the parameters file to specify the release rate for a given trip. The plug-in uses the name of the API coefficient variable to identify the trip, and the variable name has to be of the form “Trips Zone ‘O’ to Zone ‘D,’” where O is the origin zone and D is the destination zone. Once the rates are loaded, the plug-in then uses random numbers to release the vehicles at approximately the release rate specified (*PARAMICS Programmer User Guide* (2000)). (Appendix A)

5.5 Measures of Effectiveness for Calibration Study

For this dissertation, the relative error of flow and density are taken as the main measures of effectiveness and the minimum relative error, which optimize the mean headway and the mean reaction time, are used as the objective function for the calibration study. Every 3 min, the average values of flow and density are applied for more accurate comparisons.

The objective function takes the following form:

$$F = \sum_{INTERVAL} \sum_{DETECTOR} \sum_{LANE} \left(\frac{\|K_{real} - K_{sim}\|}{K_{real}} + \frac{\|Q_{real} - Q_{sim}\|}{Q_{real}} \right), \quad [5.1]$$

where

K_{real} : Density for each lane and each detector on the freeway during each time interval (veh/mile)

K_{sim} : Density for each lane and each detector in simulation during each time interval (veh/mile)

Q_{real} : Flow for each lane and each detector on the freeway during each time interval (veh/h/ln)

Q_{sim} : Flow for each lane and each detector in simulation during each time interval (veh/h/ln)

5.6 Calibration Process (Under-Congested Traffic Flow Condition)

5.6.1 Calibration of Headway and Reaction Time

The difference between the density and the flow obtained from the Freeway Service Patrol real-world data and the PARAMICS simulation results are used as input for the objective function that is to be minimized. Thus, the main objective is to search for the values of the key parameters that minimize the relative error between real-world data and the PARAMICS simulation model. The key parameters selected for this calibration study were mean headway and mean reaction time. The data for this study were selected from the morning peak data of September 30, 1993, which was collected at one-minute intervals; it includes flow in vehicles per hour, speed in miles per hour, and density in vehicles per mile.

Table 5.2 Average flow, speed, and density of morning peak data (three-minute intervals)

Time	Flow (Veh/hr)	Speed (mile/hr)	Density (veh/mile)
09:03	1,147	60.43	18.86
09:06	1,190	60.58	19.58
09:09	1,230	61.12	20.16
09:12	1,123	59.77	18.74
09:15	1,167	60.52	19.19
09:18	1,110	61.19	18.07
09:21	1,157	60.78	18.90
09:24	1,277	59.63	21.23
09:27	1,167	59.60	19.48
09:30	1,010	61.48	16.44
09:33	1,057	59.83	17.59
09:36	1,117	60.43	18.44
09:39	1,223	58.57	20.83
09:42	1,103	59.10	18.60
09:45	1,120	60.63	18.33
09:48	1,170	60.16	19.39
09:51	1,273	61.12	20.77
09:54	1,113	60.57	18.28
09:57	1,197	59.77	19.97
10:00	975	60.88	15.95

The simulation was run for one hour, from 9:00 AM to 10:00 AM. The reason for using one hour of data is that the total flow follows a similar trend for the same time period across various days. An ANOVA test was performed to test whether this one day's worth of data is representative of all other data collection periods of other days. The mean flow and mean density data for seven randomly selected different days were compared. The F-values for the ANOVA test for mean flow and mean density were 1.16 and 1.33, respectively. These values were lower than the F critical

value, which was 2.12 at the 95 percent confidence level and 2.85 at the 99 percent confidence level. This means the flow and density data of September 30, 1993 can be assumed to represent all other days.

The initial points of the two variables (x_1, x_2) , where x_1 is the mean headway and x_2 is the mean reaction time, were set to (1.00, 1.00), respectively. The sum of the relative errors of the flow and the density were used to generate new values of θ for the SPSA algorithm every 3 min. To prevent very high or very low values for the mean headway or mean reaction time in the SPSA algorithm, we limit the mean headway to between 0.2 and 2.5, and mean reaction time of between 0.2 and 2.0 s.

Optimization of the objective function using the SPSA algorithm:

$$\text{Minimize } F = \sum_{INTERVAL} \sum_{DETECTOR} \sum_{LANE} \frac{\|K_{real} - K_{sim}\|}{K_{real}} + \frac{\|Q_{real} - Q_{sim}\|}{Q_{real}} \quad [5.2]$$

Constraints:

- 1) Mean headway: $0.2 < x_1 < 2.5$
- 2) Mean reaction time: $0.2 < x_2 < 2.0$

Table 5.3 Relative errors, depending on mean headway and mean reaction time

Mean headway	Mean reaction time	Loss function		Relative error
		$\hat{L}(\theta + c_k \Delta_k)$	$\hat{L}(\theta - c_k \Delta_k)$	
1.00	1.00	24.74	27.83	-3.09
1.62	0.38	24.96	23.89	1.07
1.77	0.23	28.49	24.85	3.64

1.35	0.65	26.93	25.76	1.17
1.23	0.54	25.26	26.29	-1.03
1.14	0.63	24.97	26.82	-1.85
1.29	0.48	23.55	24.49	-0.94
1.22	0.41	24.80	25.83	-1.03
1.29	0.33	26.54	24.48	2.06
1.43	0.20	25.99	24.34	1.65
1.33	0.30	25.80	24.93	0.87
1.27	0.25	24.56	25.57	-1.01
1.22	0.20	25.70	25.05	0.65

5.6.2 The SPSA Iteration Process (Spall (2003))

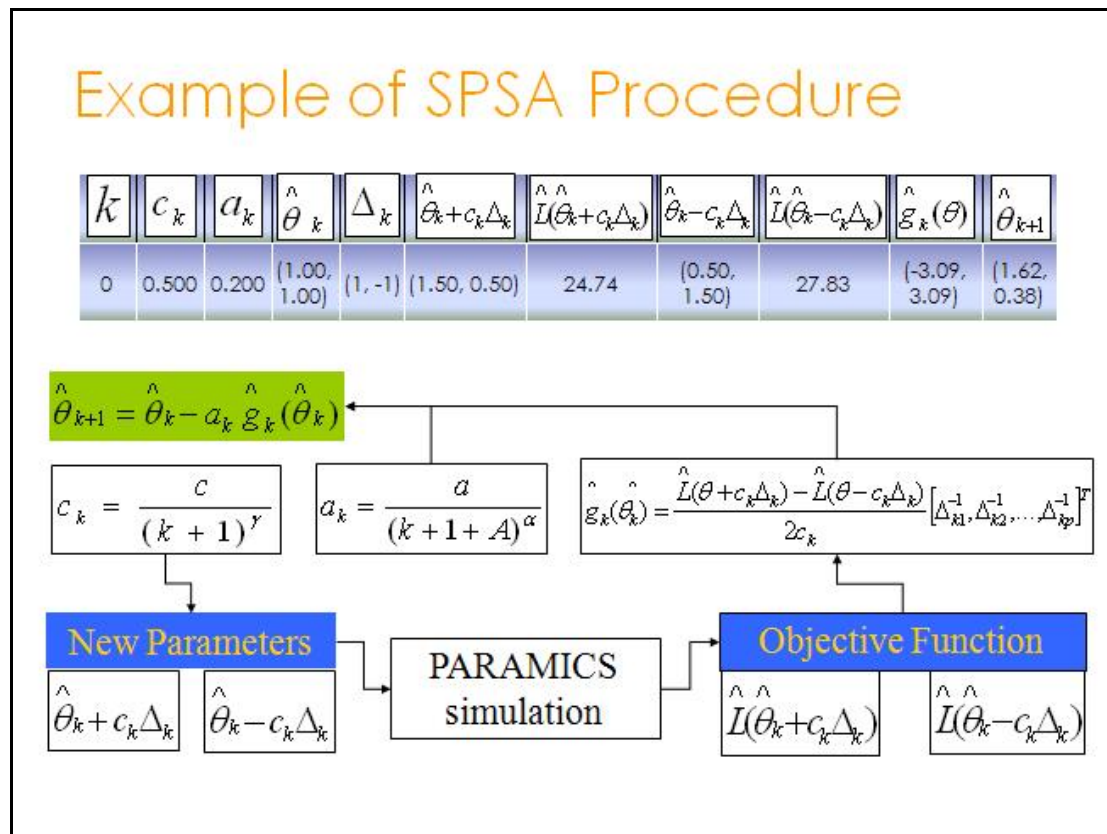


Figure 5.3 The example of the SPSA algorithm procedure

Step 0: Initialization and coefficient selection

Set counter index to $k=0$. The initial point $\hat{\theta}_0$ is (1.00, 1.00) and nonnegative coefficients a , c , A , α , and γ in the gain sequence a_k and c_k are determined; these sequences are set to:

$$a_k = \frac{0.2}{(k+1)^{0.602}}, \quad c_k = \frac{0.5}{(k+1)^{0.100}}$$

Step 1: Generation of the SP vector and run the simulation with updated parameters

Generate a p -dimensional random perturbation vector Δ_k ; this vector uses a Bernoulli ± 1 distribution. The updated parameters are acquired from $\theta + c_k \Delta_k$ and $\theta - c_k \Delta_k$.

Step 2: Loss function evaluations

Evaluate the loss function; the values of c_k , Δ_k for loss function $\hat{L}(\theta + c_k \Delta_k)$ and $\hat{L}(\theta - c_k \Delta_k)$ are obtained from steps 0 and 1.

The PARAMICS simulation is performed, based on the new mean target headway and mean reaction time calculated from $\theta + c_k \Delta_k$ and $\theta - c_k \Delta_k$, respectively. The simulation results are compared with the observed data, based on loss function.

Step 3: Gradient approximation

Based on calculated two loss functions $\hat{L}(\theta + c_k \Delta_k)$ and $\hat{L}(\theta - c_k \Delta_k)$, the gradient approximation $\hat{g}_k(\hat{\theta}_k)$ from equation [3.2] is obtained and then used to generate the SP for the gradient approximation $\hat{g}_k(\hat{\theta}_k)$.

Step 4: Update θ estimate

Update $\hat{\theta}_k$ to new value $\hat{\theta}_{k+1}$, using the standard SA form.

$$\hat{\theta}_{k+1} = \hat{\theta}_k - a_k \hat{g}_k(\hat{\theta}_k)$$

Step 5: Iteration or termination

After the new value $\hat{\theta}_{k+1}$ is updated, return to step 1 with the updated $\hat{\theta}_{k+1}$ instead of $\hat{\theta}_k$.

Terminate the algorithm if the fluctuation is smaller than the change in successive iterations, or if it is lower than the first set number. $\hat{\theta}_k$ of the last iteration is the optimal value θ^* .

5.6.3 Results of the Calibration Study

The iteration process terminates at the point $\hat{\theta}_k$ (1.22, 0.20), which is lower than the initial gradient approximation $\hat{g}_k(\hat{\theta}_k)$, which was (-0.84, 0.84). The results of this calibration study are summarized in Table 5.4. The points of the two variables converge into one point where there is only a small difference between real-world

data and the PARAMICS simulation results. The difference between the two values decreased from (4.07, -4.07) when $k=2$, to (-0.84, 0.84) when $k=12$.

Figure 5.4 shows the movement of the objective function, based on the updated parameters. The sum of the relative error reduces from 25.02 when the mean target headway and mean reaction time is 1.62 and 0.38, respectively, to 23.29 when the updated parameters are 1.22 and 0.20, respectively. The error is not greatly reduced. The reason for the small reduction is that the flow number is low, so flow is not sensitively affected by mean target headway or mean reaction time. However, if the volume reaches or exceeds the capacity, the error is predicted to decrease in a more sensitive manner.

Table 5.4 The result of calibration study

k	c_k	a_k	$\hat{\theta}_k$	Δ_k	$\hat{\theta}_k + c_k \Delta_k$	$\hat{L}(\hat{\theta}_k + c_k \Delta_k)$	$\hat{\theta}_k - c_k \Delta_k$	$\hat{L}(\hat{\theta}_k - c_k \Delta_k)$	$\hat{g}_k(\theta)$	$\hat{\theta}_{k+1}$
0	0.500	0.200	(1.00, 1.00)	(1, -1)	(1.50, 0.50)	24.74	(0.50, 1.50)	27.83	(-3.09, 3.09)	(1.62, 0.38)
1	0.467	0.132	(1.62, 0.38)	(-1, 1)	(1.15, 0.85)	24.96	(2.08, 0.20)	23.89	(-1.15, 1.15)	(1.77, 0.23)
2	0.448	0.103	(1.77, 0.23)	(1, -1)	(2.22, 0.20)	28.49	(1.32, 0.68)	24.85	(4.07, -4.07)	(1.35, 0.65)
3	0.435	0.087	(1.35, 0.65)	(1, 1)	(1.78, 1.09)	26.93	(0.91, 0.22)	25.76	(1.33, 1.33)	(1.23, 0.54)
4	0.426	0.076	(1.23, 0.54)	(-1, 1)	(0.81, 0.96)	25.26	(1.66, 0.20)	26.29	(1.21, -1.21)	(1.14, 0.63)
5	0.418	0.068	(1.14, 0.63)	(1, -1)	(1.56, 0.21)	24.97	(0.72, 1.05)	26.82	(-2.20, 2.20)	(1.29, 0.48)
6	0.412	0.062	(1.29, 0.48)	(-1, -1)	(0.88, 0.20)	23.55	(1.70, 0.89)	24.49	(1.14, 1.14)	(1.22, 0.41)
7	0.406	0.057	(1.22, 0.41)	(1, -1)	(1.63, 0.20)	24.80	(0.81, 0.81)	25.83	(-1.27, 1.27)	(1.29, 0.33)
8	0.401	0.053	(1.29, 0.33)	(-1, 1)	(0.89, 0.74)	26.54	(1.69, 0.20)	24.48	(-2.57, 2.57)	(1.43, 0.20)
9	0.397	0.050	(1.43, 0.20)	(1, -1)	(1.83, 0.20)	25.99	(1.03, 0.60)	24.34	(2.08, -2.08)	(1.33, 0.30)
10	0.393	0.047	(1.33, 0.30)	(1, 1)	(1.72, 0.70)	25.80	(0.93, 0.20)	24.93	(1.11, 1.11)	(1.27, 0.25)
11	0.390	0.045	(1.27, 0.25)	(-1, -1)	(0.88, 0.20)	24.56	(1.66, 0.64)	25.57	(1.28, 1.28)	(1.22, 0.20)

			0.25)	1)				1.28)	0.20)
12	0.387	0.043	(1.22,	(-1,	(0.83, 0.59)	25.70	(1.60, 0.20)	25.05	(-0.84,
			0.20)	1)					0.84)

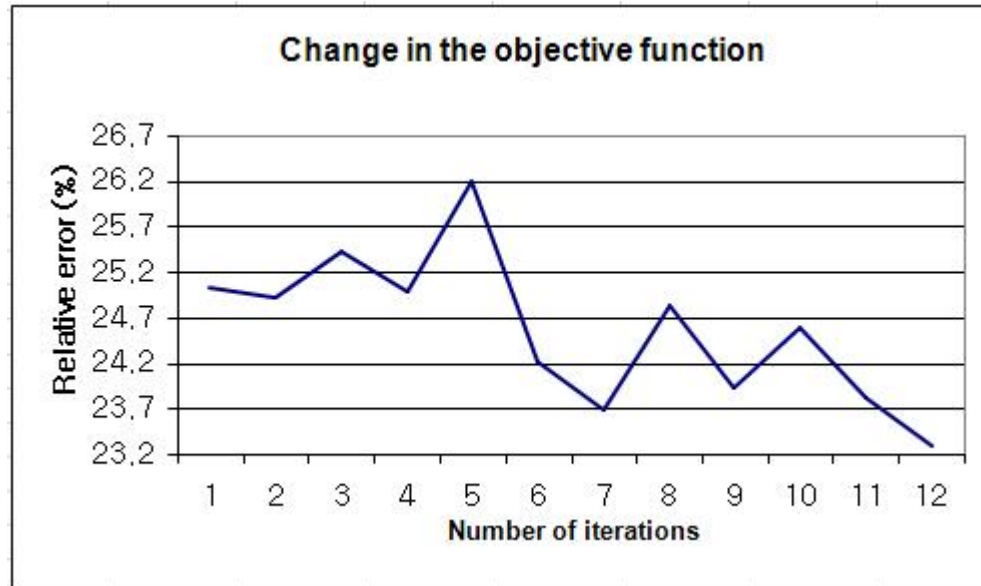


Figure 5.4 Change in the objective function (equation 5.1)

5.6.4 Goodness-of-Fit Test

Field data

The loop data from the Freeway Service Patrol network provides only flow, density, and occupancy data. However, because the loop detector does not give headway times for individual vehicles, it is extrapolated from flow data for each second. 1 s is the minimum interval that can be obtained from the detector readings; hence, the headway values are also integers, and more concentrated between 1.0 and 2.0 s. This field data follows a lognormal distribution.

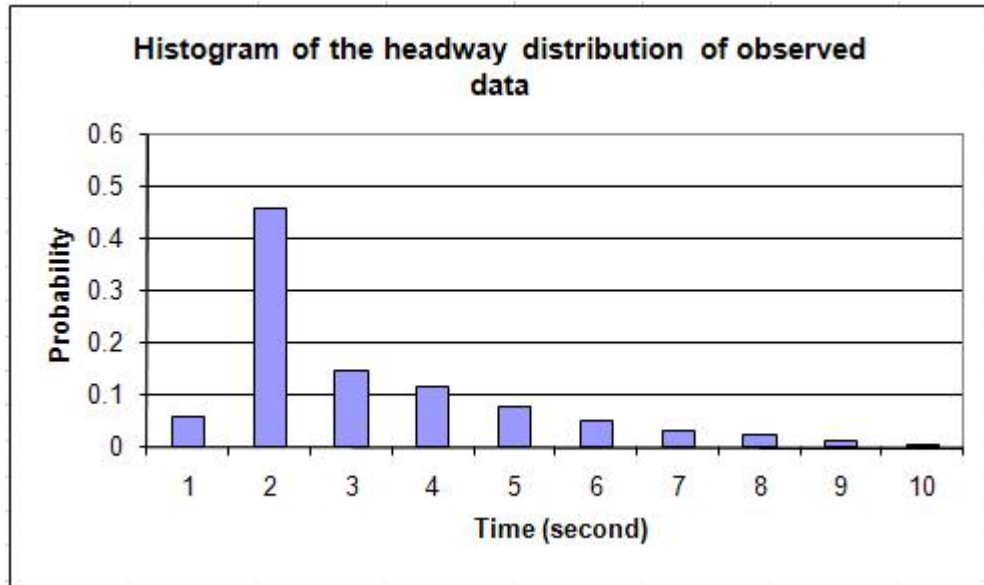


Figure 5.5 Histogram of the headway distribution of the observed data (Freeway Service Patrol (1995))

Simulation data

After basic models of the I-880 freeway in California were built in PARAMICS, calibration was performed for two key parameters namely, mean target headway and mean reaction time—which are very significant in controlling vehicle movements such as acceleration/deceleration, lane-changing, and acceptance gap. The headways of individual vehicles, based on the calibration study of mean target headway and mean reaction time, were collected from the PARAMICS simulation; headway was distributed between 1.1 and 2.1 s. This simulation data is observed to follow a lognormal distribution shown in Figure 5.6.

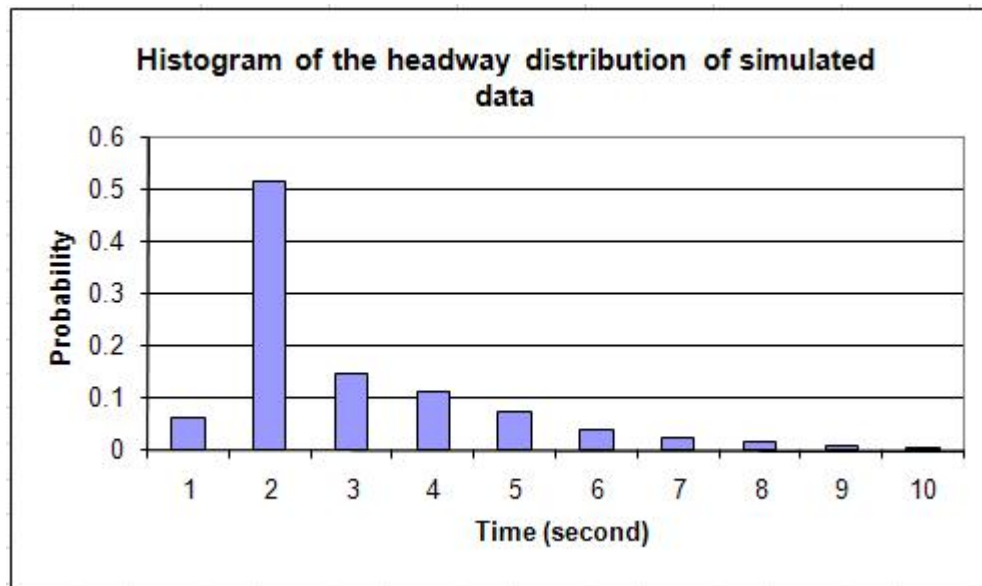


Figure 5.6 Histogram of the headway distribution of the simulated data
(PARAMICS)

Chi-square test

A chi-square test was performed on the headway distribution, as it is the most commonly used method for testing level of significance (Smith et al. (1994)). A chi-square test is used when a random variable is nonnegative and the distribution is skewed to the right (Montgomery and Runger (2005)). The best fit for the headway distribution from the observed data and the PARAMICS simulation is when the mean target headway and mean reaction are 1.22 s and 0.2 s, respectively. The null hypothesis assumes that the headway distribution from the simulation is equal to the actual headway distribution. The chi-square values from the chi-square distribution table (Montgomery and Runger (2005)) where $\chi^2=21.666$ at the 99 percent confidence level are greater than the chi-square value of the two independent samples, which is 20.639. Thus, the null hypothesis is accepted. Even if the χ^2 value is very close to the

critical region, the result of the simulation is significant. Table 5.5 shows the results of the chi-square test.

Table 5.5 Results of the chi-square test for goodness-of-fit

Interval	Frequency (FSP)	Interval	Frequency (Sim)	χ^2
1	84	1.1	86	0.048
2	631	2.1	702	7.989
3	202	3.1	200	0.020
4	160	4.1	154	0.225
5	107	5.1	99	0.598
6	69	6.1	52	4.188
7	43	7.1	34	1.884
8	32	8.1	22	3.125
9	16	9.1	11	1.563
10	9	10.1	6	1.000
		Table	21.666	20.639

5.6.5 Sensitivity Analysis

A sensitivity analysis was also performed by varying the mean target headway; this was done by making changes to flow and density. By increasing or decreasing mean target headway every 0.1 s, the flow and density values were compared. When mean target headway was increased by 0.1 s from the optimized headway of 1.22 s, the total discrepancy of flow and density increases from 5.28 to 6.11. If the mean target headway decreases by 0.1 s, the total discrepancy of flow and density increases to 5.58. As a result, with either an increase or a decrease to mean target headway, the total discrepancy will be greater than the optimal value. Figures

5.7 and 5.8 show the sensitivity analysis of the mean target headway, based on flow and density.

The sensitivity analysis was performed, based on upper and lower bounds for the parameter values. The parameter constraints limited the mean target headway to between 0.2 and 2.5 s, and the mean reaction time to between 0.2 and 2.0 s. For four different cases—(2.5, 2.0), (2.5, 0.2), (0.2, 2.0), and (0.2, 0.2)—calibrations were carried out. Figure 5.9 shows the values of flow and density with extreme parameters.

Table 5.6 Sensitivity analysis depending on the headway

	Headway, reaction time	Flow	Density	Sum
Initial value	1.00, 1.00	2.96	2.93	5.89
0.2 sec. Decrease	1.02, 0.20	2.50	2.92	5.42
0.1 sec. Decrease	1.12, 0.20	3.01	2.57	5.58
Optimized value	1.22, 0.20	2.60	2.68	5.28
0.1 sec. Increase	1.32, 0.20	3.11	3.00	6.11
0.2 sec. Increase	1.42, 0.20	3.23	2.90	6.13
	2.50, 2.00	6.76	25.68	32.44
	2.50, 0.20	1.98	6.56	8.54
	0.20, 2.00	3.06	8.33	11.39
	0.20, 0.20	5.15	7.66	12.81

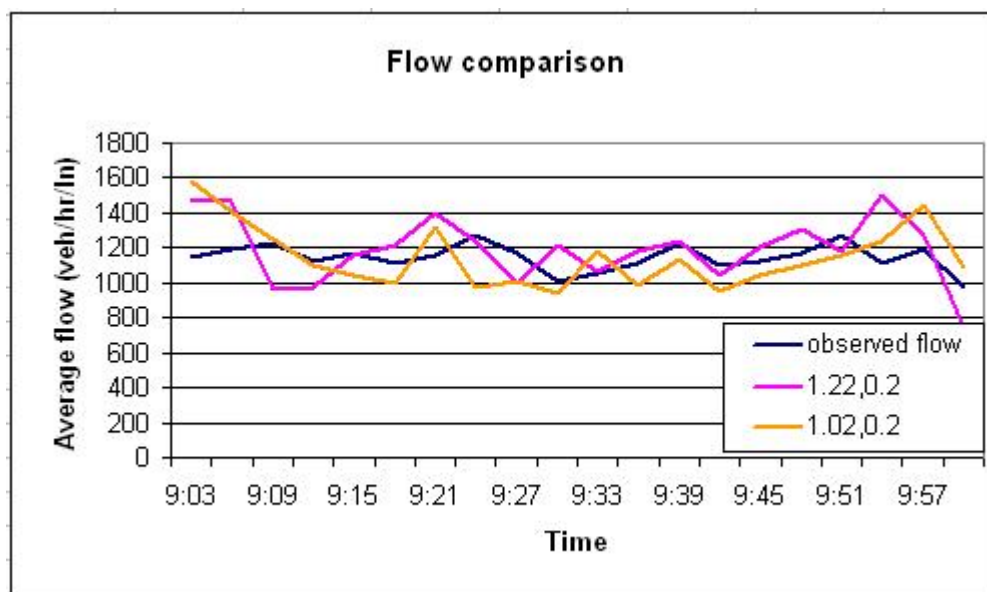


Figure 5.7 (a) Decreased mean target headway (0.2)

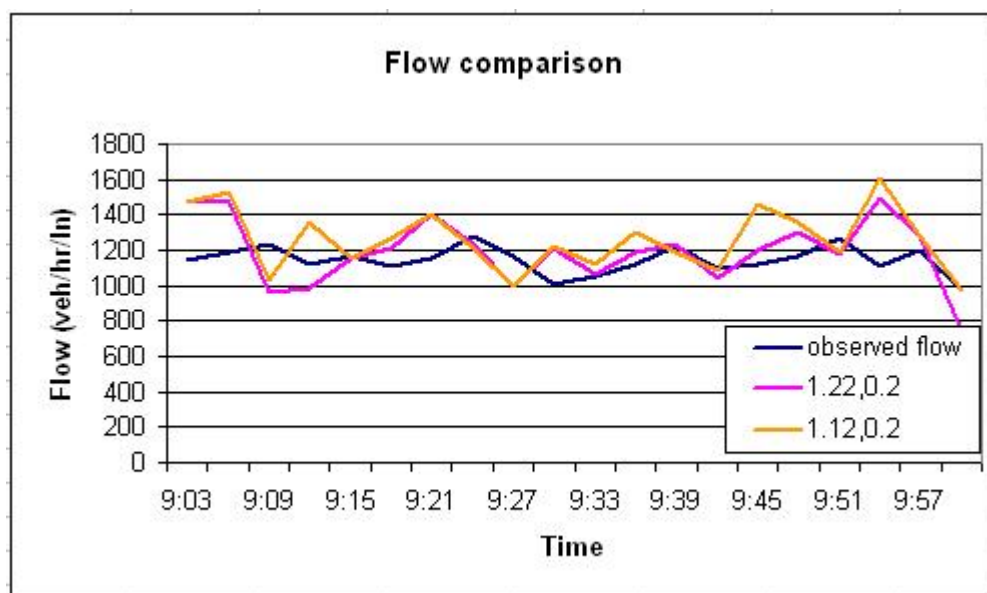


Figure 5.7 (b) Decreased mean target headway (0.1)

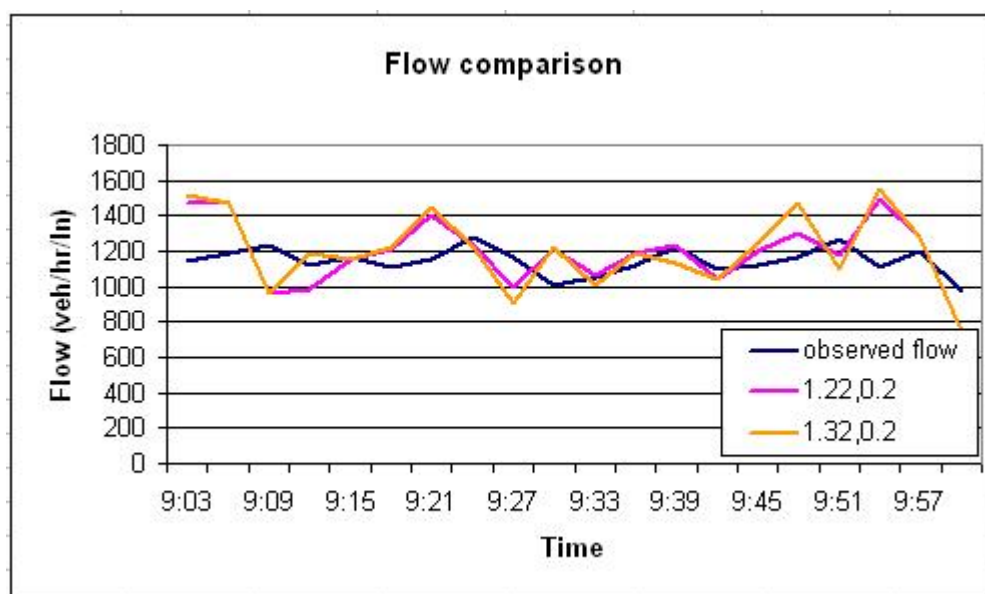


Figure 5.7 (c) Increased mean target headway (0.1)

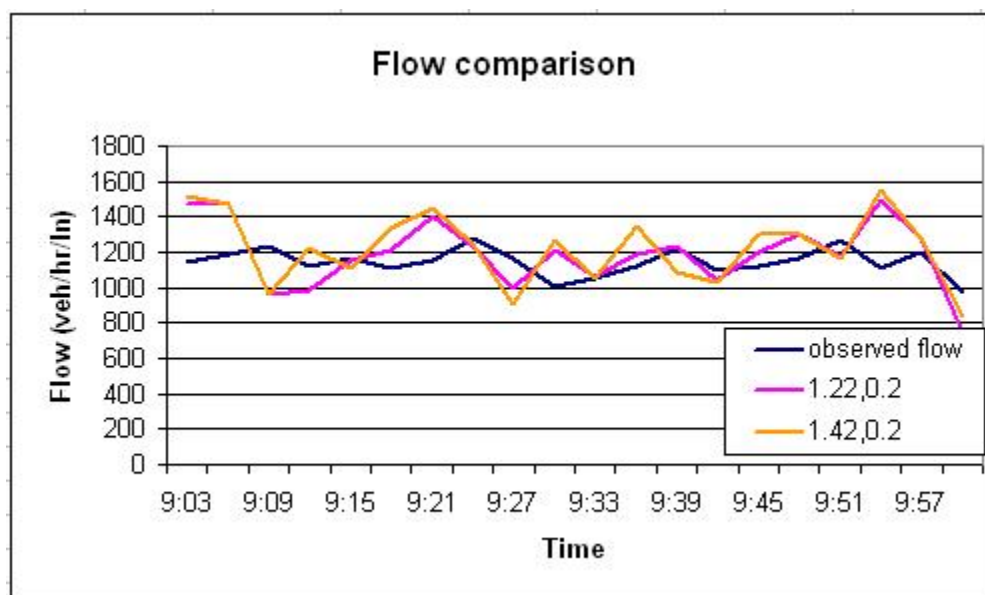


Figure 5.7 (d) Increased mean target headway (0.2)

Figure 5.7 Sensitivity analysis of mean target headway (flow comparison)

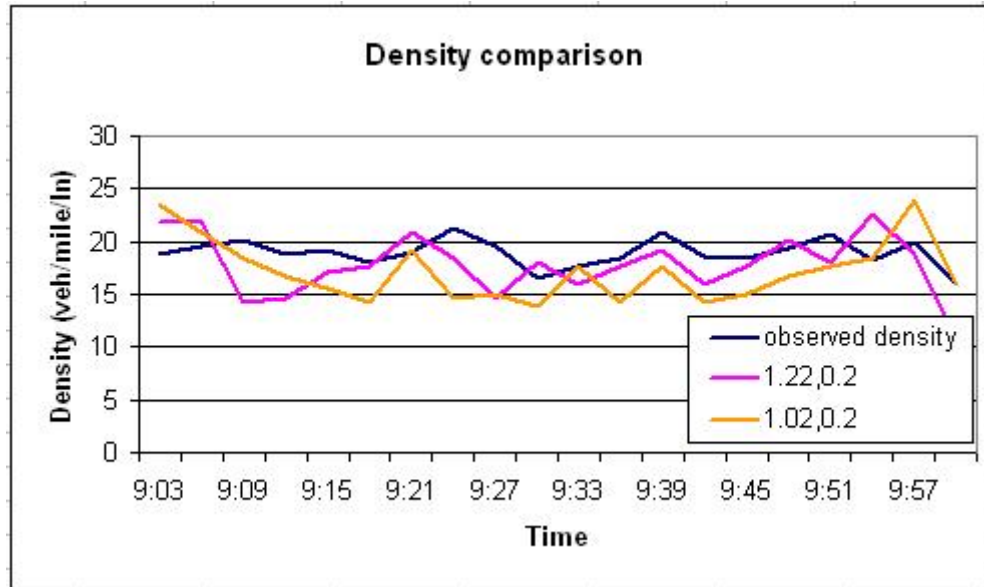


Figure 5.8 (a) Decreased mean target headway (0.2)

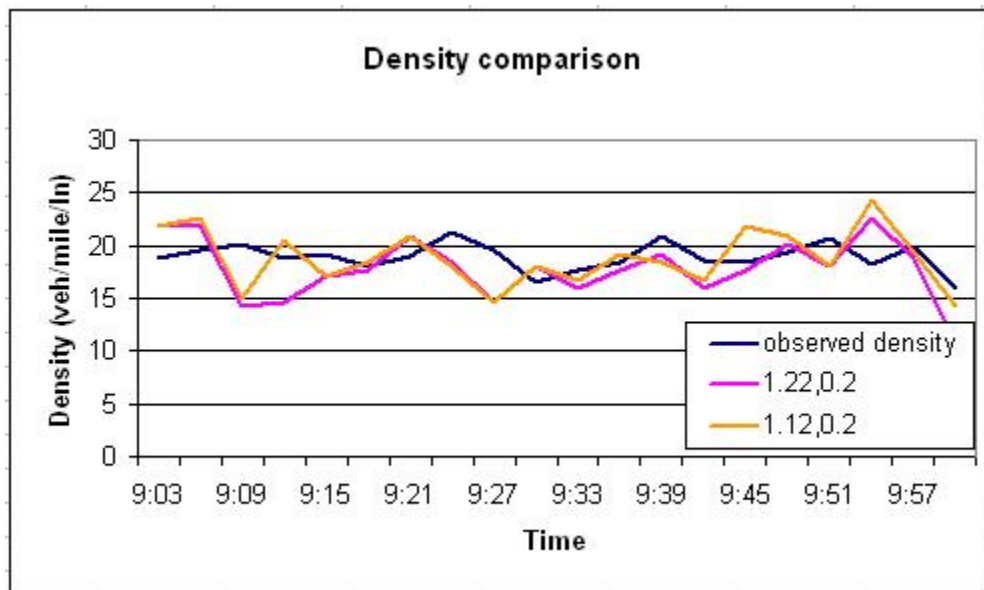


Figure 5.8 (b) Decreased mean target headway (0.1)

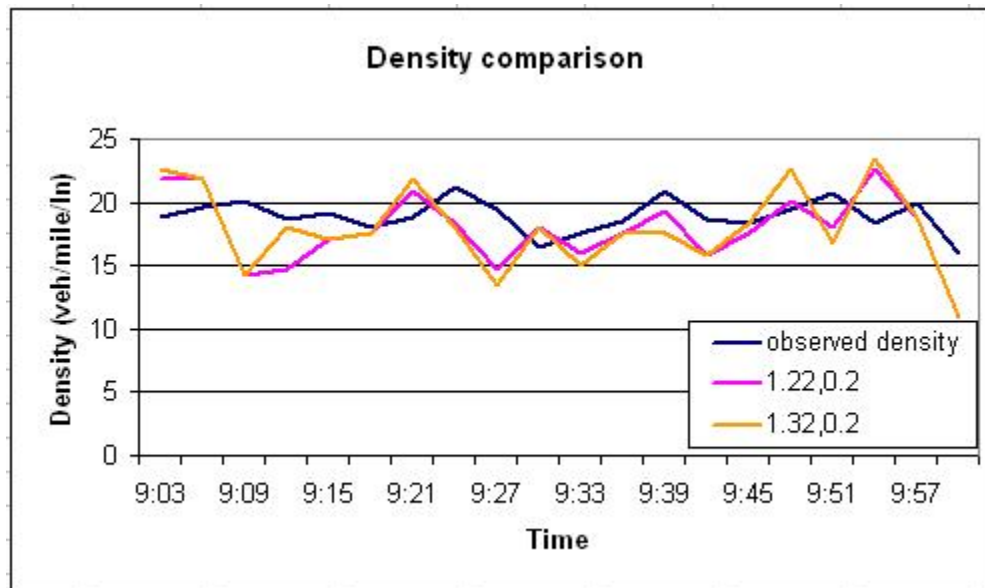


Figure 5.8 (c) Increased mean target headway (0.1)

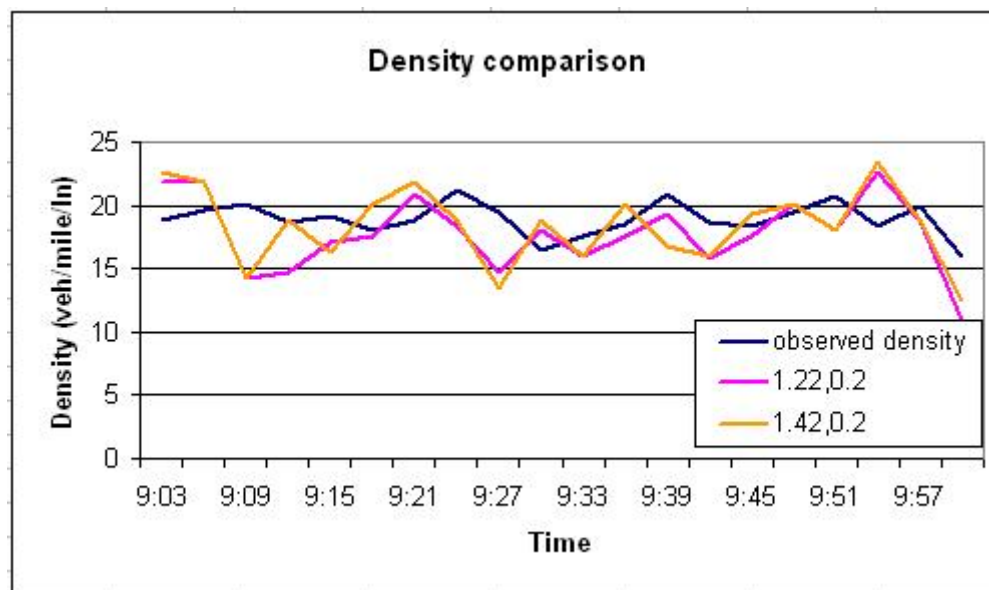


Figure 5.8 (d) Increased mean target headway (0.2)

Figure 5.8 Sensitivity analysis of mean target headway (density comparison)

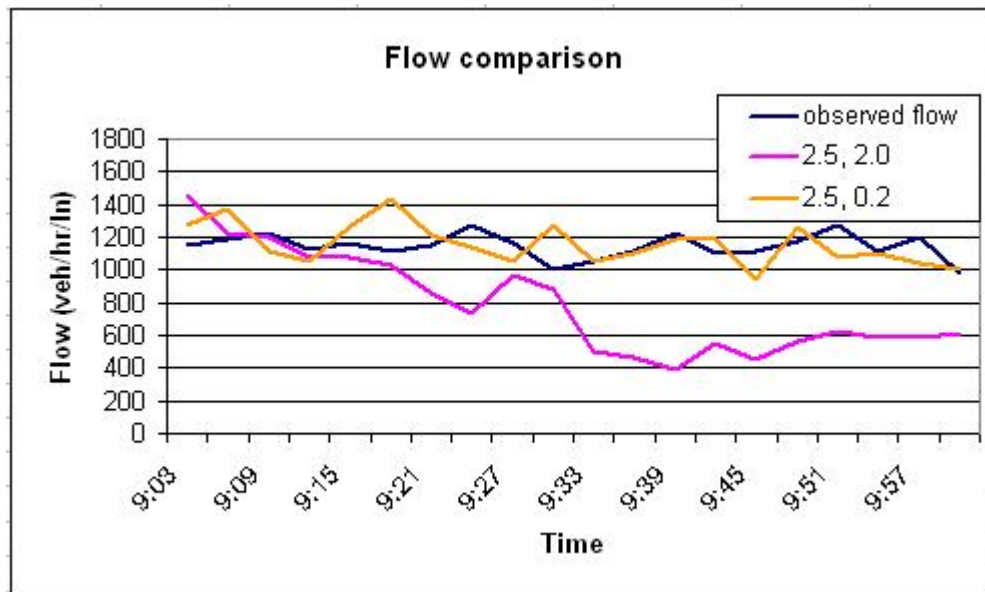


Figure 5.9 (a) Flow comparisons with upper and lower bounds of the parameters (2.5, 2.0), (2.5, 0.2)

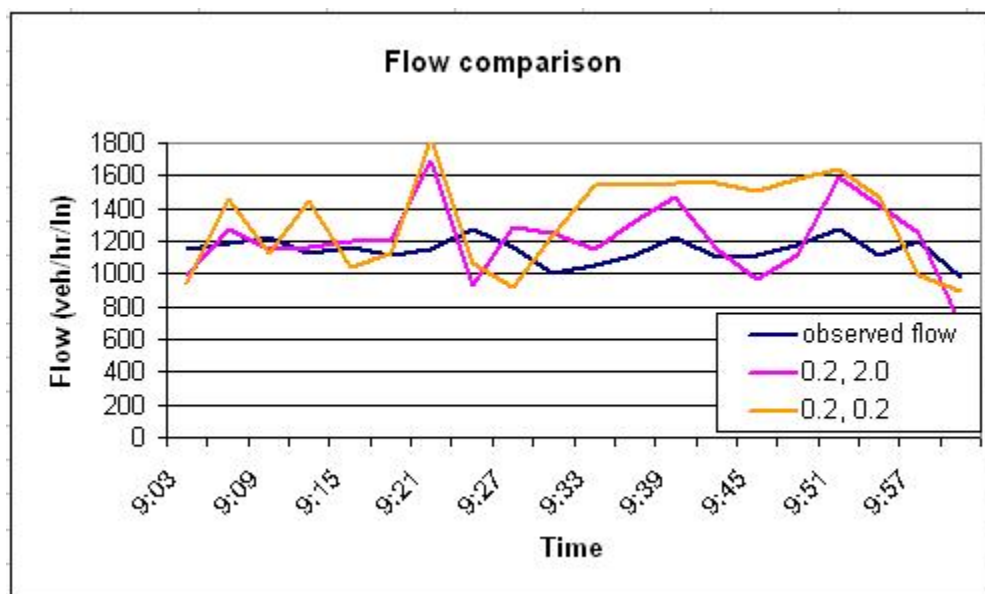


Figure 5.9 (b) Flow comparisons with upper and lower bounds of the parameters (0.2, 2.0), (0.2, 0.2)

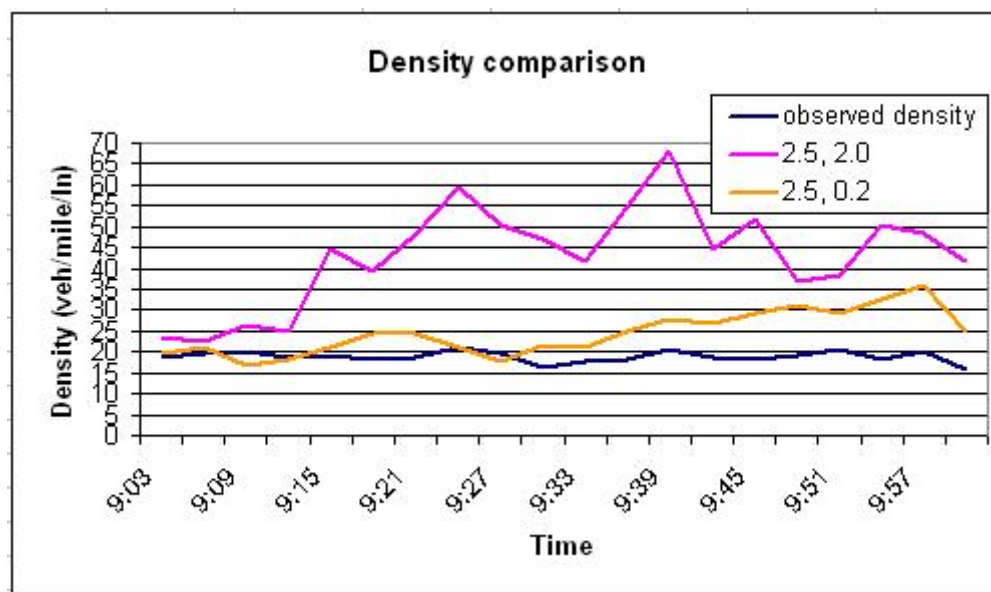


Figure 5.9 (c) Density comparisons with upper and lower bounds of the parameters
(2.5, 2.0), (2.5, 0.2)

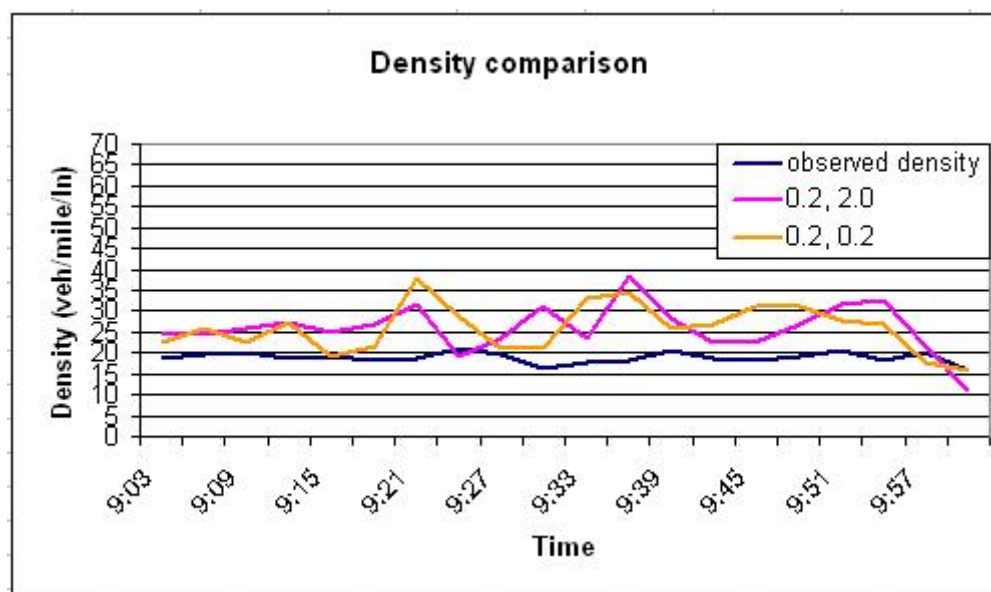


Figure 5.9 (d) Density comparisons with upper and lower bounds of the parameters
(0.2, 2.0), (0.2, 0.2)

Figure 5.9 Sensitivity analysis with upper and lower bounds of the parameters (flow and density comparison)

In addition to the above test, a significance test was carried out for the headway distribution, for each value of the mean target headway. All other values were kept at a constant value. By changing the mean target headway by 0.1 s, the chi-square test was performed. From Table 5.7, it is seen that the χ^2 value is lowest for a mean target headway of 1.22 s. In contrast, the χ^2 values for other values of mean target headway are more than the chi-square values from the chi-square distribution table (Montgomery and Runger (2005)) for the 99 percent confidence level. So, the null hypothesis is not rejected at the 99 percent confidence level, only when the mean target headway is 1.22 s.

As a result of the chi-square test of the observed and simulation headway values, the frequency fits only when the mean target headway is 1.22 s and other headways are rejected by the chi-square test. Thus, it is judged that the χ^2 value of 20.639 when the mean target headway is 1.22 s is statistically significant at the 99 percent confidence level.

Table 5.7 Chi-square test with different mean target headway values

Interval	FSP	(1.22, 0.2)		(1.02, 0.2)		(1.12, 0.2)		(1.32, 0.2)		(1.42, 0.2)	
	Frequency	Freq.	χ^2	Freq.	χ^2	Freq.	χ^2	Freq.	χ^2	Freq.	χ^2
1.1	84	86	0.05	357	887.25	184	119.05	62	5.76	28	37.33
2.1	631	702	7.99	403	82.38	596	1.94	730	15.53	775	32.86
3.1	202	200	0.02	202	0.00	206	0.08	207	0.12	221	1.79
4.1	160	154	0.23	162	0.03	148	0.90	152	0.40	127	6.81
5.1	107	99	0.60	102	0.23	100	0.46	95	1.35	85	4.52
6.1	69	52	4.19	53	3.71	49	5.80	52	4.19	52	4.19
7.1	43	34	1.88	38	0.58	34	1.88	29	4.56	32	2.81
8.1	32	22	3.13	25	1.53	26	1.13	22	3.13	24	2.00
9.1	16	11	1.56	10	2.25	13	0.56	14	0.25	10	2.25

10.1	9	6	1.00	10	0.11	9	0.00	7	0.44	6	1.00
		20.639		978.076		131.795		35.730		95.565	

5.6.6 Validation of the Calibrated PARAMICS Simulation Model

A validation process for the mean target headway and the mean reaction time, obtained through the SPSA algorithm, needs to be conducted to ensure that they are suitable for real-world conditions. A comparison between the PARAMICS simulation results and real-world data, using the new headway and reaction times, was carried out.

The PARAMICS model outputs the flow, density, and speed. Flow and density were used for the validation study. Figures 5.10 and 5.11 compare the simulation results with the real-world flow and density data gathered from the loop detectors on the freeway. The data was collected from 09:00 AM to 10:00 AM; for greater accuracy, we averaged the data every 3 min. The flow and density based on optimized parameters represent values similar to the real-world data from the loop detectors. The relative error in the calibration study is 5.28 percent, which is lower than the value of the relative error before the calibration (i.e., 5.89 percent). As mentioned above, the error reduction was not radical in this case; however, if the flow reaches or exceeds the capacity, the error is predicted to decrease in a more sensitive manner.

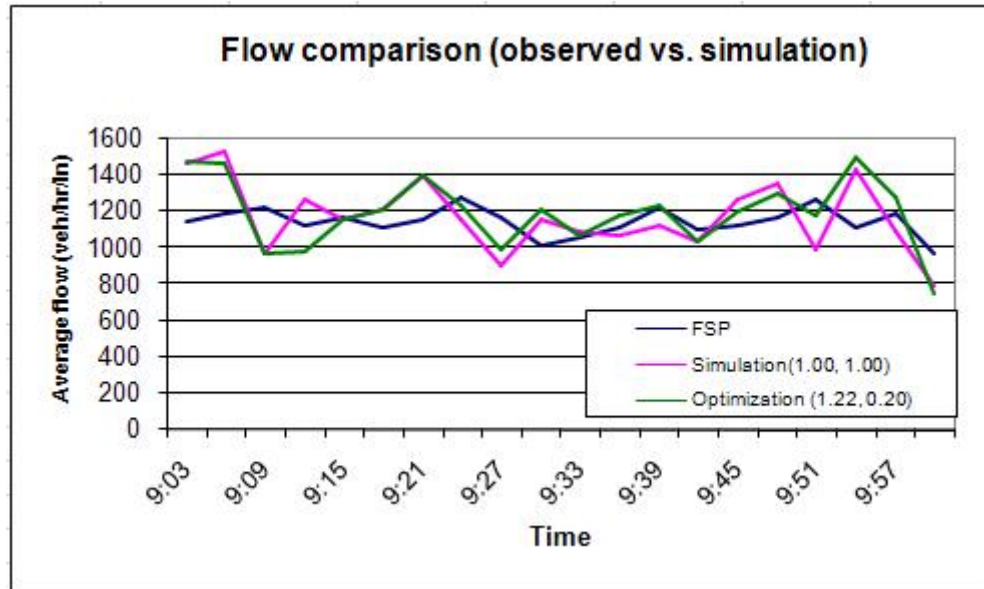


Figure 5.10 Flow comparison using the observed and simulated data

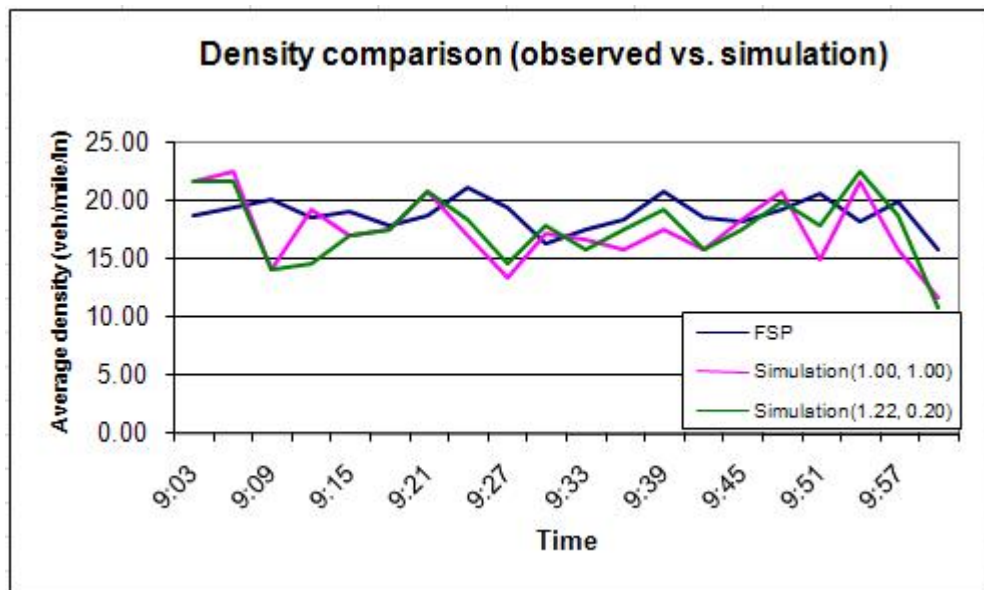


Figure 5.11 Density comparison using the observed and the simulated data

5.7 Simulation Results and Summary

Microscopic traffic simulation models are effective tools that can be used to model traffic operations on real-world traffic networks. To represent freeway traffic conditions more accurately, some of the important parameters of these tools need to be calibrated. The objective of this study was to propose an efficient methodology for calibrating microscopic simulation models. PARAMICS was chosen as the traffic simulation tool used in this study, due to its popularity among practitioners and researchers as well its well-documented capabilities; however, our expectation was to be able to use the proposed calibration methodology, irrespective of the specific simulation tool itself. Our calibration methodology is based on the SPSA algorithm proposed by Spall (1992). The main reason for using this algorithm is the fact that it has been shown to work well when applied to highly stochastic systems that are similar to the traffic models developed in PARAMICS. However, a comprehensive testing of its applicability to our problem is needed before it can be proposed as a useful algorithm for calibration. Also, our methodology calls for the careful selection of the variables to be calibrated; thus, this dissertation uses the SPSA algorithm only as an initial point for the larger problem of calibrating a complex traffic simulation model.

The calibration of PARAMICS was performed for particular parameters—namely, mean target headway and mean reaction time. The traffic conditions were found to be sensitive to the effects of these two parameters. Finding the optimal mean target headway and mean reaction time that minimize the relative error, between the real-world and simulated flow and density values, is accomplished using the SPSA

algorithm. Initially, headway and reaction time were set to 1.00 and 1.00, respectively, and the SPSA algorithm was used to update new headway and reaction times until a pre-determined convergence criterion was reached. When the gradient of the SPSA algorithm is less than 1.0, the iteration process terminates and it stops at the point $\hat{\theta}_k$ (1.22, 0.20). The difference between field data and the output of the PARAMICS simulation of flow and density with optimized mean target headway and mean reaction time was found to be 5.28 percent, which is lower than the value of relative error before the calibration (i.e., 5.89 percent). A sensitivity analysis of mean target headway was also carried out. Total relative error was calculated by varying mean target headway.

A chi-square test based on headway distribution was also performed. When a mean target headway of 1.22 s was used, the relative error was minimized; the chi-square value of 20.64 was also found to be significant, as it was lower than the value from the table, of $\chi^2_{k-1, 0.99}=21.666$.

However, the error reduction was not drastic in the test cases. It is hypothesized that this was mainly due to the fact that the flow-to-capacity ratio for the test cases undertaken thus far were low. Thus, flow is not affected very much by the mean target headway and mean reaction time at this relatively low v/c level.

Chapter 6

Calibration of a Macroscopic Traffic Simulation Model Using Enhanced SPSA Methodology

6.1 Introduction

This chapter presents an enhanced Simultaneous Perturbation Stochastic Approximation (E-SPSA) methodology to reflect the effect of the distribution of input data. Previous studies on calibration generally focused on minimizing the sum of the relative errors between the observed data from a certain period of time in a typical day and the simulation output for the same period. This static approach can be explained as calibration with data obtained at one point in time. However, this type of calibration approach cannot capture a realistic distribution of all possible traffic conditions and may produce inaccurate calibration results.

This dissertation proposes a calibration methodology based on the Bayesian sampling approach. Instead of a single demand matrix and corresponding observed traffic conditions representing a specific point in time, this calibration methodology uses randomly generated demand matrices and corresponding traffic conditions from an observed statistical distribution of these variables. The goal of using input values generated from an observed distribution of demands is to accurately represent a wide

range of all likely demand conditions observed at a facility. Moreover, at each iteration, the proposed calibration methodology reestimates optimal parameters by using a stochastic optimization algorithm known as the SPSA algorithm. A macroscopic simulation model of a portion of I-880 in California based on the cell transmission approach is calibrated with the proposed methodology. The proposed enhanced SPSA algorithm outperforms a simple SPSA algorithm based on several case scenarios studied as part of this dissertation.

6.2 Proposed Enhanced Methodology for Calibrating Cell Transmission Model (CTM)

Calibrating the parameters of a traffic simulation model can be formulated as an optimization problem in which the analytical form of the objective function is unknown. This simulation–optimization problem can be more formally stated as the minimization of the sum of measures of accuracy for various inputs to the simulation model. This function is calculated at the j^{th} iteration as shown in equation [6.1].

$$L(D_1^j, D_2^j, \dots, D_I^j, \Theta_1^j, \Theta_2^j, \dots, \Theta_I^j) = \sum_{i=1}^I \{g_1(Q_i^{Ob}, Q_i^S) + g_2(D_i^0, D_i^j) + g_3(\Theta_i^0, \Theta_i^j)\} \quad [6.1]$$

subject to constraints,

$$Q_k^S = A(D_1^j, D_2^j, \dots, D_k^j, \Theta_1^j, \Theta_2^j, \dots, \Theta_k^j) \text{ for } k \in (1, \dots, I)$$

$$\underline{\Theta}_i \leq \Gamma_i^j \leq \overline{\Theta}_i$$

where

D_i^j is the O-D demand vector for the i^{th} time interval,

D_i^0 is the starting O-D demand vector for the i^{th} time interval

Θ_i^j is the parameter vector for the i^{th} time interval,

Θ_i^0 is the starting parameter vector for the i^{th} time interval,

$\underline{\Theta}_i, \overline{\Theta}_i$ are the lower and upper bounds for the parameter vectors, respectively,

Q_i^{Ob} is the vector of the observed set of flows for the i^{th} time interval,

Q_i^S is the vector of the simulated set of flows for the i^{th} time interval,

$A(D_1^j, D_2^j, \dots, D_k^j, \Theta_1^j, \Theta_2^j, \dots, \Theta_k^j)$ is the autoregressive assignment matrix for the k^{th} period,

L is the objective function in the optimization process, and

g_1, g_2, g_3 are measures of accuracy for traffic flows, O-D demands, and the parameter set, respectively.

In addition to the objective function that does not have a closed-form representation, the calibration problem is a “stochastic optimization” problem. Variables of many traffic simulation models have a stochastic component to reflect random variations in real-world observations. Thus, the traffic simulation calibration problem has to be approached as a multivariable stochastic optimization problem that does not have a closed form of objective function.

The functional form of the objective function in stochastic approximation (SA) algorithms is probabilistic. Each algorithm can be divided into two general

categories: gradient and gradient-free settings. The stochastic root-finding algorithm by Robbins and Monro (1951) is generally used for nonlinear problems when the gradient function is available. SPSA, one of the well-known SA algorithms, can be applied in both stochastic gradient and gradient-free settings; it can also be applied to solve optimization problems that have a large number of variables.

In this dissertation, flows and densities were obtained with a macroscopic simulation model based on the CTM proposed by Daganzo (1994). Since the goal in this dissertation is to introduce a new calibration methodology, a well-accepted but easy-to-implement approach was chosen for the simulation component of the study. However, it is clear that the proposed calibration methodology can be implemented in conjunction with any other simulation tool. The CTM is a simple and accurate representation of traffic situations such as acceleration–deceleration, stop and go, and shockwaves. CTM limits the flow to the minimum value between the upstream capacity and downstream capacity of the cell (Daganzo (1994)). The maximum number of vehicles in the undercongested condition is the product of the jam density (K_j) and cell length at cell i , and the maximum number of vehicles in the overcongested condition is the capacity of the cell $i - 1$.

Previously, Munoz et al. (2004) calibrated a cell-transmission-based model of a portion of westbound I-210 in Southern California. Free-flow speed and congestion parameters were calibrated using a constrained least-square fit on the flow–density relationship.

The free-flow velocities v_i at the j^{th} detector:

$$\phi_j v_j = Y_j$$

where

$\phi_j = [\rho_{d_j}(k_{5:00}) \cdots \rho_{d_j}(k_{6:00})]^T$ is the measured densities, and

$Y_j = [q_{d_j}(k_{5:00}) \cdots q_{d_j}(k_{6:00})]^T$ indicates flows over the specified time interval

The equation for the congestion parameter:

$$\phi_j \begin{bmatrix} w_j \\ w_j \rho_{J,j} \end{bmatrix} = Y_j$$

where

$$\phi_j^T = \begin{bmatrix} -\rho_{d_j}(k_1) \cdots -\rho_{d_j}(k_{N_c}) \\ 1 \cdots \cdots \cdots 1 \end{bmatrix}, \text{ and}$$

$$Y_j = \begin{bmatrix} q_{d_j}(k_1) + \frac{l_j}{T_s} \Delta \rho_{d_j}(k_1) \\ \cdot \\ \cdot \\ q_{d_j}(k_{N_c}) + \frac{l_j}{T_s} \Delta \rho_{d_j}(k_{N_c}) \end{bmatrix}$$

The difference between the simulated and the observed total travel times (TTT) is the objective function used to evaluate the performance of the simulation.

$$TTT = T_s \sum_{k=k_{5:00}}^{k_{11:45}} \sum_{i \in C_d} l_i \rho_i(k)$$

Here, C_d indicates the set of cells.

However, this approach focused only on the deterministic aspects of the calibration problem.

Almasri and Friedrich (2005) performed a calibration study of a macroscopic model developed using a cell transmission model.

The difference between the simulated and the observed total delay was selected as the objective function to evaluate the performance of the simulation.

$$f = \min \sum_i \sum_j d_j(t)$$

where

f indicates the sum of delays.

They used genetic algorithm (GA) to solve optimization problem; it minimized the relative error between observed data and simulation output.

Park and Won (2006) used Latin Hypercube Design (LHD) algorithm to reduce the number of combinations of parameters. Even if more parameter sets provide more accurate simulation results, it takes a considerably high amount of time to run the simulation. Thus, Authors performed a calibration of microscopic and stochastic simulation models developed in VISSIM and CORSIM, based on LHD-based parameters. The result of the verification test showed that real-world conditions for other days can be fairly captured by the calibrated simulation model.

This dissertation proposes using the SPSA approach proposed by Spall (1992) in conjunction with a Bayesian sampling methodology. Figure 6.1 shows a flowchart of the proposed combined E-SPSA calibration and validation methodology.

The basic steps of the proposed methodology can be summarized as follows:

1. Increment iteration: $\text{iteration} = \text{iteration} + 1$

Iteration:

- a. Generate the O-D demand matrix from a probability distribution function of demands developed with real-world data by using the Bayesian sampling methodology (Gelman et al. (2004)).
 - b. Use the SPSA algorithm to determine the optimal parameters given the demand matrix generated.
2. Compare the output of simulation for the given demand matrix in the current iteration—namely, flows and densities—with the observed distribution of flows and densities to determine the correlation between the two distributions. If it is satisfactory, terminate the iterative process and proceed to the validation step. If unsatisfactory, return to Step 1.
 3. If verification and validation tests are satisfactory, then stop. If not, return to Step 1.

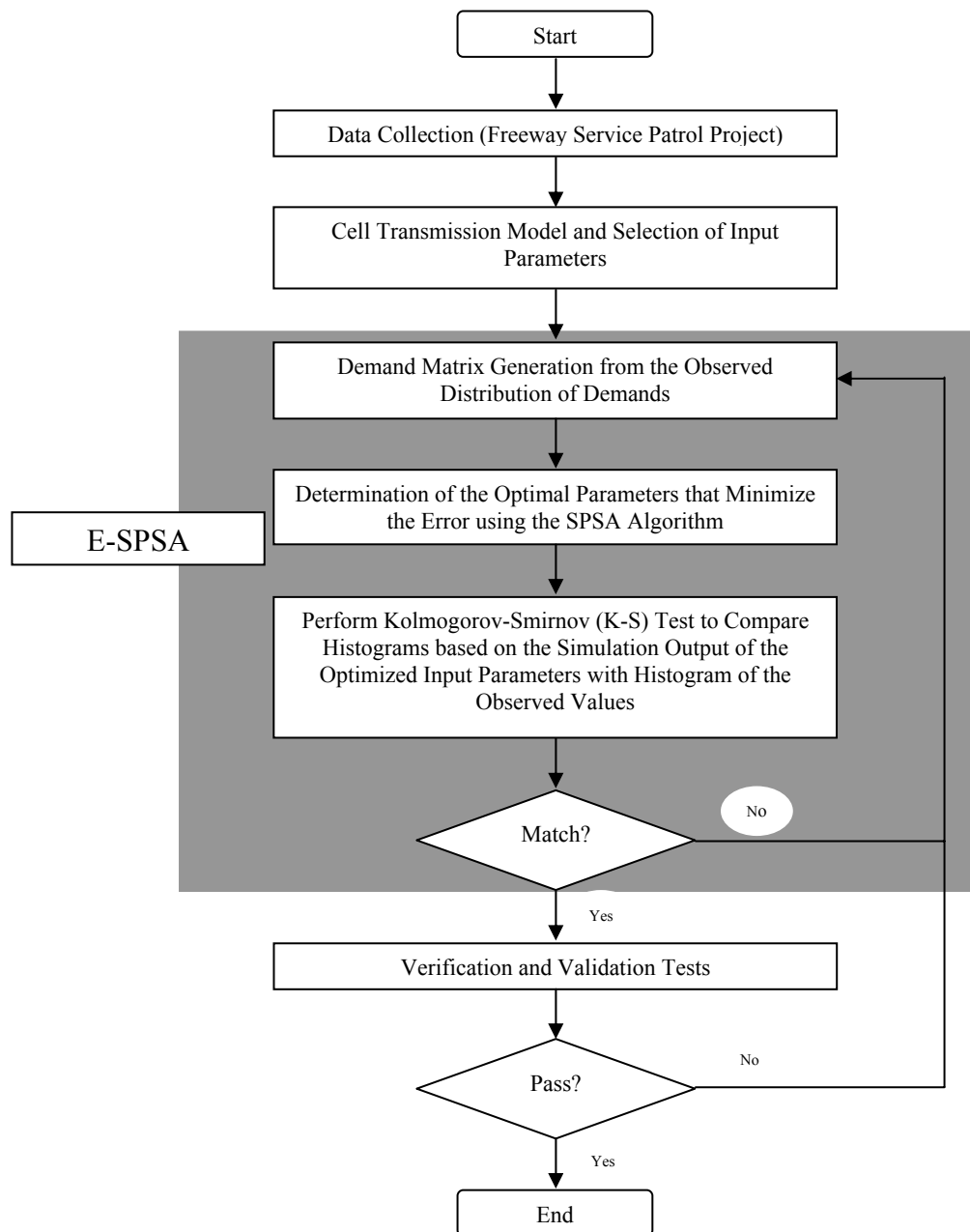


Figure 6.1 Proposed combined enhanced SPSA simulation calibration methodology

6.3 Description of Sampling Methodology

The initial distribution consists of random samples generated from the observed demand matrix, using WinBUGS, a software package (<http://www.mrc->

bsu.cam.ac.uk/) that performs Markov chain Monte Carlo simulations to randomly generate time-dependent O-D demand matrices. Each randomly generated demand (d_k) ($k \in (1, \dots, I)$, n indicates the number of demand matrix) is a random sample of the initial demand distribution. This initial distribution is used to find the optimal input parameter values of the free-flow speed and the jam density. At each iteration, these input parameters are determined by using the SPSA algorithm, as discussed in the preceding section.

6.4 Implementation Details of E-SPSA Calibration Methodology for a Freeway Segment

To test the effectiveness of the E-SPSA calibration methodology, a freeway segment with and without ramps was considered.

6.4.1 Demand Matrix Generation from Observed Distribution of Demands

In traffic simulation models, the vehicular demand is modeled by using traffic zones. In the case of freeway segments, these zones are usually placed at a segment upstream of the segment under study. If the study segment is relatively short and the flow is observed on all sections (before and after ramps), the demand generated from the zone will, on an average, be equal to the flow observed at the segment under study. So, it can be assumed that the flow observed at a point on the freeway is the resulting effect of the same amount of demand generated at a zone upstream of the segment. In this dissertation, the demand matrices were generated by using the traffic counts (i.e., flows from loop detectors). Hence the autoregressive assignment function A as

described in equation [6.1] will depend only on the current O-D demand D_1^j and parameters Θ_1^j . In the case study presented (shown in Figure 6.2), flows are observed on all sections. Hence, the demands could be determined uniquely. At each iteration, a new demand matrix is formed from the flows, which are randomly selected from the distribution of observed flows, which is the prior distribution. Thus, each generated demand matrix is effectively a sample from the initial distribution.

Depending on the existence of intermediate ramps, a random demand matrix is formed from the distribution of observed flows for the two distinct geometries. The basic calibration procedures of demand originating from a single zone and demand originating from two zones may differ slightly because of the sampling methodology. For the on-ramp scenario, the prior distribution is obtained from the relationship between the flow on the mainline and that on a ramp. For generating the demands from two zones, the demands for the mainline and ramp (the two components of D_1^j) are sampled simultaneously formed from the flows Q_i^{Ob} . To take into account the existence or lack of correlation between the two demands, the demand matrix is generated by using conditional or independent samples, respectively. The existence of the autoregressive assignment function shows that there can be a correlation (through Q_i^{Ob}) between the ramp demands and mainline demands D_1^j .

Table 6.1 Possible demand sampling method

Demand Sampling	Single Zone	Two Zones (On-ramp scenario)
Not Correlated	Independent sampling	Independent sampling
Correlated	Not applicable	Conditional sampling

6.4.2 Determination of Optimal Parameters That Minimize the Error Using the Enhanced SPSA Algorithm

Based on the randomly generated demand matrix, the calibration parameters are reestimated at each iteration. To select the optimum values of the parameters, a stochastic optimization algorithm, the SPSA algorithm, is used. The format of the objective function for the given simple freeway section is of the form shown in equation [6.2].

$$L = \sum_i \sum_{lane} \left[\frac{|Q_i^{real} - Q_i^{sim}|}{Q_i^{real}} + \frac{|K_i^{real} - K_i^{sim}|}{K_i^{real}} \right] \quad [6.2]$$

where

L : objective function,

Q_i^{real} : observed flows for a given time period i and lane (vph),

Q_i^{sim} : simulated flows for a given time period i and lane (vph),,

K_i^{real} : observed density for a given time period i and lane (vpm),

K_i^{sim} : simulated density for a given time period i and lane (vpm), and

i : time period $i \in (1, \dots, I)$.

It is apparent from the explanation in the section on demand matrix generation that the demands D_i^j and flows Q_i^S are directly correlated. If the function for the measure of accuracy can be assumed to be the same—namely, relative error—then the objective function will have same terms repeating twice. Therefore, the objective function to be optimized reduces to that shown in equation [6.2]. Because CTM is a

macroscopic simulation model, there is an additional term K_i^{real} density that can be measured and calibrated easily.

CTM simulation is then run multiple times with different random seeds to consider the variability in the simulation at each step of the SPSA algorithm. The random seeds are an important factor that is studied to determine their effect on the simulation results. In the stochastic analysis, the random seeds produce more accurate results by representing measurement noise (Hollander and Liu (2008)). In the CTM methodology used, the random seeds directly affect the demand and hence the flow. Thus, to minimize the variance of errors, it is important to run the simulation with several different random seeds. At the end of each simulation run, the relative error between the observed and the simulated is calculated with equation [6.2]. The SPSA algorithm is implemented to optimized loss function L . Ding (2003) suggested that the values of a , c , α , and γ in equation [3.4] be set to 0.2, 0.5, 0.602, and 0.01, respectively; those values are used in this dissertation.

6.4.3 Perform Kolmogorov-Smirnov (K-S) Test

Random samples from the prior distribution are generated from the observed demand matrix. The SPSA algorithm for each generated demand matrix calibrates these parameters. When one iteration of the calibration procedure is completed and the optimized parameter values are found by the SPSA algorithm, the evaluation process is performed. The distribution of the flows and densities from the cell transmission is compared with the distribution of the observed values by using the K-

S test. If there are random samples x_1, x_2, \dots, x_n from a cumulative distribution function $F_m(x)$, and the empirical cumulative distribution function is denoted by

$$F_n(x) = \frac{1}{n}(\text{Observed_data} \leq x)$$

H_o : For all random samples x_1, x_2, \dots, x_n , $F_m(x) = F_n(x)$

H_a : For at least one data of random samples x_1, x_2, \dots, x_n , $F_m(x) \neq F_n(x)$

A K-S test determines whether the data follow a specific distribution based on the difference between $F_n(x)$ and $F_m(x)$.

$$D_{n,m} = \sup |F_n(x) - F_m(x)|$$

Here, sup indicates the supremum of $|F_n(x) - F_m(x)|$. For example, $\sup\{10, 11, 12\}=12$.

Normally, the null hypothesis is that the data follows a specific distribution and if the test statistic $\sqrt{\frac{nm}{n+m}} D_{n,m}$ is more than a critical value, the null hypothesis is rejected at the chosen alpha level.

If the two distributions pass the K-S test, the procedure moves to the validation step. If they do not pass the test, the sampling process is repeated. The advantage of using a nonparametric statistical test such as the K-S test is that it does not depend on the distribution of the parameter in question. Kim et al. (2005)

performed the K-S test to ensure that the distribution of the simulation travel time represented real traffic conditions. Hollander and Liu (2008) mentioned that a comparison of the probability density function by using the K-S test is better validation method than the examination of individual observation.

6.5 Case Study

The calibration of a single zonal demand case was performed to test the effectiveness of the proposed E-SPSA approach. Additionally, the calibration was done with two demand zones over an extended road segment (mainline and on-ramp).

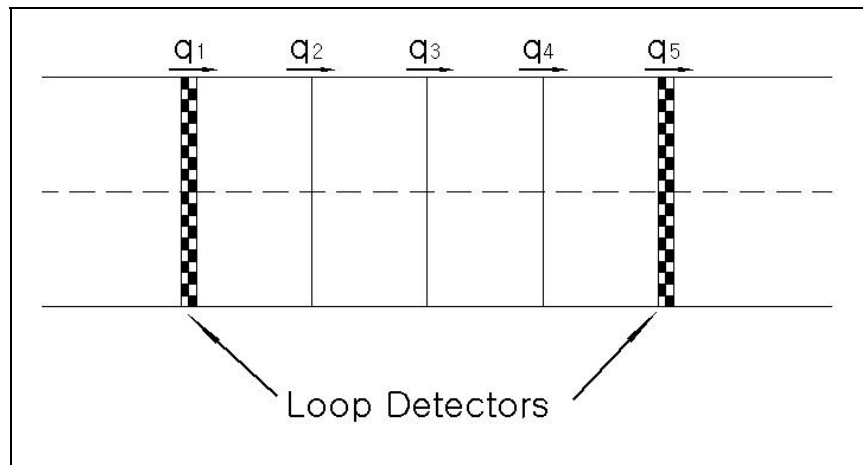
6.5.1 Data Collection

Data were obtained from the database of the Freeway Service Patrol project for a portion of the I-880 freeway in Hayward, California (Skabardonis et al. (1998)). Data were collected from September 27 to October 29, 1993, from 05:00 to 10:00 and from 14:00 to 20:00 for weekdays and were aggregated into 5-minute counts. The data were used differently depending on the existence or nonexistence of an intermediate ramp. Flow data for all the time periods for 17 different days were estimated in the cases with no intermediate ramp. When intermediate ramps were present, data were divided into four intervals: depending on morning or evening and on peak (reach the capacity) or nonpeak (uncongested) period (05:00 to 07:30, 07:30 to 10:00, 14:00 to 17:00, and 17:00 to 20:00). In the case of a freeway with a single zone (no intermediate ramp), the selected freeway segment is a two-lane one-way road and the length of the section is 1 mile. In the case of a freeway with an

intermediate ramp, one lane for the mainline and on-ramp, respectively, is used and the length of the section is 1.2 miles.

6.5.2 CTM and Selection of Input Parameters

In the case of single zonal demand (no intermediate ramp), the road segments in CTM are initially modeled as a simple road segment to test the effectiveness of the E-SPSA approach. The selected freeway segment is a two-lane one-way road and the length of the section is 1 mile. The case of an intermediate ramp is modeled as an extended road segment as described by Daganzo (1995) (Figure 6.2). The selected freeway segment is one lane for the mainline and on-ramp, respectively, and the length of the mainline is 1.2 miles. Because the zonal demand, one of the major input variables, is sensitive to the flow–density relationship, free-flow speed (V_f) and jam density (K_j) were selected as the input parameters.



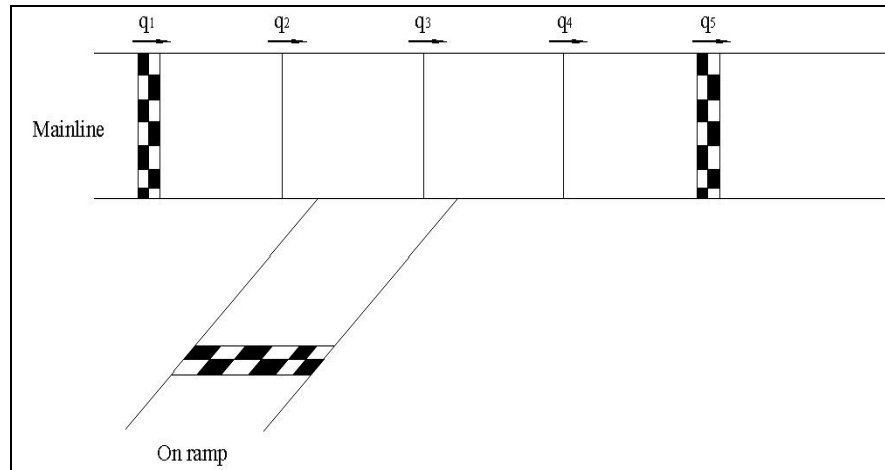


Figure 6.2 The network geometry

6.5.3 Demand Matrix Generation from Observed Distribution of Demands

When a ramp exists, the demand matrix (formed from flows) is generated depending on whether the flows from the two zones are correlated. The main assumption is that there is no correlation between these flows, which makes it possible to sample the mainline and ramp flows independently.

Figures 6.3 and 6.4 show the histogram of the observed demand matrix formed from the flows.

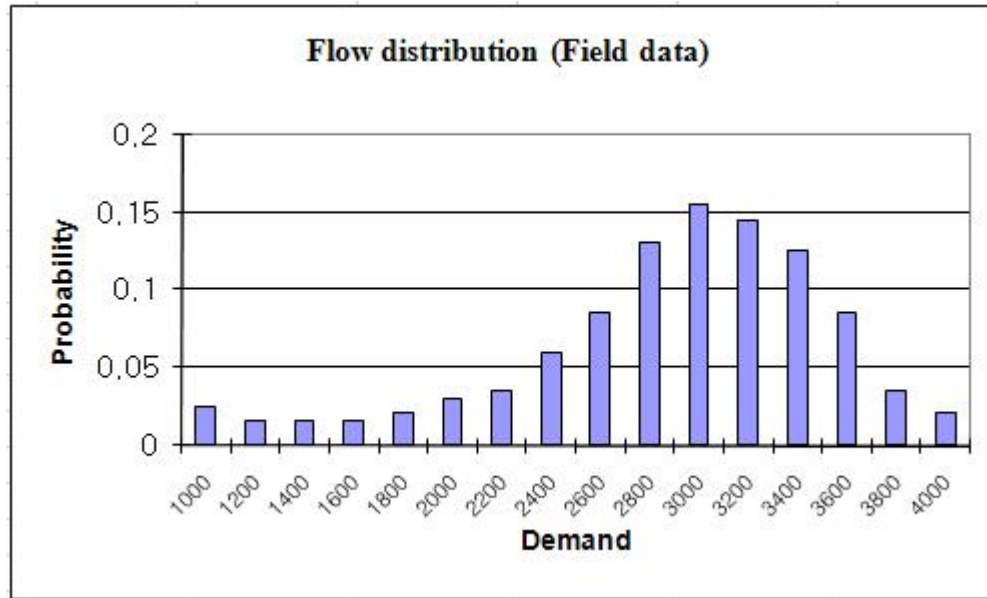


Figure 6.3 Histogram based on the distribution of 17 days of observed demand

matrix: no intermediate ramp

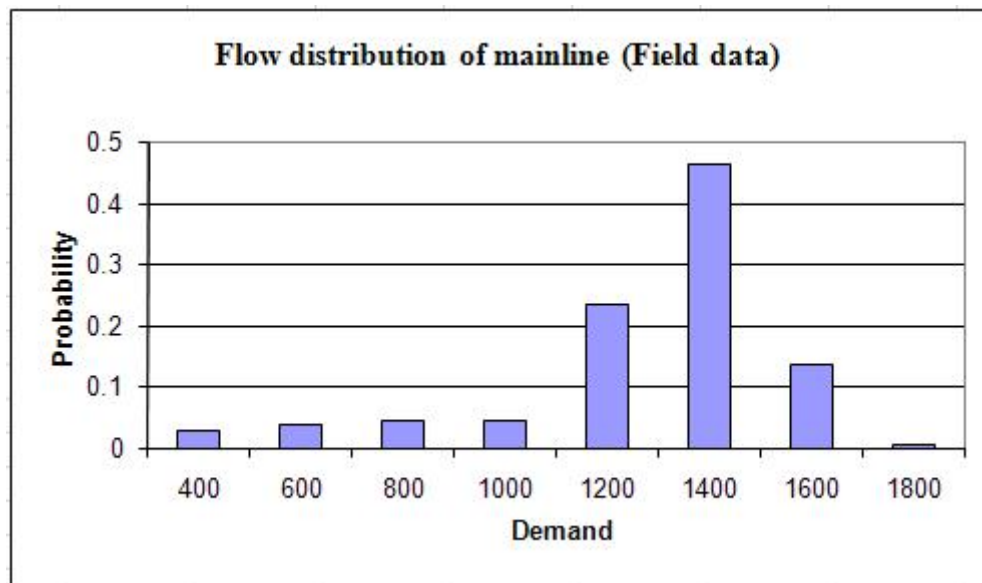


Figure 6.4 (a) Mainline

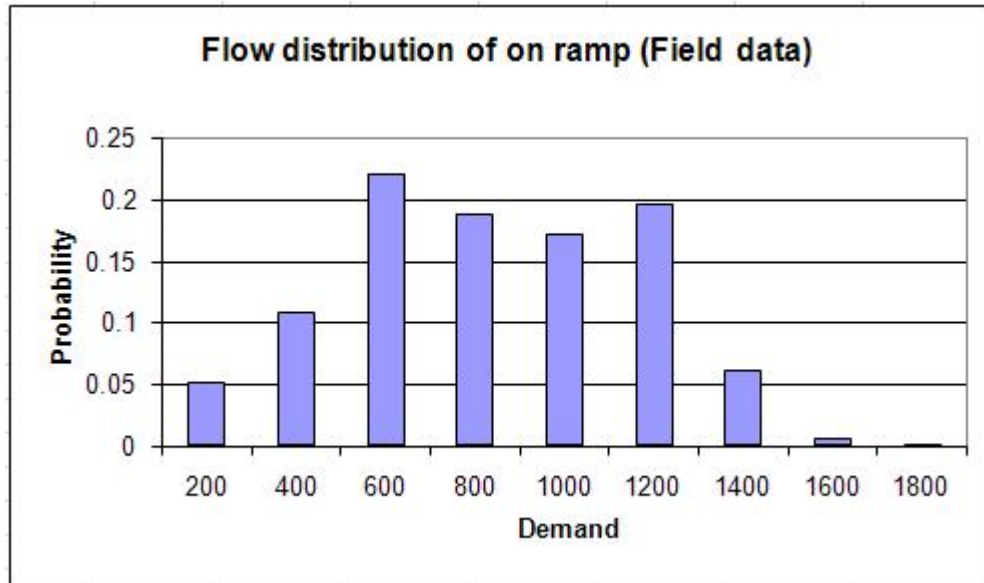


Figure 6.4 (b) On ramp

Figure 6.4 Histogram based on the distribution of 17 days of observed demand

matrix: intermediate ramp

6.5.4 Determination of Optimal Parameters That Minimize Error Using the Enhanced SPSA Algorithm

No intermediate ramp

For single zonal demand (no intermediate ramp), the initial values of free-flow speed and jam density are taken as 55 mph and 110 vehicles per mile for two lanes, respectively. The SPSA algorithm is used to determine the “optimal” values of the calibrated simulation parameters for each iteration. The same procedure is repeated until the sum of the relative error between observed and simulated values is less than the acceptable error of 5%. Each iteration is performed with three different random seeds when using the SPSA algorithm.

The input parameters converge when there is only a small difference between the simulated and observed values of flow and density. These are the optimized input parameter values for each generated demand matrix. The best fit for flow and density is observed for optimized input parameters of 59.6 mph and 107.0 vehicles per mile for two lanes, respectively.

Intermediate Ramp

For two zonal demand (mainline and on ramp), the resulting output of the calibrated cell transmission model is compared with the observed data. The initial parameters of free-flow speed and jam density are set to 60 mph and 60 vehicles per mile for four time periods. The sum of relative errors for four time periods (05:00 to 07:30, 07:30 to 10:00, 14:00 to 17:00, and 17:00 to 20:00) were found to be 4.71, 4.06, 3.97, and 4.43, respectively. Table 6.2 summarizes the results for optimal calibration parameters.

Table 6.2 Optimal calibration parameters and other statistics

Time Period	Optimal Free flow speed (mph)	Optimal Jam density (vpm)	Sum of Relative Error of Flow	Sum of Relative Error of Density	Sum of Total Errors
5:00 ~ 7:30	59.4	60.7	2.01	2.70	4.71
7:30 ~ 10:00	58.7	61.3	2.02	2.04	4.06
14:00 ~ 17:00	58.6	59.1	1.83	2.14	3.97
17:00 ~ 20:00	59.3	60.7	2.53	1.90	4.43

6.5.5 Description of the Kolmogorov-Smirnov Test (Munoz et al. (2004))

The obtained flow and density distributions of the macroscopic simulation output based on the optimized input parameters were compared with the observed distributions, using the K-S test (Miller et al. (1990)).

For the single zonal demand case, the K-S test values for flow and density distributions are 0.019 and 0.139, respectively. These values are less than the critical values of 0.247 and 0.340 obtained from the K-S table at the 95% confidence level. For the two zonal demand cases, the critical K-S values from the K-S table are greater than the K-S values for flow and density distributions, as shown in Table 6.3. For the scenario with two simple road segments, the null hypothesis could not be rejected, so there is no reason to doubt about its validity; the null hypothesis states that the simulation flow and density distributed are not different from the observed distributions. Figures 6.5, 6.6 and 6.7 show the distribution of simulated flow and density values when the optimized values of input parameters are used.

Table 6.3 Kolmogorov-Smirnov values for each time period (Intermediate ramp case)

Time Period	K-S Value of Flow	K-S Value of Density	Critical Value from K-S Table for Flow (95 %)	Critical Value from K-S for Density (95 %)
05:00~07:30	0.096	0.089	0.340	0.544
07:30~10:00	0.038	0.063	0.389	0.453
14:00~17:00	0.040	0.032	0.453	0.544
17:00~20:00	0.019	0.025	0.340	0.453

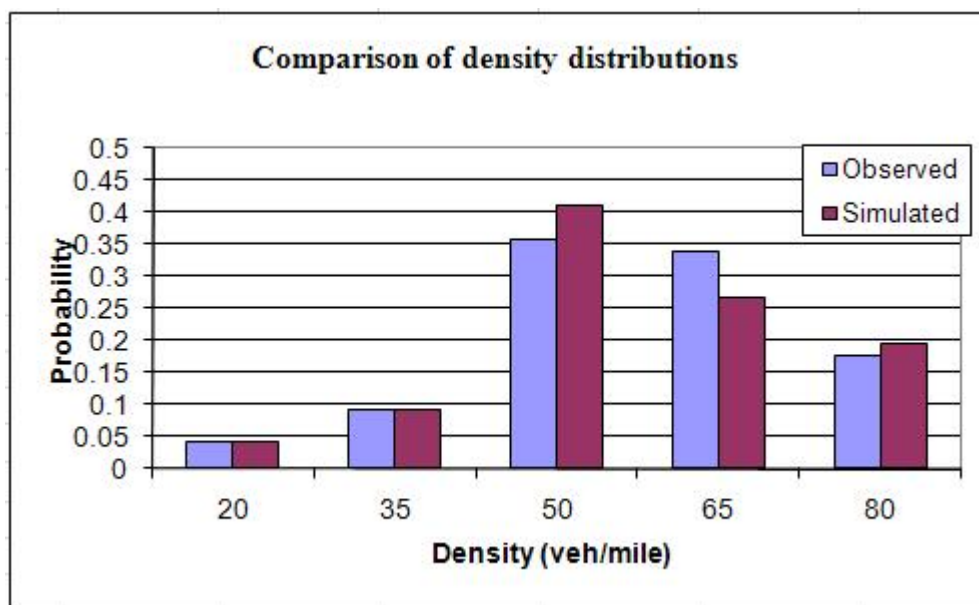
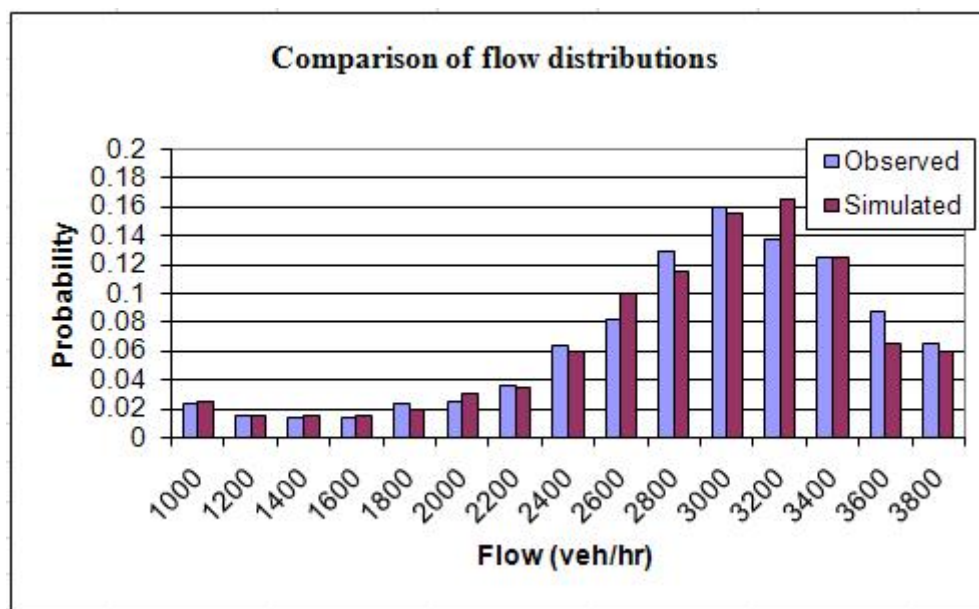


Figure 6.5 Comparison of simulated and observed flow and density distributions: no intermediate ramp

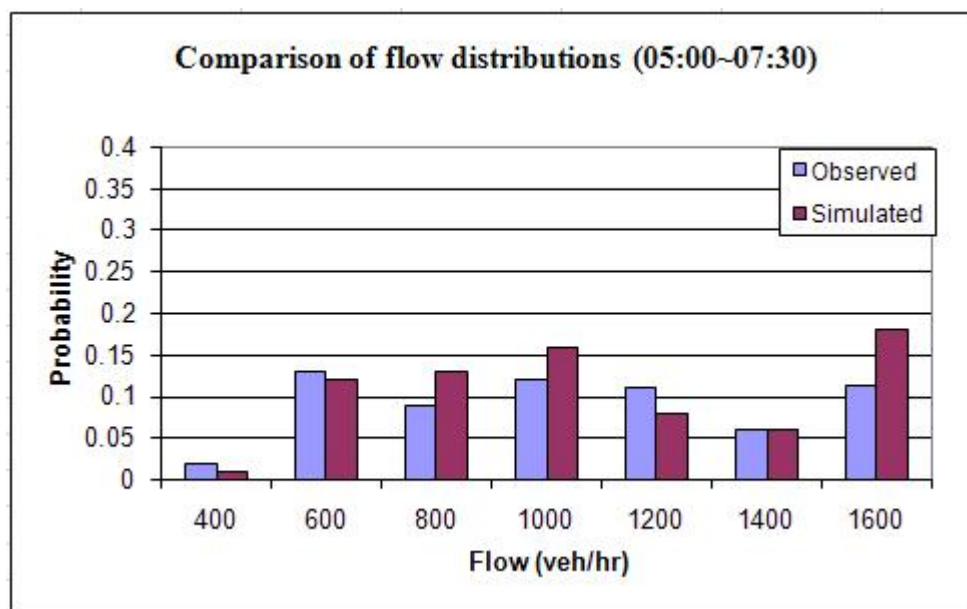


Figure 6.6 (a) 05:00~07:30

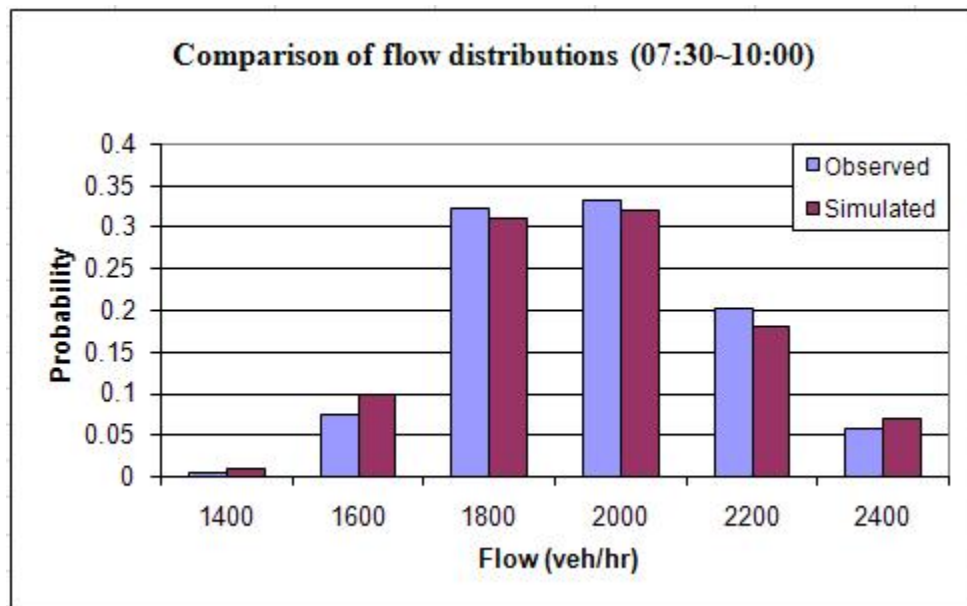


Figure 6.6 (b) 07:30~10:00

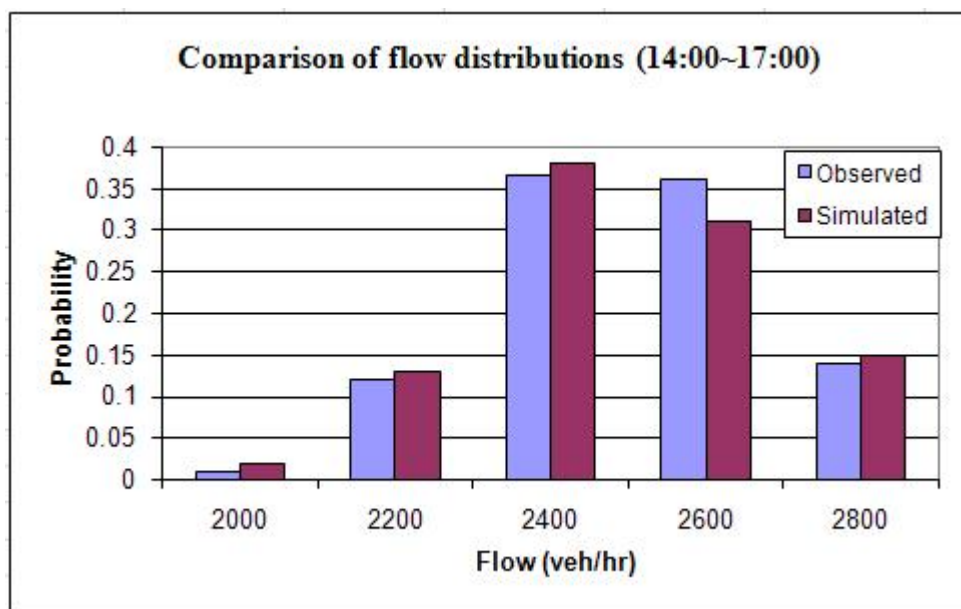


Figure 6.6 (c) 14:00~17:00

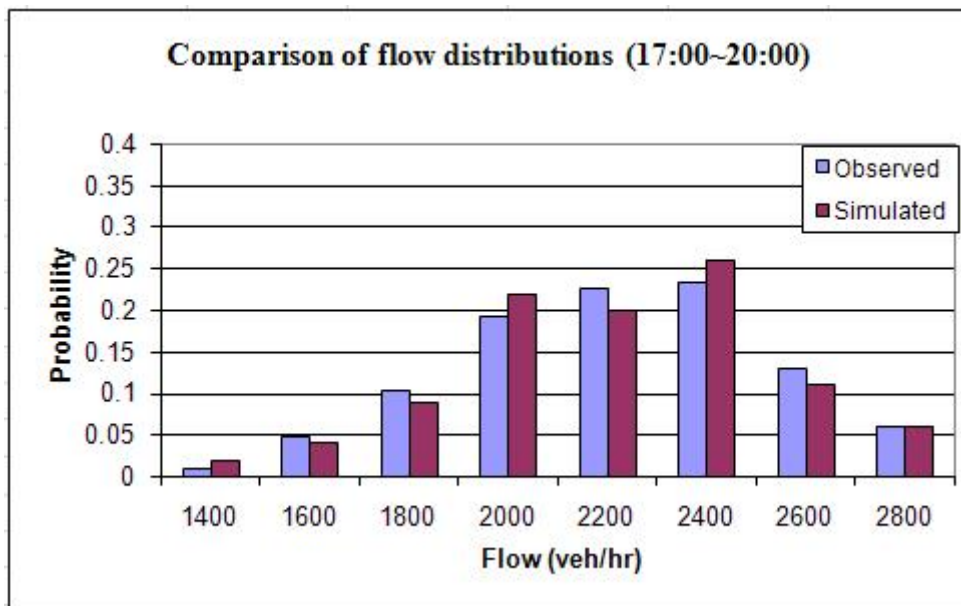


Figure 6.6 (d) 17:00~20:00

Figure 6.6 Comparison of simulated and observed flow distributions: intermediate ramp

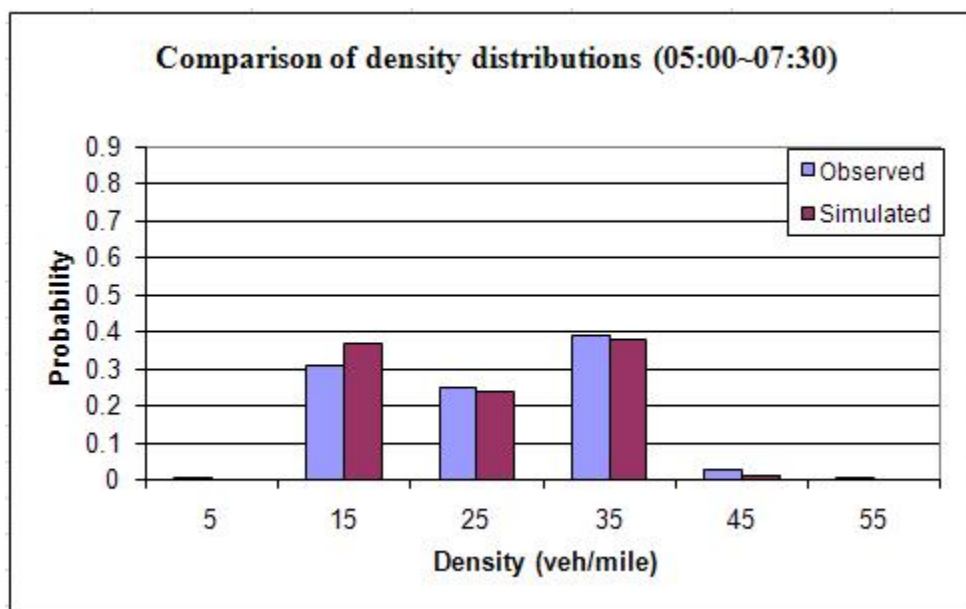


Figure 6.7 (a) 05:00~07:30

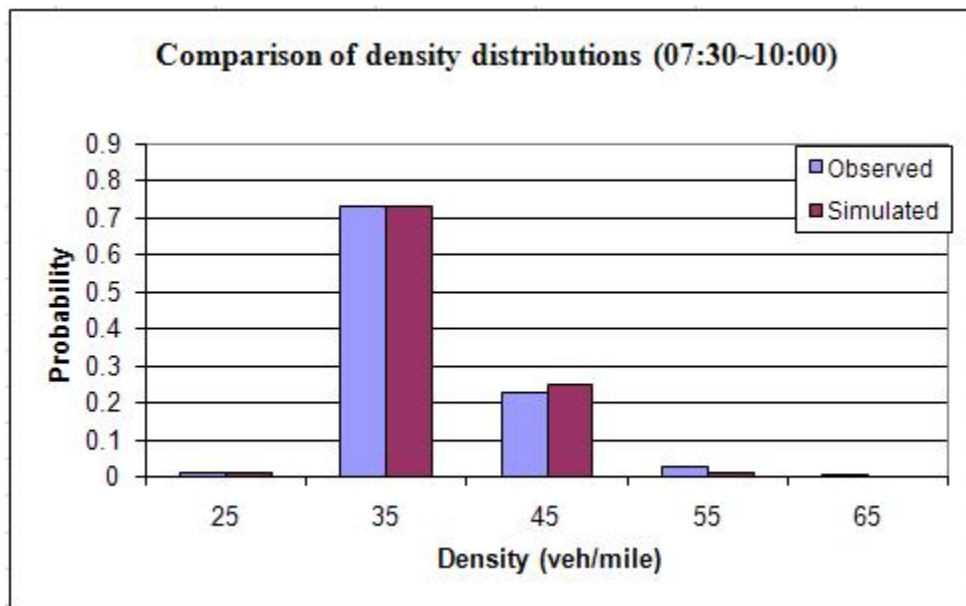


Figure 6.7 (b) 07:30~10:00

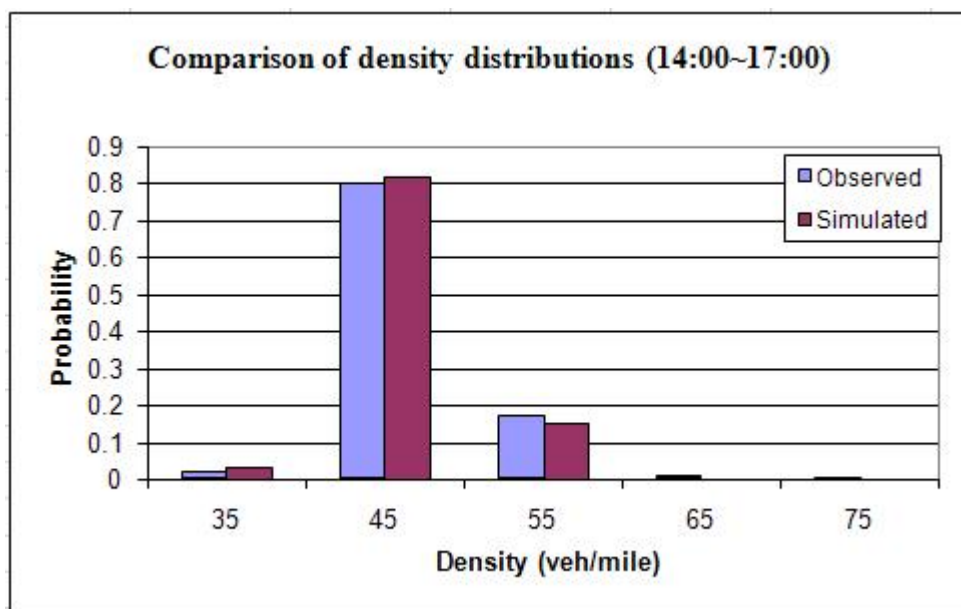


Figure 6.7 (c) 14:00~17:00

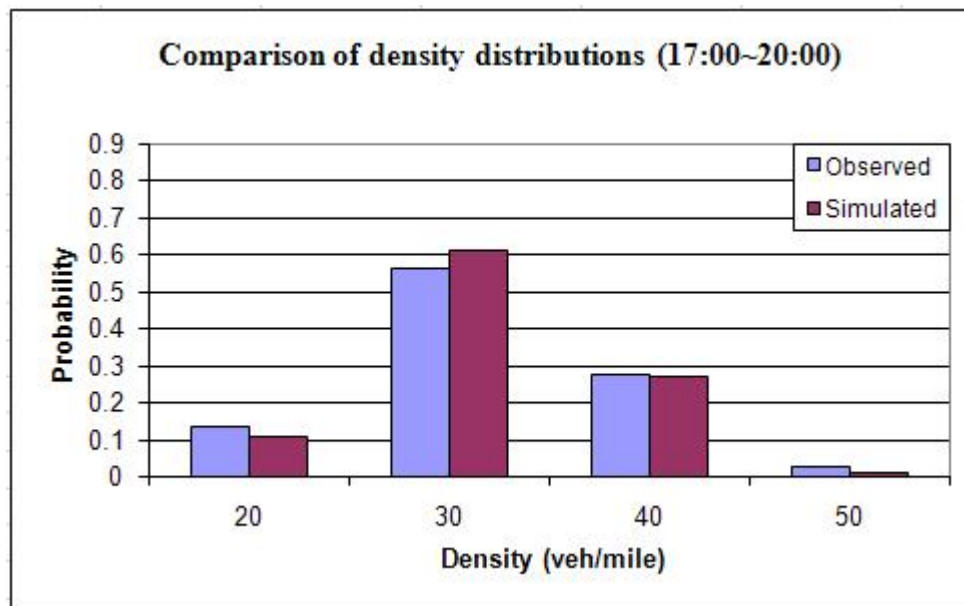


Figure 6.7 (d) 17:00~20:00

Figure 6.7 Comparison of simulated and observed density distributions: intermediate ramp

6.5.6 Verification and Validation Tests

The verification test was performed to ensure that the determined optimal input parameters (the free-flow speed and jam density) represent realistic and accurate values under real traffic conditions. This verification analysis tested whether the objective function could satisfy the predetermined stopping criteria (5%). The result of this verification test and the performance of the simulation tool show that real-world conditions can be fairly captured by the calibrated simulation model.

When the verification processes were satisfied, the validation of calibrated parameter values was performed for different days in the same time period and for the same network. It is difficult to compare the calibrated model performance with the similar performance results found in other calibration papers. However, the mean square variation (MSV) that Sanwal et al. (1996) used is a good method to compare the degree of deviations with the observed values.

Fitness criteria for MSV are shown below:

$$R_{fit}^v = 1 - E[(v - v_m)^2] / E[v_m^2], \quad [6.3]$$

Here, v_m and v denote measured speeds and model speeds, respectively.

$$R_{fit}^T = 1 - E[(T - T_m)^2] / E[T_m^2], \quad [6.4]$$

Here, T_m and T denote measured travel times and computed travel times, respectively. If the model's estimations are close to real-world measurements then the MSV should be close to one.

The optimized parameter values were used to simulate randomly selected days as a part of the validation process. The results of the validation for the case of the two geometric configurations (with and without intermediate ramp) are discussed below.

No intermediate ramp

The optimized parameter values were used to simulate two randomly selected days. The distributions of flow and density based on the optimized parameter values are compared with the observed data distributions (Figures 6.8 and 6.9). Based on the K-S test, the values of the flow distributions for September 30, 1993, and October 13, 1993, were 0.019 and 0.018, both less than the critical K-S value from the table (0.194). The values of density distributions 0.037 and 0.012 are also less than the critical K-S value of 0.453 at the 95% confidence level. According to the K-S test, observed and simulated flow and density distributions are proven to have an acceptable level of similarity (fit) with respect to each other.

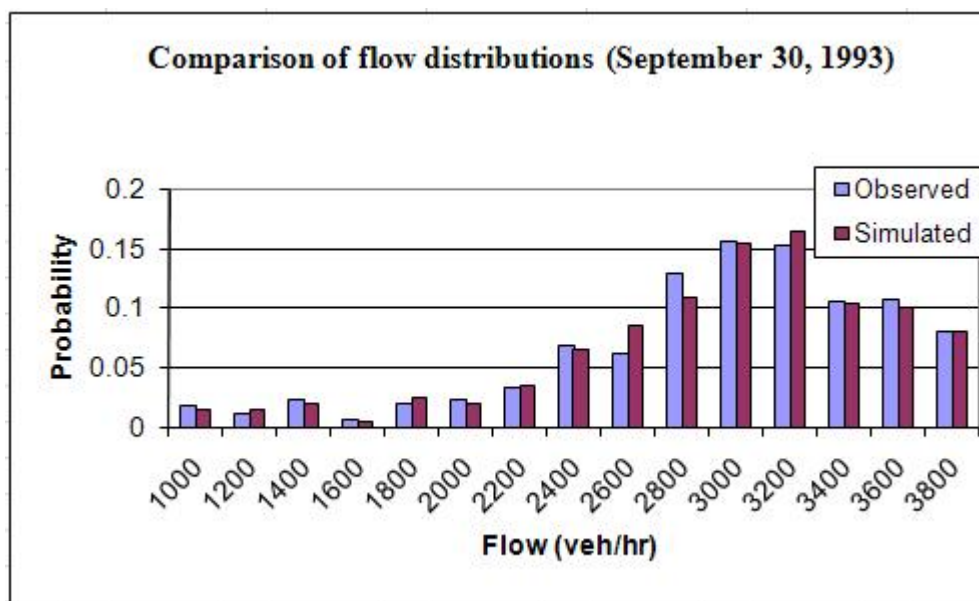


Figure 6.8 (a) Flow on September 30, 1993

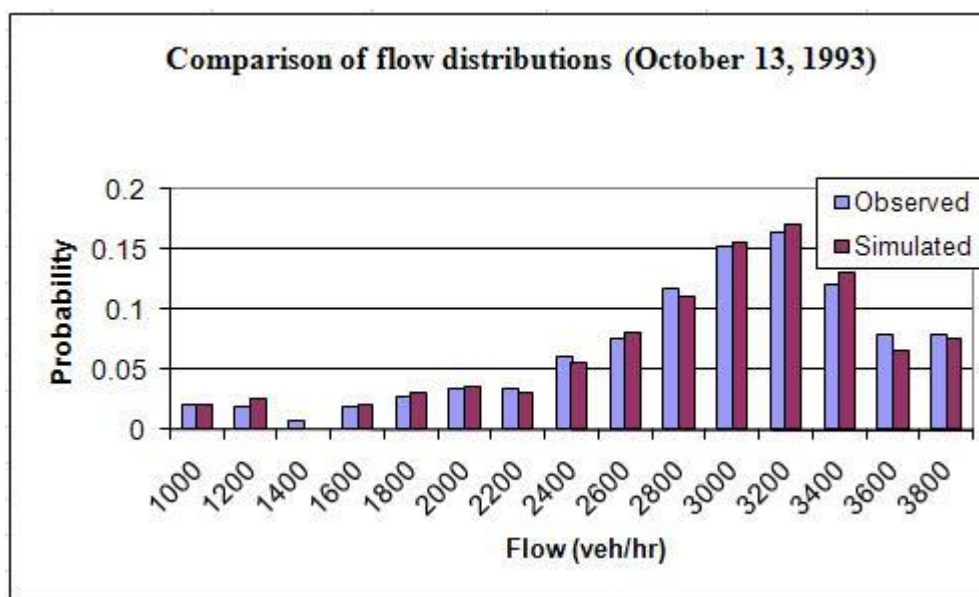


Figure 6.8 (b) Flow on October 13, 1993

Figure 6.8 Comparison of simulated and observed flow distributions

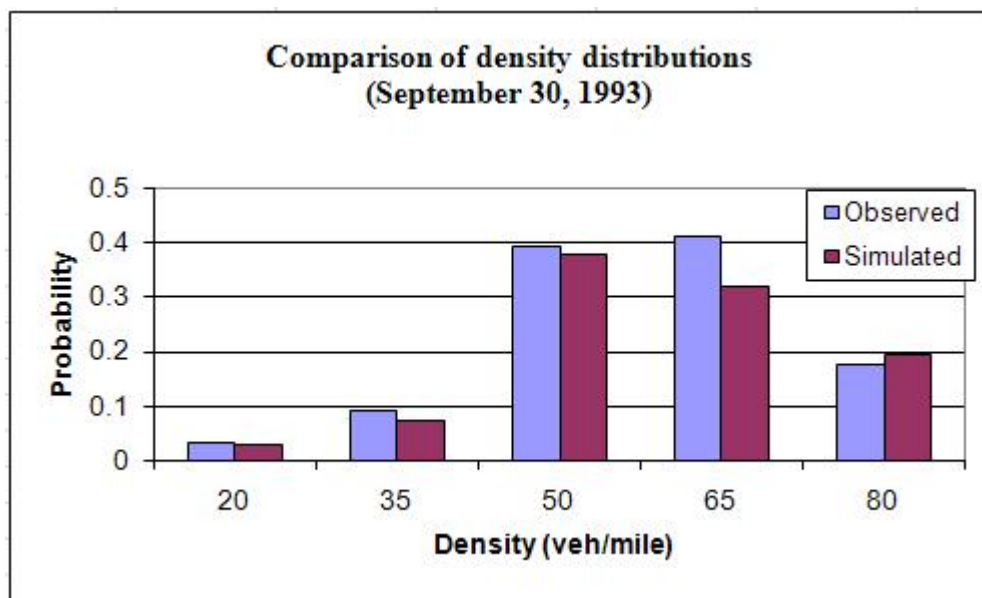


Figure 6.9 (a) Density on September 30, 1993

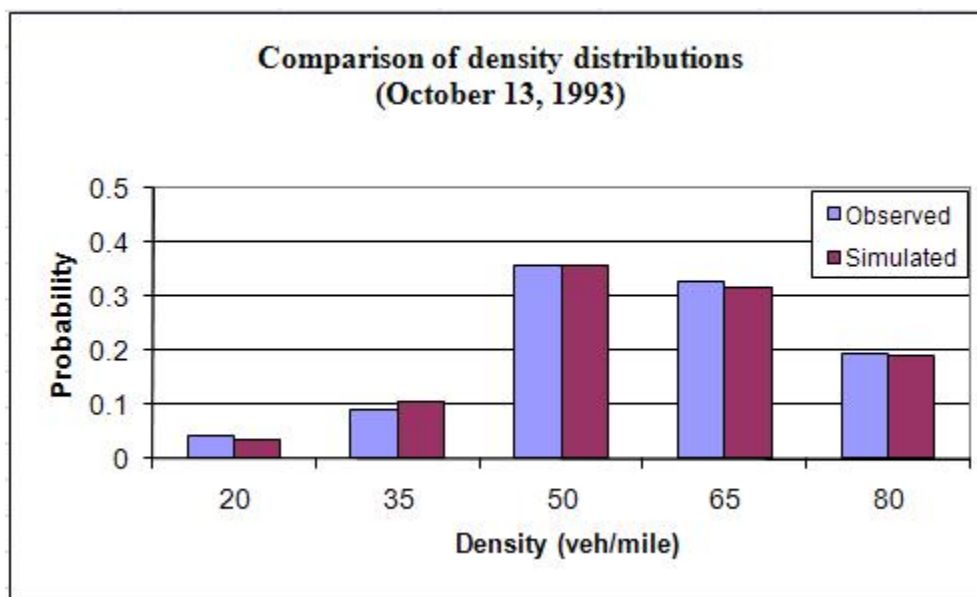


Figure 6.9 (b) Density on October 13, 1993

Figure 6.9 Comparison of simulated and observed density distributions

Intermediate ramp

The validation test was performed for three scenarios. The first scenario used the E-SPSA approach for four randomly selected days. The second and third scenarios tested the SPSA algorithm without the sampling methodology for single and multiple days. These tests were performed to determine the effectiveness of the E-SPSA approach compared with the SPSA-only approach. Finally, the MSV measure used by Sanwal et al. (1996) was applied as an evaluation criterion to compare the degree of deviations from the observed values.

First Scenario Optimized parameter values of four time periods match well with the distributions of observed values shown in Table 6.3. The optimized parameter values were used for four randomly selected days that were not used in the calibration process. The statistical test results of this process are shown in Table 6.4.

Table 6.4 Kolmogorov-Smirnov values for each time period

Time Period	K-S Value of Flow	K-S Value of Density	Critical Value from K-S Table for Flow (95 %)	Critical Value from K-S for Density (95 %)
05:00~07:30	0.042	0.034	0.272	0.389
07:30~10:00	0.116	0.026	0.453	0.453
14:00~17:00	0.028	0.036	0.247	0.453
17:00~20:00	0.087	0.080	0.194	0.389

For all periods of the time, each calculated K-S value was less than the critical K-S values given by the table. This result also shows that two distributions between the observed and the simulated flow and density fit closely. Figures 6.10 and 6.11

show the fitness between the observed and the simulated distributions of flow and density for each time period.

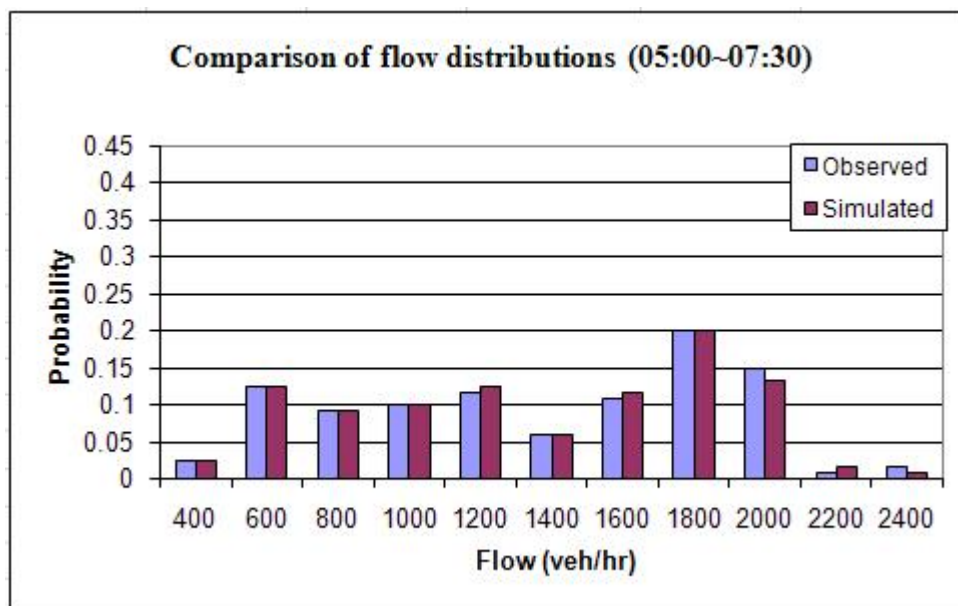


Figure 6.10 (a) 5:00~7:30

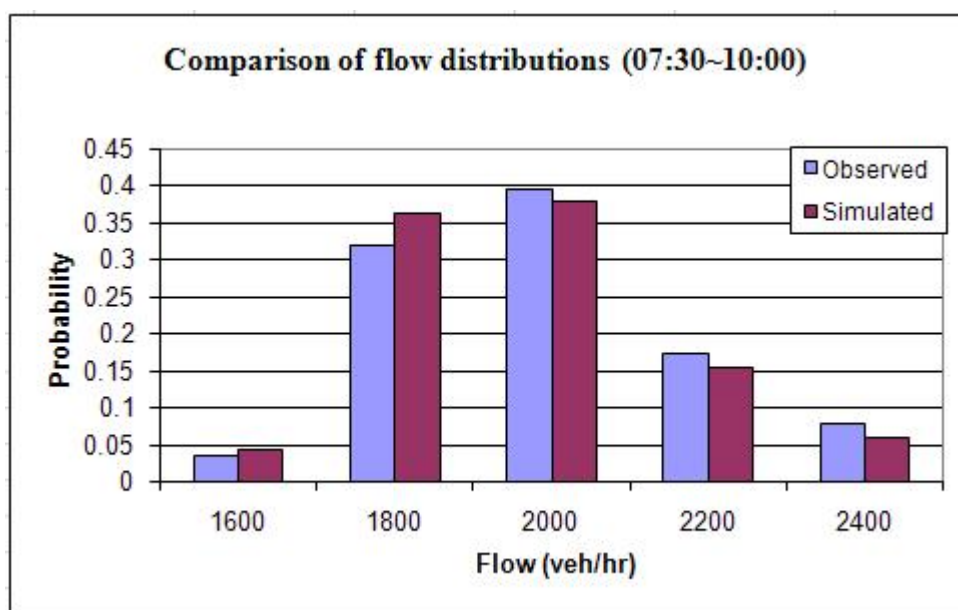


Figure 6.10 (b) 7:30~10:00

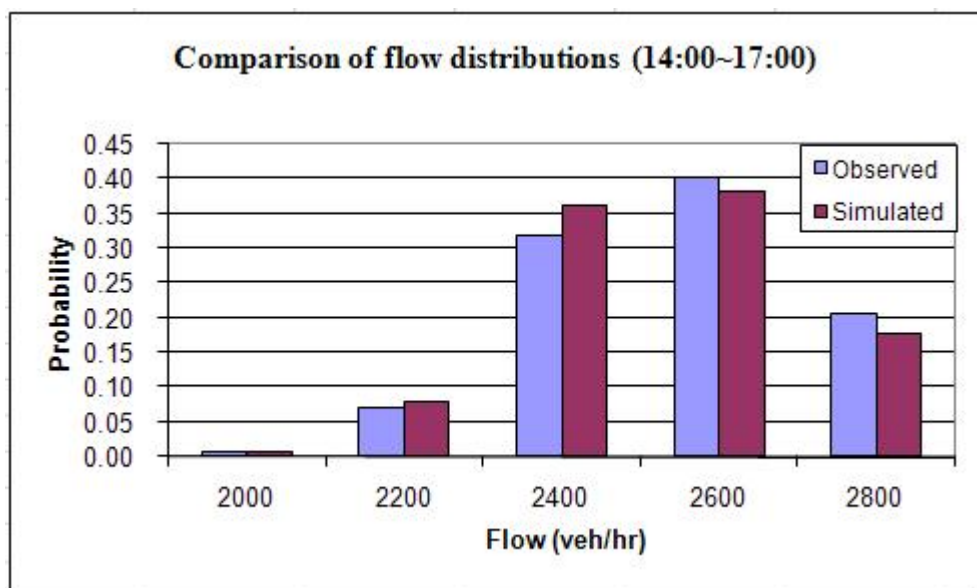


Figure 6.10 (c) 14:00~17:00

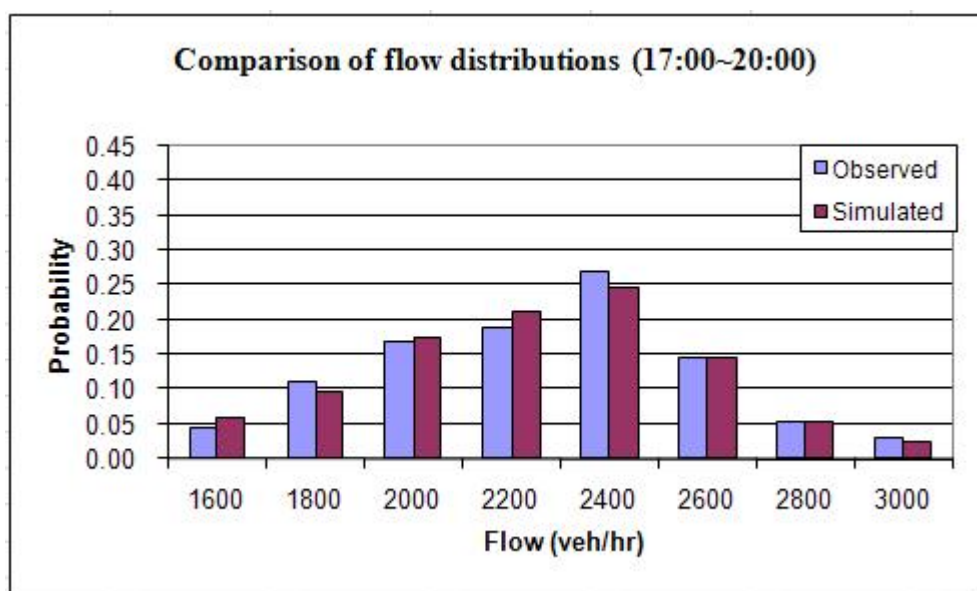


Figure 6.10 (d) 17:00~20:00

Figure 6.10 Comparison of simulated and observed flow distributions

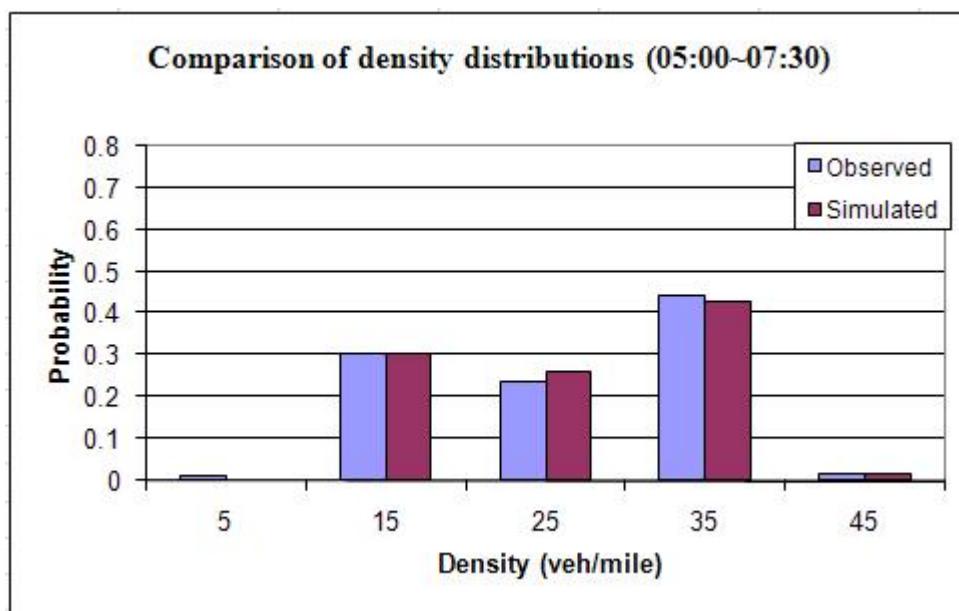


Figure 6.11 (a) 5:00~7:30

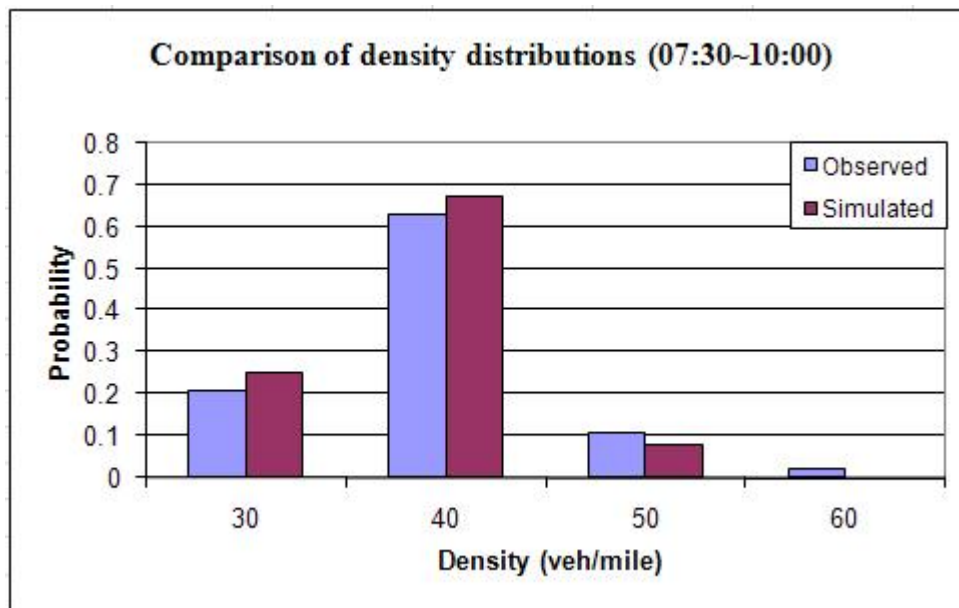


Figure 6.11 (b) 7:30~10:00

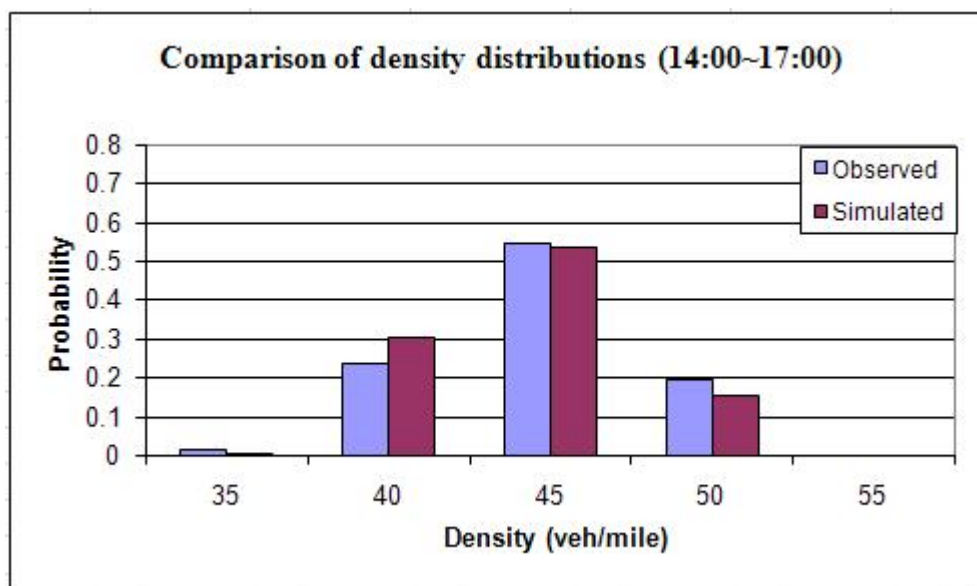


Figure 6.11 (c) 14:00~17:00

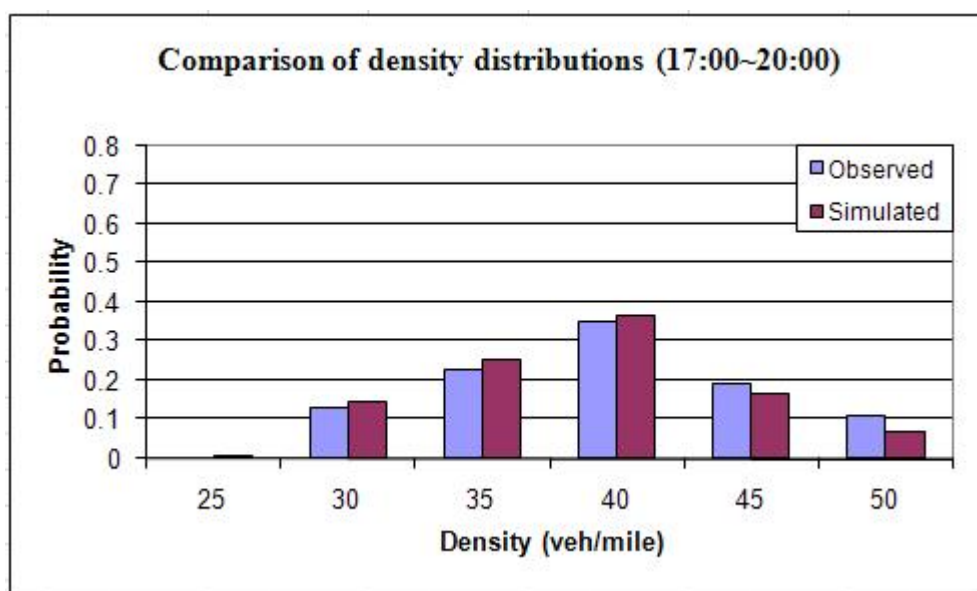


Figure 6.11 (d) 17:00~20:00

Figure 6.11 Comparison of simulated and observed density distributions

Second Scenario In the second scenario, the validation test was performed for the calibration process based on the SPSA-only algorithm. Calibration was performed with a single day's data until the error was within the bounds. September 30, 1993, data were tested to determine optimal parameter values and the resulting relative errors were calculated as 2.13, 2.66, 3.51, and 4.56. For three randomly selected days, the error was calculated using these optimized parameter values. In the case of the third time period, 14:00 to 17:00, the relative errors range from a low of 3.53 on October 13, 1993, to a high of 13.53 on October 5, 1993. The resulting relative errors are summarized in Table 6.5. On the basis of the SPSA-only algorithm result, flow and density distributions for the time period 07:30 to 10:00 on October 13, 1993, were compared with observed data distributions using the K-S test. The critical value of the K-S test for flow and density distributions is 0.272, which is more than the value calculated for simulated flow distribution (0.207) and less than the calculated value for the simulated density distribution (0.448). Thus, the null hypothesis is rejected for density distribution.

Table 6.5 Sum of relative errors for the validation test for three randomly selected days

Days	Sum of relative Error of Flow and Density			
	05:00~07:30	07:30~10:00	14:00~17:00	17:00~20:00
09/30/93	2.13	2.66	3.51	4.57
10/05/93	8.25	11.17	13.53	5.79
10/13/93	7.36	13.49	3.53	4.06
10/18/93	5.73	5.51	6.55	6.41
Average	5.87	8.21	6.78	5.21

Third Scenario In the third scenario, the validation test was performed for the same time period on multiple days and relative errors of 4.58, 4.82, 4.19, and 4.88 were obtained. The optimized parameter values based on the SPSA algorithm were used for four randomly selected days and for four different time periods on those days. The relative errors increased to 10.42, 16.21, 17.58, and 15.52. With this type of calibration approach (SPSA), the two independent data sets for the same facility can be different, even if the mean of the observed data distribution closely matches the simulated data. Hence, it is concluded that the optimal parameter values from the SPSA algorithm are not always transferable to data sets from the same time periods on different days.

On the basis of the variation approach proposed by Sanwal et al. (1996), the MSV of flow of four randomly selected days was compared with the simulation results obtained from the simulation model calibrated using the E-SPSA algorithm. From the morning period between 05:00 and 07:30 to the evening period between 17:00 and 20:00, the MSVs of flow are 0.968, 0.979, 0.981, and 0.950. Sanwal et al. (1996) obtained a value of 0.945 for the variation of speed and 0.968 for the variation of travel time when they applied the optimized parameters from one day to another.

At this point, Even if the reverse case could be happened, normally, the simulation results with optimized parameters are more accurate rather than the results with applying the optimized parameters for other days. However, the result of the transferability tests from Sanwal et al. (1996)'paper was shown that the variation of travel time when they applied the optimized parameters to another day had more accurate result. The MSV value was 0.885 after parameter fitted and when they

applied the optimized parameters to another day, the value was obtained to 0.968. However, the values of MSVs of flow for our approach stand for improving the results of simulation calibration by accurately capturing a wide range of real-world conditions while Sanwal et al. (1996) tested for limited time period.

6.6 Simulation Results and Summary

Careful calibration of traffic simulation models is necessary to accurately represent prevailing traffic conditions. In this chapter, a new calibration methodology based on the Bayesian sampling approach is proposed. Instead of using a single demand matrix and corresponding observed traffic conditions that represent one point in time, the new methodology uses randomly generated demand matrices and corresponding traffic conditions from an observed distribution of these variables. The goal of using input values, generated from the observed distribution of demands, is to enable an accurate wide-range representation of all likely demand conditions observed at a facility. Observed demand values were used to determine a distribution of observed demands for 17 days.

Bayesian sampling approach was applied as part of the proposed calibration methodology to better represent the distribution of the observed traffic characteristics. The main purposes of using Bayesian analysis were to overcome the over- and underestimation of calibration parameters and to acquire a realistic distribution of all possible traffic conditions. Previously, the Bayesian analysis method was not extensively used because of its complex computational requirements. However,

improved performance of modern computers, coupled with efficient computational techniques, allows the Bayesian method to be widely used in a number of areas.

At each iteration of the proposed Bayesian sampling framework, a new demand matrix, which is randomly sampled from this distribution, is loaded into the macroscopic simulation model. Moreover, at each iteration, the proposed calibration methodology re-estimates optimal parameters by using a stochastic optimization algorithm, SPSA, and distributions of flow and density from the macroscopic simulation are compared with the distribution of the observed flow and density (Gelman et al. (2004)).

A cell transmission-based macroscopic simulation model of a portion of I-880 in California was calibrated with the proposed methodology. Two relatively simple road segments, shown in Figure 6.2, one with a single zonal demand (no intermediate ramp) and the other with two zonal demands (mainline and on-ramp), were used as case studies. The distribution of output from CTM was obtained by loading demand matrices randomly sampled from the distribution of observed demand and from the calibrated input parameters, which are the free-flow speed and jam density. The distribution of simulation output was compared with the observed data distribution by using the K-S test. The null hypothesis for the K-S test stated that simulated flow and density distributions are not different than their observed counterparts. For all scenarios, the null hypothesis could not be rejected at the 95% confidence level. Thus, it can be concluded that the differences between the distributions of observed and simulated flow and density values are not statistically significant.

The validation test with a single zonal demand was also performed over two randomly selected cases using the same time period and network. On the basis of optimized input parameters, the flow and density distributions were compared. The differences between the observed and the simulated flow and density distributions were found to be statistically insignificant at the 95% confidence level. Thus, these parameters can be considered to have been validated.

As an extended simulation model, a road segment with an intermediate ramp was modeled using the CTM. The sum of relative errors for four time periods (05:00 to 07:30, 07:30 to 10:00, 14:00 to 17:00, and 17:00 to 20:00) were found to be 4.71, 4.06, 3.97, and 4.43, respectively. For three different scenarios, the model parameters were tested for validation and for the effectiveness of the E-SPSA approach. From Table 6.4, the results of four different time periods were found to satisfy the statistical test for accepting the null hypothesis, and it is concluded that parameter values calibrated by using E-SPSA are applicable to data from a different day. On the other hand, in the second and third scenarios, where SPSA was used without the sampling approach as the main calibration algorithm, predetermined validation constraints were not always satisfied. According to Table 6.5, none of the average values of the sum of relative error of flow and density values satisfied the constraint of an acceptable relative error of 5%. In addition, in the scenario, in which parameters were calibrated with the SPSA-only methodology, the distributions of simulated flow and density values for the time period 07:30 to 10:00 on October 13, 1993 were compared with observed data distributions using the K-S test. The critical value of the K-S test for flow and density distributions is 0.272, which is less than the calculated value for the

simulated density distribution (0.448). The null hypothesis is rejected for density distribution. Therefore, the E-SPSA method was found to improve the results of simulation calibration by accurately capturing a wide range of real-world conditions.

Chapter 7

Calibration of a Microscopic Simulation Model Using Extended-SPSA Methodology

7.1 Introduction

In microscopic simulation, the parameter values are determined from input data that is changeable. To accurately represent real traffic conditions, the parameter values need to be calibrated for each input datum generated from an observed distribution. However, calibration with the data from multiple days and a wide range of time periods makes it too expensive to run the simulation. In addition, a consideration of the uncertainties that need to be explained is another issue. Simulations for predicted future conditions with parameter values that are optimized with a certain day's data have limitations in representing accurate traffic conditions. Waller et al. (2001) studied the influence of demand uncertainty and they compared using a single determined value for future demand with true expected future performance. Molina et al. (2005) used the Bayesian approach to overcome these problems and predicted the behavior of traffic at a signalized intersection in Chicago. The Bayesian analysis method proposed by Molina et al. (2005) enables one to find the posterior distribution of the parameters of Demand (λ) and turning probability

(P), given the data (C) denoted by $\pi(\lambda, P | C)$ that is acquired from a prior distribution for λ and P, with the data density, given λ and P. However, they did not use a stochastic optimization method to find “best” values for the calibration parameters.

This chapter presents the calibration methodology using the Bayesian sampling approach, in conjunction with the application of the SPSA stochastic optimization method (Ex-SPSA) to produce more effective calibration of traffic simulation models.

7.2 Proposed Methodology for the Calibration of a Microscopic Simulation Model

In this dissertation, we propose the use of the Bayesian sampling approach in conjunction with the SPSA approach proposed by Spall (1992). Flows and speeds are obtained using a microscopic simulation model based on PARAMICS, which was developed by Quadstone Limited (*PARAMICS Programmer User Guide* (2000)). The objective function is shown below:

$$F = \sum_{lane} \sum_{time} \left[\frac{|Q_{real} - Q_{sim}|}{Q_{real}} + \frac{|S_{real} - S_{sim}|}{S_{real}} \right], \quad [7.1]$$

where

F : The objective function,

Q_{real} : Observed flows for a given time period, (vph)

Q_{sim} : Simulated flows for a given time period, (vph)

S_{real} : Observed speed for a given time period, (mph)

S_{sim} : Simulated speed for a given time period (mph).

Since, the value of the objective function shown in equation [7.1] is determined using a stochastic simulation tool, a stochastic optimization technique is required to determine optimal values of calibration parameters that will minimize equation [7.1]. The SPSA algorithm is a well-known and efficient stochastic optimization technique, which was described in the chapter 3. In addition to using the SPSA as the optimization approach, Bayesian sampling approach is used to be able to obtain input values that represent the complete range of the observed demand values to ensure a more robust calibration of the simulation model for a complete range of possible traffic conditions.

The basic steps of our proposed methodology can be summarized as follows:

1. Increment iteration: iteration=iteration+1

Iteration:

- a. Generate the demand from a probability distribution function of demands developed using real-world data.
- b. Based on the sampled “ m ” number of data points, which cover the whole range of input distributions, the mean target headway (h_j) and mean reaction time (r_j) are optimized by the SPSA algorithm. Then estimate the distribution of h_i and r_i based on the set of optimized values for the complete distribution of demands noted as, I_i (where $i = 1, 2, \dots, n$, $j = 1, 2, \dots, m$, $m < n$).

2. Compare the output of a simulation for the demand I_k given h_k and r_k in the current iteration—namely, flows—with the observed distribution of flows to determine the statistical similarity between the two distributions (where $k = 1, 2, \dots, 100$). If it is satisfactory, terminate the iterative process and proceed to the validation step. Else return to Step 1.

3. If verification and validation tests are satisfactory, then stop. Else return to Step 1.

Figure 7.1 shows a flowchart of the proposed combined Ex-SPSA calibration and validation methodology.

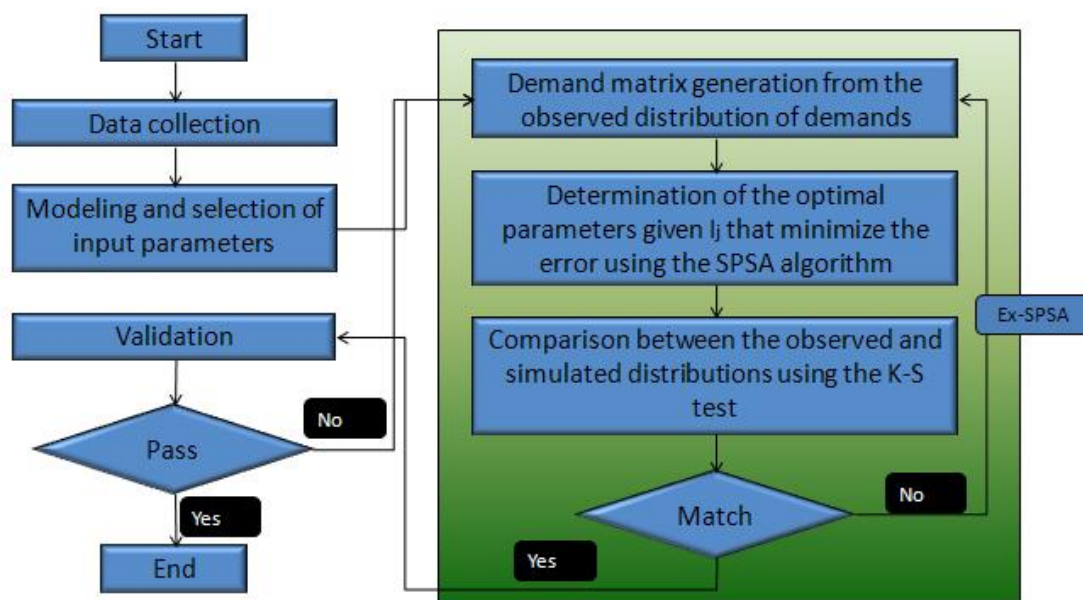


Figure 7.1 Proposed extended SPSA calibration methodology and validation methodology

7.3 Implementation Details of the Proposed Ex-SPSA Calibration Methodology

The calibration of PARAMICS is performed to prove the effectiveness of the Ex-SPSA approach. Using Ex-SPSA, a more effective calibration of traffic simulation models is produced.

7.3.1 Data Collection

Data were obtained from the database of the Freeway Service Patrol project for a portion of the I-880 freeway in Hayward, California (Skabardonis et al. (1998)). Data from 06:00 AM to 10:00 AM weekdays were collected over September 27, 1993 to October 29, 1993 and aggregated into 15-minute counts. Data for all time periods for 16 different days were estimated.

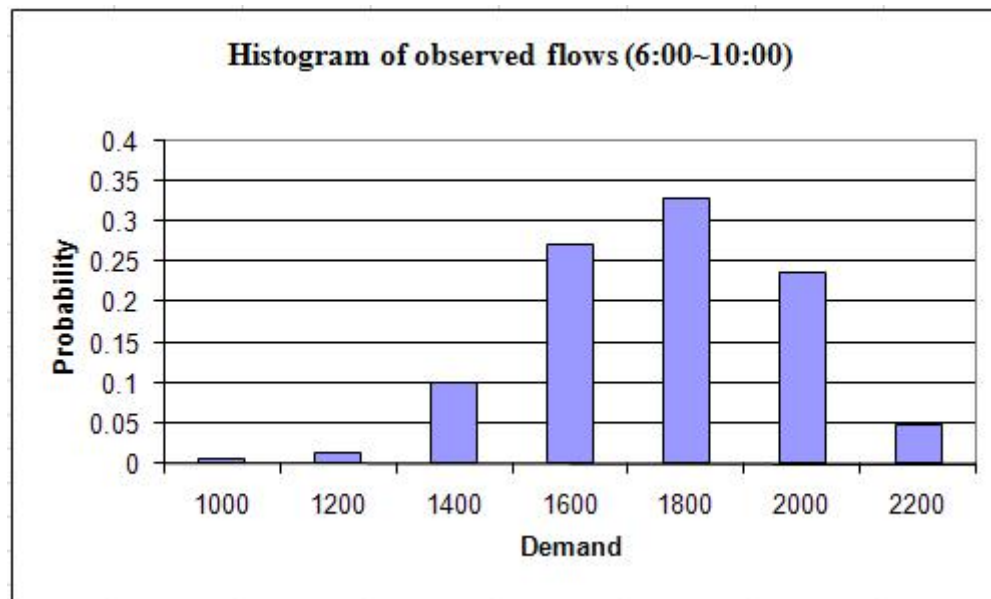


Figure 7.2 Histogram based on the distribution of 16 days of observed demand
(Skabardonis et al. (1998))

The network was created in the PARAMICS model according to the data from the Freeway Service Patrol study (Skabardonis et al. (1998)). The layout of the study segment is shown in Figure 7.3.

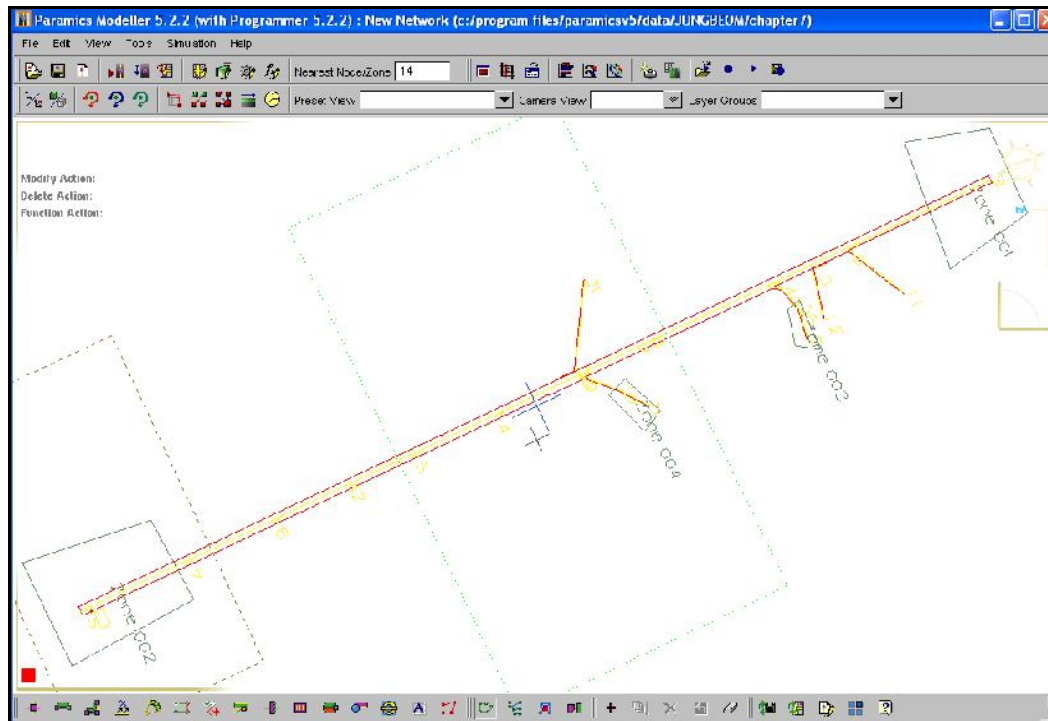


Figure 7.3 The layout of the study segment modeled using PARAMICS

7.3.2 Demand Matrix Generation from the Observed Distribution of Demands

Selecting a best-fit distribution for the data histogram is crucial to accurate data analysis because an inappropriate distribution causes incorrect input data generation. How well the selected distribution matches the data distribution is determined by a goodness-of-fit test such as the Kolmogorov-Smirnov (K-S) test, Anderson-Darling test, or Chi-Square test. Easyfit software is used to determine the best-fit distribution for the data set and deals with uncertainties. In addition, the

software shows the parameter values and the results of a goodness-of-fit test for 40 different distributions (www.mathwave.com).

Easyfit software is used to determine that beta distribution whose parameter values are $\alpha_1=3.56$, $\alpha_2=2.18$, $a=944.5$ and $b=2100.5$ as the best fit for our data set (where, a indicates the minimum value and b stands for the maximum value of the data). Figure 7.4 shows a histogram for the data, with the distribution fitting.

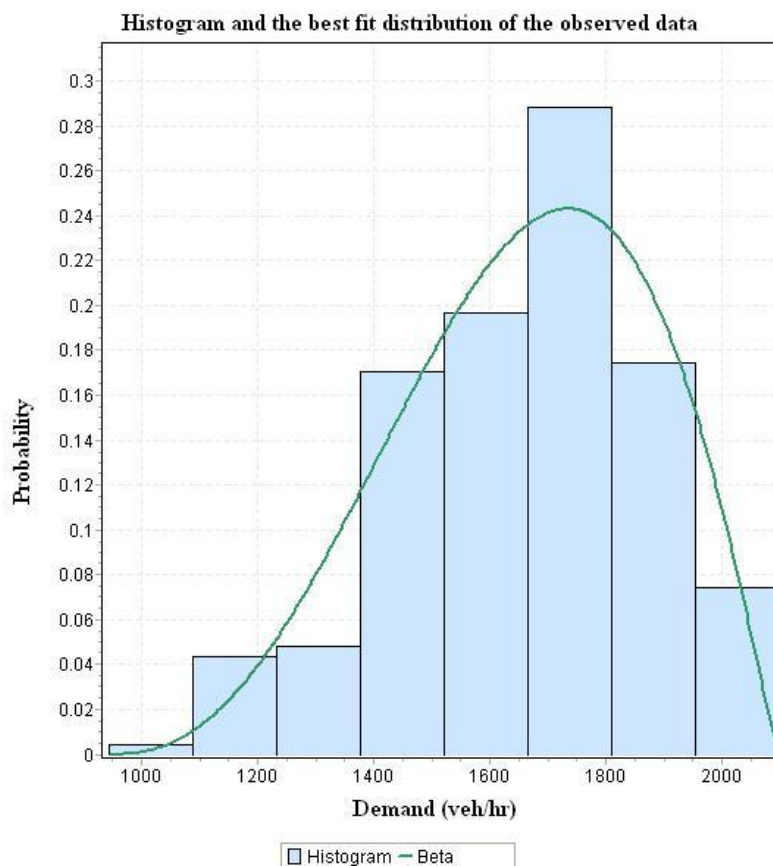


Figure 7.4 Histogram and the best fit distribution of the observed data

(www.mathwave.com)

The obtained beta distribution is compared with the observed data distribution, using the K-S test (Miller et al. (1990)). The K-S test is appropriate in our case because its critical values do not rely on the distribution's shape. In contrast, Anderson-Darling is only applicable to a few types of distributions and a chi-square test requires sufficient sample size.

The null hypothesis states that there is not a statistically significant difference between the beta distribution and the observed flow distribution. On the basis of the results of the K-S test, summarized in Table 7.1, the null hypothesis cannot be rejected at any reasonable confidence levels, i.e., the sampling from the beta distribution can be assumed to represent the distribution from the data histogram.

Table 7.1 Results of the K-S test

Kolmogorov-Smirnov test					
Sample Size	230				
Statistic	0.05362				
P-Value	0.50858				
α	0.2	0.1	0.05	0.02	0.01
Critical Value	0.071	0.081	0.090	0.100	0.108
Reject?	No	No	No	No	No

7.3.3 Determination of the Optimal Parameters that Minimize the Error using the Extended SPSA Algorithm

For input data I , the parameter values—mean target headway and mean reaction time—of PARAMICS are determined using the SPSA algorithm. In previous

studies, simulation calibration was performed with a single input datum I_1 obtained at one point in time and parameter values were optimized using a specific methodology, such as the genetic, simplex, or trial-and-error method shown in Figure 7.5 (Gardes et al. (2002); Lee et al. (2001); Toledo et al. (2004)).

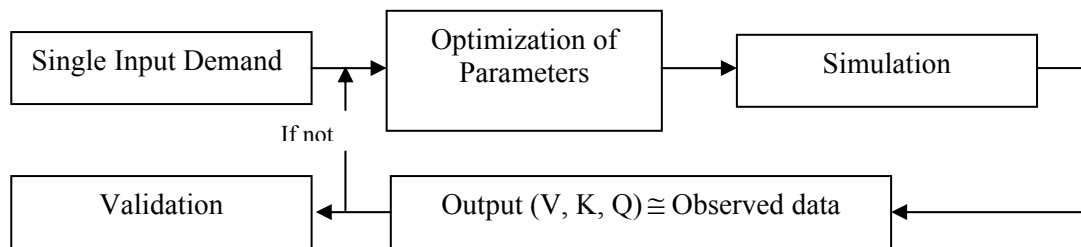


Figure 7.5 A conceptual representation of traditional calibration methods (Gardes et al. (2002); Lee et al. (2001); Toledo et al. (2004))

However, a simulation model calibrated using traffic data obtained from a limited time period over certain days under an unknown input distribution might not be able to represent the traffic conditions on other days. A more robust approach is to calibrate for the entire range of the input data (I_i) to be able to represent a complete range of possible traffic conditions as shown Figure 7.6 (where $i = 1, 2, \dots, n$). However, this method requires considerable computing resources to run the simulation for each replication of demand. In addition, because traffic flow is variable and all the predicted future traffic counts cannot be observed, there are limitations in accurately representing predicted traffic conditions with predetermined parameter values that are optimized using a certain day's data. Therefore, rather than calibrating using input

data from certain time periods only, calibration with the data obtained from a complete input distribution is deemed to be necessary.

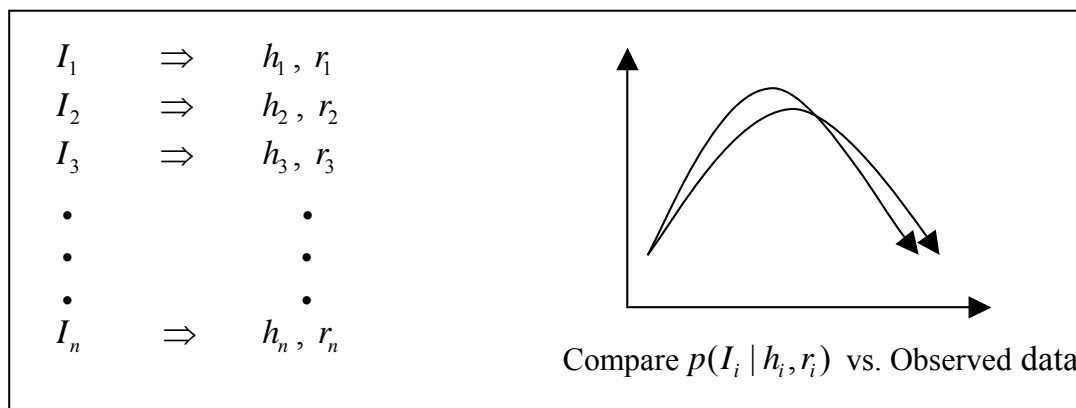


Figure 7.6 A conceptual representation of calibration method of complete range of possible traffic conditions

In this chapter, based on the randomly sampled “ m ” number of input data points, which cover the whole range of the input distribution, the mean target headway (h_j) and mean reaction time (r_j) are optimized using the SPSA algorithm for each sample, and the distributions of the h_i and r_i given the values of I_i (where $i = 1, 2, \dots, n$, $j = 1, 2, \dots, m$, $m < n$) are determined. This process for finding the distribution of $(h_i, r_i | I_i)$ is shown in Figure 7.7.

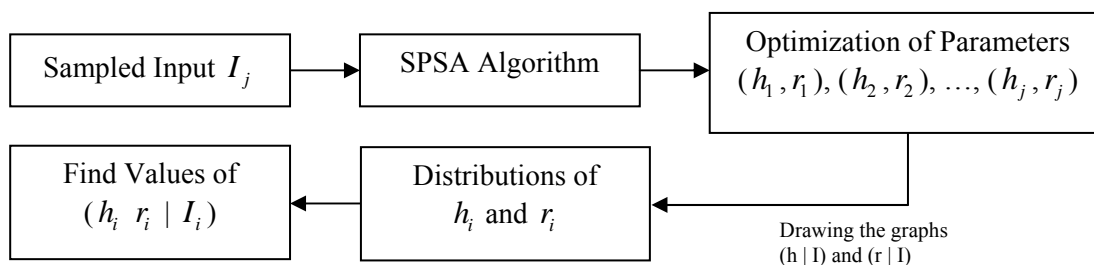


Figure 7.7 The conceptual representation of the proposed methodology for finding the distribution of h_i and r_i given I_i ($h_i, r_i | I_i$)

Based on the optimized values of h_j and r_j as a function of demand, the trend lines and their functional representations are also obtained for both of them. These relationships for the mean target headway distribution given demand ($h_i | I_i$) and for the mean reaction time given demand ($r_i | I_i$) are shown in Figures 7.8 and 7.9.

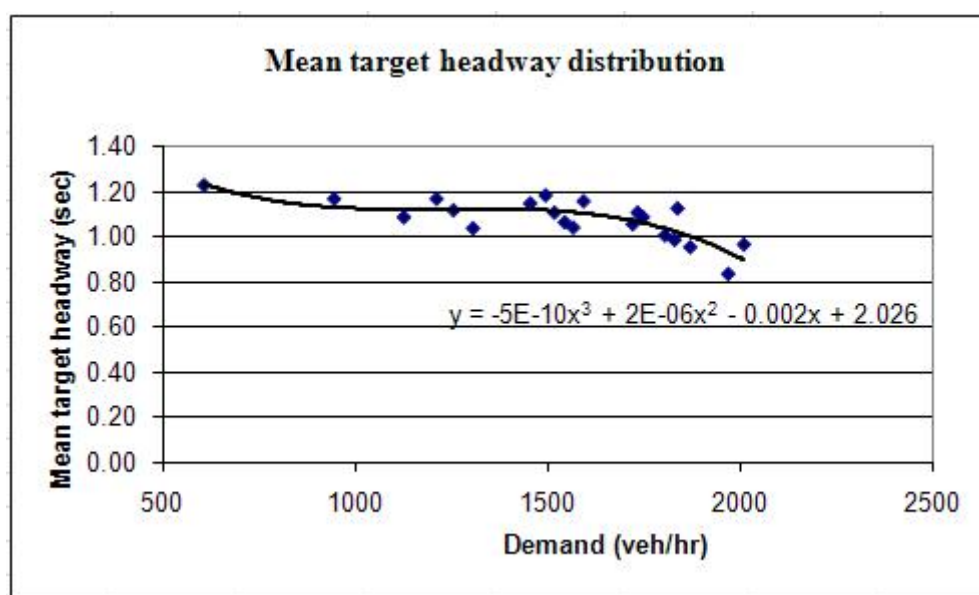


Figure 7.8 Mean target headway distribution

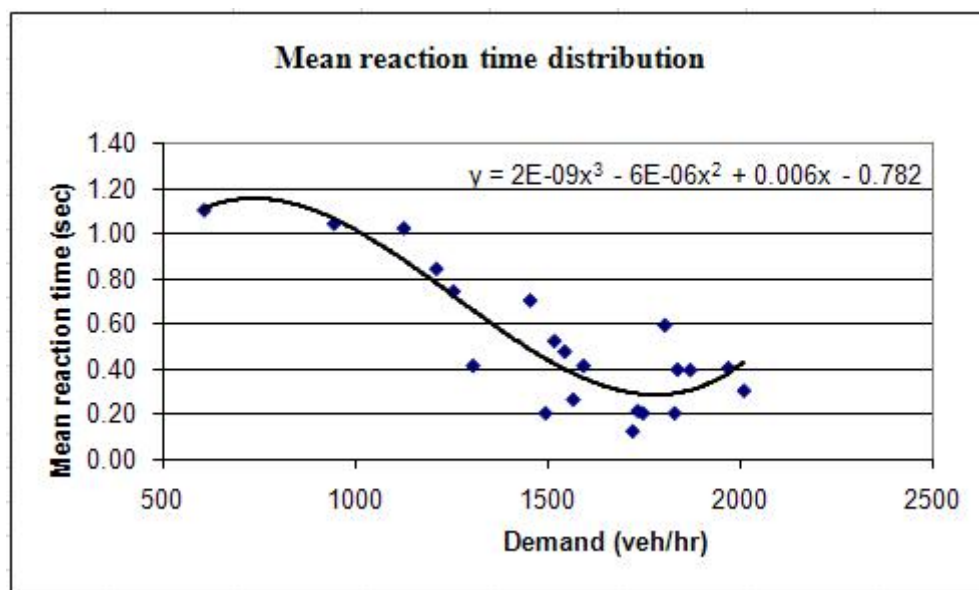


Figure 7.9 Mean reaction time distribution

The calibration test was performed to ensure that the inferred optimal input parameters from the trend lines, given the demand, represent realistic and accurate values under real traffic conditions for different days. Based on the estimated parameter values from the trend lines, given demand, the flow and speed values are compared for October 28, 1993 and October 29, 1993. The data from these days were not used in the calibration process. The sums of the relative errors for flow and speed values calculated using equation [7.1] were found to be 4.45 for October 28, 1993 and 4.14 for October 29, 1993. These results satisfied the requirement of an acceptable relative error of less than 5%. Figures 7.10 and 7.11 compare the flow and speed values based on the estimated parameter values with the observed data for those two dates.

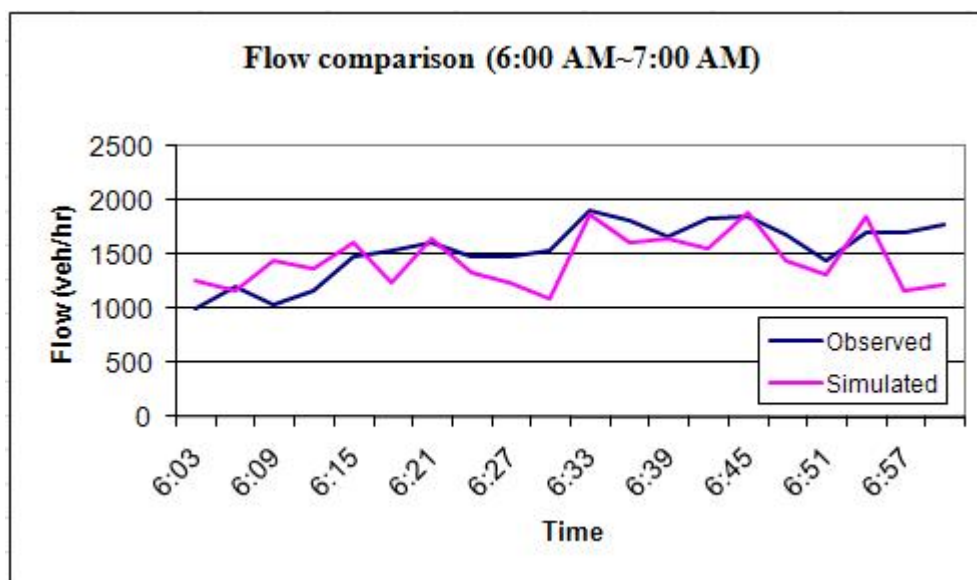


Figure 7.10 (a) Flow

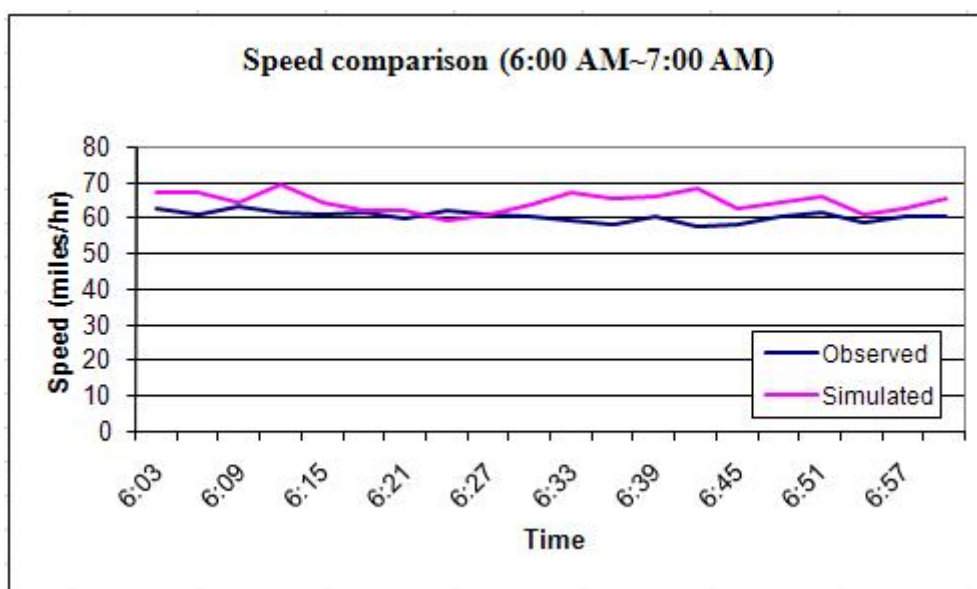


Figure 7.10 (b) Speed

Figure 7.10 Comparison between observed and simulated flow and speed (October 28, 1993) (Skabardonis et al. (1998))

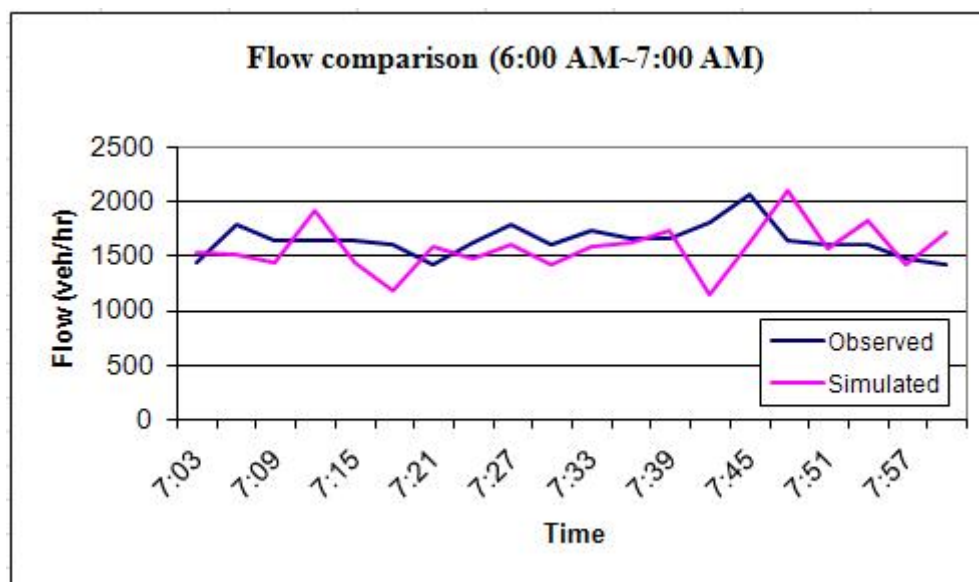


Figure 7.11 (a) Flow

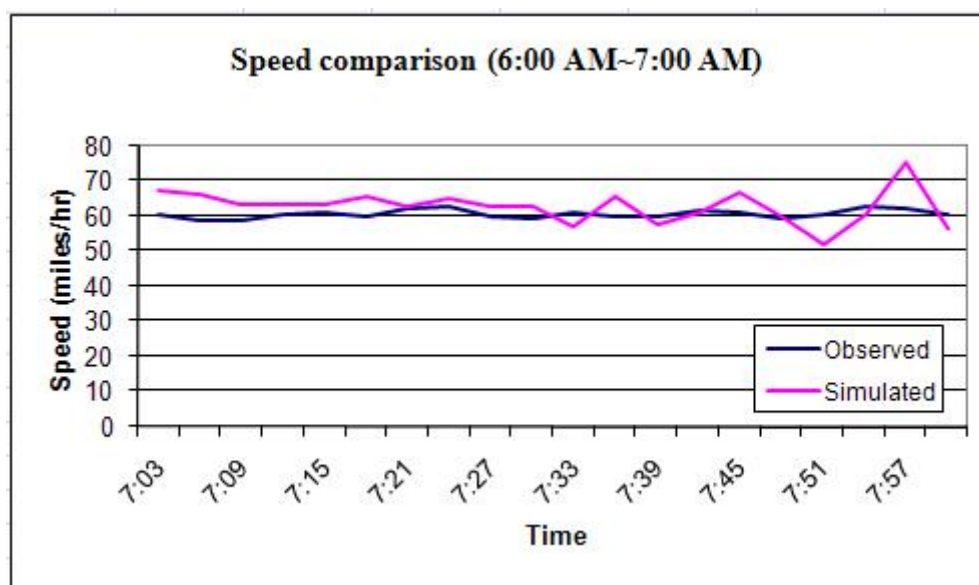


Figure 7.11 (b) Speed

Figure 7.11 Comparison between observed and simulated flow and speed (October 29, 1993) (Skabardonis et al. (1998))

7.3.4 Verification Test

On the basis of the method of Sanwal et al. (1996) presented in chapter 6, the mean square variation (MSV) of speed was compared with the simulation results obtained from the calibrated simulation model using the SPSA algorithm. The MSV is calculated by subtracting the mean square error from one and the value is close to one that states the model's estimations are close to real-world measurement.

The values for October 18, 1993 and October 11, 1993 were estimated at 0.897 and 0.905, respectively, which are greater than the variation of speed, 0.888, obtained from Sanwal et al. (1996)'s paper, i.e., even if between the SPSA-only methodology and variation approach did not have remarkable differences, the SPSA-only methodology leads to obtain relatively more accurate results.

7.3.5 Analysis of the Simulation Output for the Optimized Input Parameters

A simulation output is a function of input data given mean target headway and mean reaction time, denoted by $F[(I_i | h_i, r_i)]$. One hundred sampled input data (I_k) and optimized parameter values, given I_k , were the inputs to PARAMICS, and the outputs of the simulation were compared with the observed data distribution obtained from real data. Figure 7.12 shows the plot of the distribution of the sampled data from a beta distribution using the Bayesian sampling approach. For each sample, the generated sample data I_k , the mean target headway, and the mean reaction time calculated using the estimated equations shown in Figure 7.8 and Figure 7.9. This process is summarized in Table 7.2. The K-S test is performed as a goodness-of-fit

test to compare the distribution obtained from the simulation outputs using the optimized input parameters with the distribution obtained using observed data.

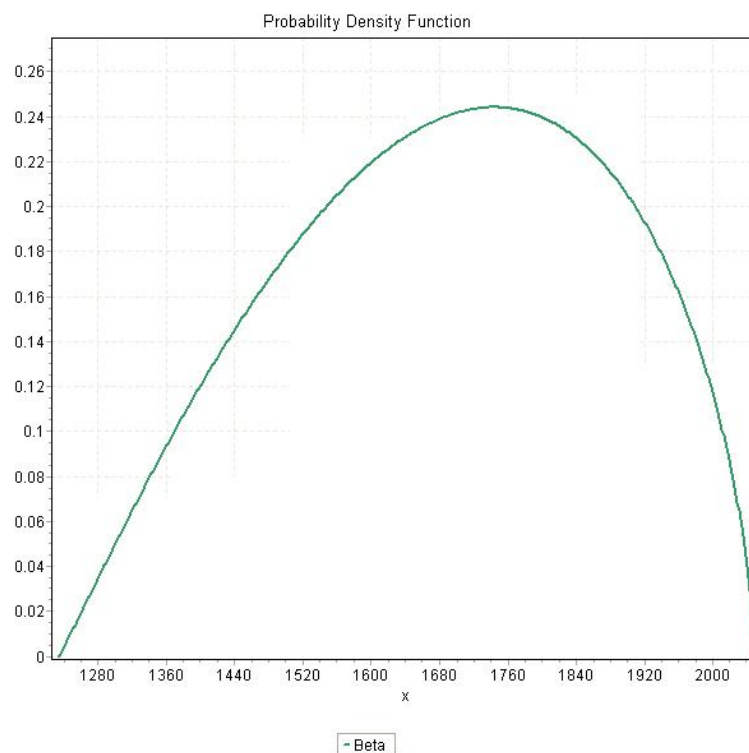


Figure 7.12 The estimated distribution of sampled flow data (www.mathwave.com)

Table 7.2 Simulated data, mean target headway, and mean reaction time given flow

Data	Headway	Reaction time	Data	Headway	Reaction time	Data	Headway	Reaction time	Data	Headway	Reaction time
1,861	0.98	0.24	1,970	0.95	0.20	1,518	1.04	0.48	1,586	1.03	0.44
1,934	0.96	0.20	1,683	1.01	0.37	1,676	1.01	0.37	1,780	0.99	0.30
1,516	1.05	0.49	1,380	1.07	0.58	1,853	0.98	0.25	1,714	1.01	0.35
1,817	0.99	0.27	1,563	1.04	0.45	1,888	0.97	0.22	1,899	0.97	0.22
1,411	1.07	0.56	1,614	1.03	0.42	1,835	0.98	0.26	1,722	1.00	0.34
1,787	0.99	0.30	1,569	1.03	0.45	1,590	1.03	0.43	1,698	1.01	0.36
1,821	0.98	0.27	1,930	0.96	0.20	1,466	1.06	0.52	1,659	1.02	0.39
1,869	0.97	0.24	1,560	1.04	0.45	1,642	1.02	0.40	1,462	1.06	0.52
1,894	0.97	0.22	1,723	1.00	0.34	1,930	0.96	0.20	1,825	0.98	0.27
1,776	0.99	0.30	1,601	1.03	0.43	1,581	1.03	0.44	1,897	0.97	0.22
1,887	0.97	0.23	1,572	1.03	0.45	1,855	0.98	0.25	1,525	1.04	0.48
1,942	0.96	0.20	1,923	0.96	0.20	1,623	1.02	0.41	1,591	1.03	0.43

1,325	1.08	0.62	1,777	0.99	0.30	1,909	0.97	0.21	1,863	0.98	0.24
1,896	0.97	0.22	1,691	1.01	0.36	1,235	1.10	0.68	1,762	1.00	0.31
1,897	0.97	0.22	1,723	1.00	0.34	1,638	1.02	0.40	1,385	1.07	0.58
1,704	1.01	0.35	1,578	1.03	0.44	1,827	0.98	0.27	1,605	1.03	0.42
1,971	0.95	0.20	1,623	1.02	0.41	2,048	0.94	0.20	1,362	1.08	0.59
1,936	0.96	0.20	1,249	1.10	0.67	1,734	1.00	0.33	1,474	1.05	0.51
1,718	1.00	0.34	1,920	0.96	0.20	1,406	1.07	0.56	1,279	1.09	0.65
1,361	1.08	0.59	1,735	1.00	0.33	1,593	1.03	0.43	1,802	0.99	0.28
1,697	1.01	0.36	1,795	0.99	0.29	1,998	0.95	0.20	1,780	0.99	0.30
1,317	1.09	0.62	1,587	1.03	0.44	1,656	1.02	0.39	1,817	0.99	0.27
1,956	0.96	0.20	1,717	1.01	0.34	1,764	1.00	0.31	1,549	1.04	0.46
1,923	0.96	0.20	1,540	1.04	0.47	1,844	0.98	0.26	1,416	1.07	0.56
1,621	1.02	0.41	1,695	1.01	0.36	1,712	1.01	0.35	1,763	1.00	0.31

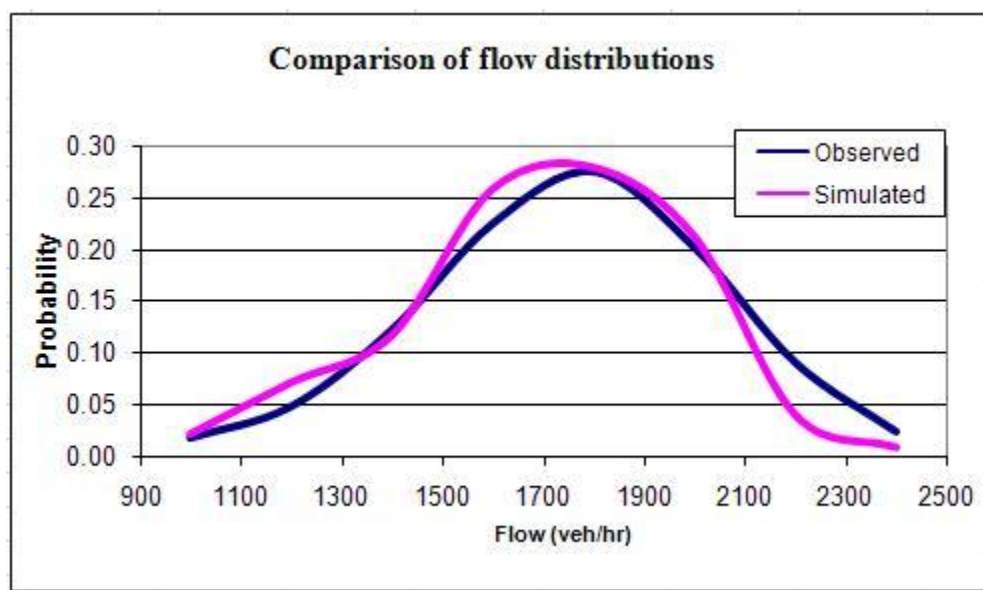
7.3.6 Statistical Comparison of the Distributions Obtained Using Simulated and Observed Data

Kolmogorov–Smirnov (K-S) test was performed to ensure that the distribution of the simulation results represented real traffic conditions. A comparison was made between the observed data distribution and the distribution of the simulation results acquired from 100 sampled input data and their optimal parameter values shown in Table 7.2.

The K-S test value for flow distribution was 0.059, which is less than all of the critical values obtained from the K-S table shown in Table 7.3. This result indicates that there is no statistically significant difference between the two distributions and thus calibrated simulation model represents real-world conditions. Figure 7.13 shows a probability comparison between the observed data and simulation results.

Table 7.3 Results of the Kolmogorov-Smirnov test

Kolmogorov-Smirnov test				
Sample Size	100			
Statistic	0.059			
P-Value	0.368			
α	0.1	0.05	0.025	0.01
Critical Value	0.173	0.192	0.209	0.231
Reject?	No	No	No	No

**Figure 7.13** Comparison of the observed and simulated probabilities of flow

The MSV of flow was also estimated to verify the effectiveness of Ex-SPSA methodology. The MSV value of speed was 0.940, which is the greater than the variation of speed obtained from SPSA-only and from Sanwal et al. (1996)'s paper, i.e., the Ex-SPSA methodology enables one to most accurately represent actual traffic conditions.

A worst-fit distribution for the data histogram is selected for data analysis to test if the use inappropriate distribution causes inaccurate results. Easyfit software provides the worst-fit data distribution to a lognormal distribution whose parameter values are $\sigma = 0.13731$ and $\mu = 7.4049$. The obtained lognormal distribution is compared with the data distribution, using the K-S test (Miller et al. (1990)). As a result of the K-S test, the null hypothesis is rejected at confidence levels of less than 95 percent shown in Table 7.4.

Table 7.4 Results of the Kolmogorov-Smirnov test

Kolmogorov-Smirnov test			
Sample Size	229		
Statistic	0.09483		
P-Value	0.03041		
α	0.2	0.1	0.05
Critical Value	0.071	0.081	0.090
Reject?	Yes	Yes	Yes

One hundred sampled input data from the lognormal distribution was the input to PARAMICS model, and the output of the simulation were compared with the observed data distribution. A goodness-of-fit test is performed to compare the distribution based on the simulation outputs for the optimized input parameters with the observed data distribution. The K-S test value for flow distribution was 0.322, and this value is more than all the critical values obtained from the K-S table shown in Table 7.5. This result indicates that there is a difference between the two distributions and thus simulation outputs from sampled input data from the lognormal distribution

do not accurately represent real-world conditions. Figure 7.14 shows a probability comparison between the observed and simulated data.

Table 7.5 Results of the Kolmogorov-Smirnov test

Kolmogorov-Smirnov test				
Sample Size	100			
Statistic	0.322			
P-Value	0.368			
α	0.1	0.05	0.025	0.01
Critical Value	0.173	0.192	0.209	0.231
Reject?	Yes	Yes	Yes	Yes

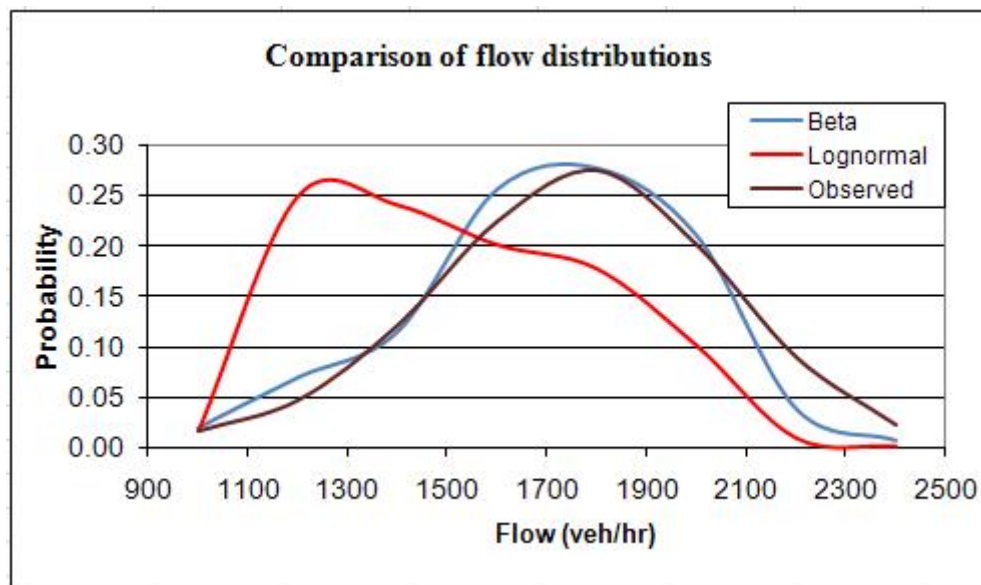


Figure 7.14 Comparison of the observed and simulated values of traffic flow

7.3.7 Validation Test

After the K-S test was satisfied for the calibration step, a validation test was performed for the hold out data that belongs to a different time period that was not

used for the calibration study. For the 15-minute flow range of 1200–1400 vehicles, eight different days' simulation output distributions were compared with the observed data distributions. Figure 7.15 shows a comparison between the observed data and simulation probability results.

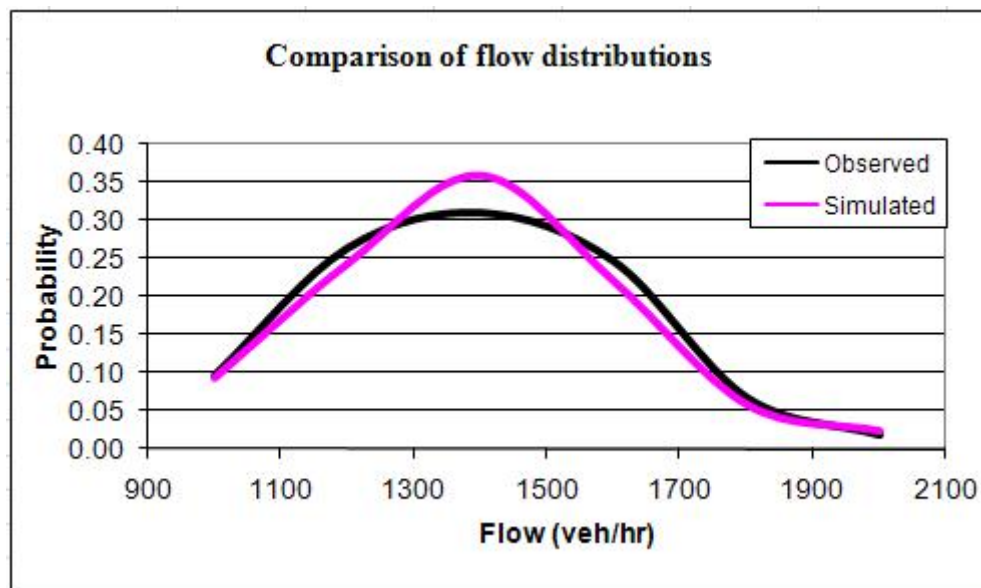


Figure 7.15 Comparison of the observed and simulated probabilities of flow (For the range of 1200~1400)

The K-S test was performed to verify the null hypothesis that there is not a statistically significant difference between the distribution of the simulation results and that of the observed flow. Based on the K-S test, the value of the flow distribution, 0.028, was less than the critical value of 0.192 obtained from the K-S table at the 95% confidence level. This demonstrated that the observed and simulated flow distributions have an acceptable level of similarity (fit) with each other.

7.4 Simulation Results and Summary

In this chapter, a new calibration methodology using the Bayesian sampling approach, in conjunction with SPSA stochastic optimization method, was proposed. This methodology enables the use of a wide range of traffic conditions from an observed data distribution. It also considers uncertainties. Data were obtained for a portion of the I-880 freeway in Hayward, California and aggregated into 15-minute counts for 16 different days. The input distribution was estimated using Easyfit software.

A section of the I-880 in California was first modeled in PARAMICS and then calibrated using the proposed methodology. The simulation results of a microscopic model varies in sensitivity based on the input parameters such as geometries, signposting, or factors related to the behavior of drivers. Thus, the calibrated parameters for a single demand matrix might not generate accurate results for other demands that are likely to occur depending on the time of the day, day of the week, the month, or the season.

The Ex-SPSA approach allows for the calibration of a simulation model for the whole range of input data and helps to determine the optimized parameter values for this wide-range. In this chapter, based on “ m ” number of sampled data points from complete distribution of demands that covers the whole range of the input distribution, input parameters were optimized using a well-known stochastic optimization algorithm, SPSA, at each iteration $(h_j, r_j | I_j)$ (where $j=1,2,...,m$). The distributions of h_i and r_i given I_i $(h_i, r_i | I_i)$ were assumed to follow the trend lines shown in Figures 7.8 and 7.9.

A verification test over two randomly selected time periods was also performed. On the basis of the estimated input parameters, the sums of the relative errors for the flow and speed values were found to be 4.45 and 4.14 for October 28, 1993 and October 29, 1993, respectively, which satisfied the constraint of an acceptable relative error of less than 5%. The differences between the observed and the simulated flow and speed were found to be statistically significant. Thus, these parameters were considered to be validated.

The distribution of simulation output for one hundred samples of input data (I_k) was compared with the distribution of the observed data. The optimized parameter values given I_k were determined from Figures 7.8 and 7.9. The K-S test was used to ensure that the distribution of the simulation results represented real traffic conditions. The K-S test value for flow distribution was 0.059, which was less than all of the critical values obtained from the K-S table, that is, the calibrated simulation model can capture real-world conditions.

The Ex-SPSA methodology was compared with the SPSA-only calibration method and a variation approach proposed by Sanwal et al. (1996) to evaluate accuracy of the proposed Ex-SPSA calibration approach vis-à-vis other calibration methods. MSV value of the Ex-SPSA methodology was 0.940, which was better than the ones obtained from the SPSA-only methodology (0.897 for October 18, 1993) or the variation approach (0.888). In other words, on the basis of the MSV values, the SPSA-only methodology and variation approach by Sanwal et al. (1996) did not have major differences but SPSA-only methodology was able to produce slightly more accurate results. Thus, it can be safely stated that the Ex-SPSA methodology could

more accurately represent a complete range of traffic conditions than the SPSA-only or the variation approach proposed by Sanwal et al. (1996).

A validation test was also performed to verify that the parameter values obtained by using the Ex-SPSA were applicable to data from different days that were not included in the calibration dataset. For the 15-minute flow range of 1200–1400 vehicles, the simulation output distributions for eight different days were compared with the observed data distributions. Based on the K-S test, the value of the flow distribution (0.028) was less than the critical K-S value (0.192) obtained from the K-S table at the 95% confidence level, i.e. the simulated flow distribution was not statistically different from the observed flow distribution.

This analysis showed that the Ex-SPSA based calibration method can capture day-to-day randomness of traffic because it employs a wide-range of data coming from a representative distribution of traffic over different days and within day time periods. On the other hand, there are limitations in capturing traffic conditions accurately if one wants to perform calibration using SPSA-only or variation approaches for the complete input distribution. This is because these methods require considerable computational time to run the simulation for each input, and still cannot reflect day-to-day randomness of traffic flow mainly due to a lack of robust sampling approach that can guarantee an accurate representation of the complete input distribution. Therefore, the Ex-SPSA which uses the Bayesian sampling approach was found to improve the results of simulation calibration process by accurately capturing a wide range of time-dependent real-world conditions, overcoming the limitations of previous calibration studies.

Chapter 8

Conclusions and Recommendation for Future Research

In this dissertation, calibration and validation for a section of the I-880 freeway was performed using PARAMICS and CTM. Even though, many papers about traffic simulation models have been published, their calibration methodology is generally based on fitting the simulation output to the observed data from a certain period of time in a typical day that is a part of an unknown demand distribution. However, this type of calibration approach cannot represent a realistic distribution of all possible traffic conditions and may produce inaccurate calibration results. Thus, the main purpose of this dissertation is to present a new calibration methodology that works well for a wide range of data distributions.

In this dissertation, first the calibration of the CTM and PARAMICS simulation models were performed using the SPSA algorithm. The SPSA algorithm can be applied in both stochastic gradient and gradient-free settings; it can also be applied to solve optimization problems that have a large number of variables. As the results of the simulations, the SPSA algorithm was found to be an effective when it was applied to small sample of demand calibration. However, alike previous studies,

this static approach can be only explained as calibration with data obtained at one point in time.

Second, the CTM calibration was performed using E-SPSA approach to reflect the effect of the distribution of input data. Previous studies on calibration generally focused on minimizing the sum of the relative errors between the observed data from a certain period of time in a typical day and the simulation output for the same period.

Instead of calibrating using a single demand matrix, E-SPSA uses randomly generated demand matrices and corresponding traffic conditions from an observed distribution of these variables. In the case of single zonal demand (no intermediate ramp), the road segments in CTM are initially modeled as a simple road segment to test the effectiveness of the E-SPSA approach and the case of an intermediate ramp is modeled as an extended road segment. For the single zonal demand case, the K-S test values for flow and density distributions are 0.019 and 0.139, respectively. These values are less than the critical values of 0.247 and 0.340 obtained from the K-S table at the 95% confidence level. For the two zonal demand cases, the critical K-S values from the K-S table are greater than the K-S values for flow and density distributions, as shown in Table 6.3. The null hypothesis states that the simulation flow and density distributed are not different from the observed distributions. For the scenario with two simple road segments, the null hypothesis could not be rejected, so there is no reason to doubt about its validity. Thus, calibration using input values generated from an observed distribution of demands can accurately represent a wide range of all likely demand conditions observed at a facility.

Finally, a calibration methodology that used the Bayesian sampling approach in conjunction with the application of the SPSA optimization method (Ex-SPSA) was performed to produce more effective calibration of microscopic traffic simulation models. Even if more input data provide more accurate simulation results, it takes a considerably high amount of time to run the simulation. In addition, a consideration of the uncertainties such as predicted future conditions is very important aspect to represent accurate traffic conditions. The Ex-SPSA method can be applied to calibration with wide range of data distribution and takes the uncertainties into consideration. The observed data distribution was compared with the simulation output distribution for one hundred sampled input data using the K-S test. The K-S test value for flow distribution was 0.059, and this value is less than all the critical values obtained from the K-S table. On the basis of the result of the K-S test, the simulation results and observed data distributions were successfully matched.

The Ex-SPSA methodology was compared with the SPSA-only optimization method and variation approach proposed by Sanwal et al. (1996) to ensure that the Ex-SPSA enables one to represent more realistic and accurate simulation results. On the basis of the MSV of flows, between the SPSA-only methodology and variation approach by Sanwal et al. (1996) did not have remarkable differences. However, the MSV value of the Ex-SPSA methodology was 0.940, which was notably close to one compared to the SPSA-only methodology (0.897 for October 18, 1993) and variation approach (0.888). Thus, it was concluded the Ex-SPSA methodology could more accurately represent complete range of traffic conditions than the SPSA-only or the variation approach proposed by Sanwal et al. (1996). Therefore, it was shown that

the Ex-SPSA not only overcomes the limitation of previous calibration studies but also improves the results of simulation model calibration by accurately capturing a wide range of real-world conditions.

Future research tasks include testing the Ex-SPSA for larger networks, as well as for other microscopic traffic simulations, such as CORSIM and VISSIM. In the future, other simulation parameters and more extensive data sets will be used to test the strengths and weaknesses of the proposed Ex-SPSA calibration methodology.

References

1. Ding, L., "Evaluation of ITS Technologies In South Jersey Priority Corridor Project", Master Thesis, Rutgers, The State University of New Jersey, 2003.
2. Gardes, Y., May, A. D., Dahlgren, J., and Skabardonis, A., "Freeway Calibration and Application of the PARAMICS Model", Paper Presented at the 81st Transportation Research Board Meeting, 2002.
3. Lee, D. H., Yang, X., and Chandrasekar, P., "Parameter Calibration for PARAMICS Using Genetic Algorithm", Paper presented at the 80st Transportation Research Board Meeting, 2001.
4. Toledo, T., Ben-Akiva, M. E., Darda, D., Jha, M., and Koutsopoulos, H. N., "Calibration of Microscopic Traffic Simulation Models with Aggregate Data", Transportation Research Record: Journal of Transportation Research Board, No. 1876, 2004, pp.10-19.
5. Jha, M., Gopalan, G., Garms, A., Mahanti, B.P., Toledo, T., and Ben-Akiva, M.E., "Development and Calibration of a Large-Scale Microscopic Traffic Simulation Model", Transportation Research Record: Journal of Transportation Research Board, No. 1876, 2004, pp.121-131.
6. Kim, K. O., and Rilett, L. R., "Simplex-based Calibration of Traffic Micro-Simulation Models with Intelligent Transportation Systems Data", Transportation Research Record: Journal of Transportation Research Board, No. 1855, 2003, pp.80-89.
7. Schultz, G. G., and Rilett L. R., "Analysis of Distribution and Calibration of Car-Following Sensitivity Parameters in Microscopic Traffic Simulation Models", Transportation Research Record: Journal of Transportation Research Board, No. 1876, 2004, pp.41-51.
8. Hourdakis, J., Michalopoulos, P. G., and Kottommannil, J., "A Practical Procedure for Calibrating Microscopic Traffic Simulation Models", Transportation Research Record: Journal of Transportation Research Board, No. 1852, 2003, pp.130-139.

9. Kundé, K. K., "Calibration of Mesoscopic Traffic Simulation Models for Dynamic Traffic Assignment", Master Thesis, Massachusetts Institute of Technology, 2002.
10. Park, B., and Qi, H., "Development and Evaluation of a Procedure for the Calibration of Simulation Models", Transportation Research Record: Journal of Transportation Research Board, No. 1934, 2005, pp.208-217.
11. Qin, X., and Mahmassani, H. S., "Adaptive Calibration of Dynamic Speed-Density Relations for Online Network Traffic Estimation and Prediction Applications", Transportation Research Record: Journal of Transportation Research Board, No. 1876, 2004, pp.82-89.
12. Ma, T., and Abdulhai, B., "Genetic Algorithm-Based Optimization Approach and Generic Tool for Calibrating Traffic Microscopic Simulation Parameters", Transportation Research Record: Journal of Transportation Research Board, No. 1800, 2002, pp.6-15.
13. Mahut, M., Florian, M., Tremblay, N., Campbell, M., Patman, D., and McDaniel, Z. K., "Calibration and Application of a Simulation-Based Dynamic Traffic Assignment Model", Transportation Research Record: Journal of Transportation Research Board, No. 1876, 2004, pp.101-111.
14. Molina, G., Bayarri, M. J., and Berger, J. O., "Statistical Inverse Analysis for a Network Microsimulator", 2005 American Statistical Association and the American Society for Quality Technometrics, Vol. 47, No. 4, 2005.
15. Abdulhai, B., J-B. Sheu and Recker, W., "Simulation of ITS on the Irvine FOT Area Using PARAMICS 1.5 Scalable Microscopic Simulator – Phase 1: Model Calibration and Validation", University of California at Irvine. California PATH Research Report UCB-ITS-PRR-99-12, 1999.
16. Milam, R. T., "Recommended Guidelines for the Calibration and Validation of Traffic Simulation Models", Fehr & Peers Associates, Inc. http://www.fehrandpeers.com/Papers/Guidelines_traff_simulation.pdf, Accessed Jul. 2005.
17. Sacks, J., Rouphail, N., Park, B., and Thakuriah, P., "Statistically-Based Validation of Computer Simulation Models in Traffic Operations and Management", Journal of Transportation and Statistics, Vol. 5, No. 1, 2002, pp.1-24.
18. Cheu, R. L., Jin, X., Ng, K. C., Ng, Y. L., and Srinivasan, D., "Calibration of FRESIM for Singapore Expressway Using Genetic Algorithm", Journal of Transportation Engineering, Vol. 124, No. 6, 1998, pp.526-535.

19. Gomes, G., May, A.D., and Horowitz, R., "A Microsimulation Model of a Congested Freeway using VISSIM", *Transportation Research Record: Journal of Transportation Research Board*, No. 1876, 2004, pp.71-81.
20. Boxill, S. A., and Yu, L., "An Evaluation of Traffic Simulation Models for Supporting ITS Development", Center for Transportation Training and Research, Texas Southern University, 2000.
21. "TRANSYT-7F Users Guide", University of Florida, Transportation Research Center, 1998.
22. Bottom, J., Ben-Akiva, M., Bierlaire, M., Chabini, I., Koutsopoulos, H., and Yang, Q., "Investigation of Route Guidance Generation Issues by Simulation with DynaMIT", In *Transportation and Traffic Theory* (A. Ceder, ed.), Pergamon, New York, 1999, pp.577-600.
23. "PARAMICS programmer Users Guide", 2000.
24. Balakrishna, R., Antoniou, C., Ben-Akiva, M., Koutsopoulos, H. N., and Wen, Y., "Calibration of Microscopic Traffic Simulation Models: Methods and Application", *Transportation Research Record: Journal of Transportation Research Board*, No. 1999, 2007, pp.198-207.
25. Ma, J., Dong, H., and Zhang, H. M., "Calibration of Microsimulation with Heuristic Optimization Methods", *Transportation Research Record: Journal of Transportation Research Board*, No. 1999, 2007, pp.208-217.
26. Kim, S. J., Kim, W., and Rilett, L., "Calibration of Microsimulation Models using Non-Parametric Statistical Techniques", *Transportation Research Record: Journal of Transportation Research Board*, No. 1935, 2005, pp.111-119.
27. Sanwal, K. K., Petty, K., Walrand, J., and Fawaz, Y., "An Extended Macroscopic Model for Traffic Flow", *Transportation Research Part B*. Vol. 30, No. 1, 1996, pp.1-9.
28. Dowling, R., Skabardonis, A., Halkias, J., McHale, G., and Zammit, G., "Guidelines for Calibration of Microsimulation Models: Framework and Applications", *Transportation Research Record: Journal of Transportation Research Board*, No. 1876, 2004, pp.1-9.
29. Bloomberg, L., Swenson, M., and Haldors, B., "Comparison of Simulation Models and the Highway Capacity Manual", Presented at 82nd Annual Meeting of the Transportation Research Board, Washington, D.C., 2003.

30. Spall, J. C., "Introduction to Stochastic Search and Optimization", Wiley-Interscience, 2003.
31. Nelder, J. A., and Mead, R., "A Simplex Method for Function Minimization", The Computer Journal, vol. 7, 1965, pp.308-313.
32. Robbins, H., and Monro, S., "A Stochastic Approximation Method", Annals of Mathematical Statistics, Vol. 22, 1951, pp.400-407.
33. Spall, J. C., "Multivariate Stochastic Approximation Using a Simultaneous Perturbation Gradient Approximation", IEEE Transactions on Automatic Control, Vol. 37, No. 3, 1992, pp.332-341.
34. Luo, J., "Dynamic Multi-ramp Metering Control with Simultaneous Perturbation Stochastic Approximation (SPSA)" Doctor of Philosophy Thesis, The New Jersey Institute of Technology, 2003.
35. Spall, J. C., "A One-measurement Form of Simultaneous Perturbation Stochastic Approximation", Elsevier Science Ltd. Vol. 33, No. 1, 1997, pp.109-112.
36. Spall, J. C., "Implementation of the Simultaneous Perturbation Algorithm for Stochastic Optimization", IEEE Vol. 34, No. 3, 1998, pp.817-823.
37. Spall, J. C., "Traffic-Responsive Signal Timing for System-Wide Traffic Control", Transportation Research Part C, Vol. 5, 3/4, 1997, pp.153-163.
38. Daganzo, C. F., "The Cell Transmission Model: A Dynamic Representation of Highway Traffic Consistent with the Hydrodynamic Theory", Transportation Research Part B. Vol. 28, No. 4, 1994, pp.269-287.
39. "Highway Capacity Manual", Transportation Research Board, National Research Council, Washington, D.C., 2000.
40. Koppa, R. J., Fambro, D. B., and Zimmer, R. A., "Measuring Driver Performance in Braking Maneuvers", Transportation Research Record: Journal of Transportation Research Board, No. 1550, 1996, pp.8-15.
41. Green, M., "How Long Does It Take To Stop?" Methodological Analysis of Driver Perception-Brake Times, Transportation Human Factors, 2000, pp.195-216.
42. Skabardonis, A., Petty, K., Varaiya, P., and Bertini, R., "Evaluation of the Freeway Service Patrol (FSP) in Los Angeles", California PATH Research Report. UCB-ITS-PRR-98-31, 1998.
43. Petty, K., "The Analysis Software for the FSP Project", University of California, Berkeley, 1995.

44. Smith, M., Druitt, S., Cameron, G., and MacArthur, D., "PARAMICS Final Report" Technical Report EPCC-PARAMICS-FINAL, University of Edinburgh, 1994.
45. Montgomery, D. C., and Runger, G. D., "Applied Statistics and Probability for Engineers", 2005.
46. Munoz, L., Sun, X., Sun, D., Gomes, G., and Horowitz, R., "Methodological Calibration of the Cell-Transmission Model", Proceeding of the 2004 American Control Conference, Boston, Massachusetts, June 30-July 2, 2004.
47. Munoz, L., Sun, X., Horowitz, R., and Alvarez, L., "A Piecewise-Linearized Cell Transmission Model and Parameter Calibration Methodology", Transportation Research Record: Journal of Transportation Research Board, Vol. 1965, 2006, pp.183-191.
48. Almasri, E., and Friedrich, B., "Online Offset Optimization in Urban Networks based on Cell Transmission Model", Institute of Transport, University of Hannover, Germany, 2005.
49. Park, B., and Won, J., "Simulation Model Calibration and Validation: Phase 2: Development of Implementation Handbook and Short Course", Report No. FHWA/VTRC07-CR5, 2006.
50. Gelman, A., Carlin, J. B., Stern, H. S., and Rubin, D. B., "Bayesian Data Analysis", Second edition, 2004.
51. <http://www.mrc-bsu.cam.ac.uk/>
52. Hollander, Y., and Liu, R., "The Principles of Calibrating Traffic Microsimulation Models", Transportation, Vol. 35, No. 3, 2008, pp.347-362.
53. Daganzo, C. F., "The Cell Transmission Model, Part 2: Network Traffic", Transportation Research Part B. Vol. 29, No. 2, 1995, pp.79-93.
54. Miller, I., Freund, J. E., and Johnson, R. A., "Probability and Statistics for Engineers", Fourth Edition, 1990.
55. Waller, S. T., Schofer, J. L., and Ziliaskopoulos, A. K., "Evaluation with Traffic Assignment under Demand Uncertainty", Transportation Research Record: Journal of Transportation Research Board, Vol. 1771, 2001, pp.69-74.
56. www.mathwave.com/products/easyfit.html
57. www.ivhs.mit.edu/products/simlab

Appendix A. PARAMICS Programmer API Code

```

/* -----
 * Paramics Programmer API (paramics-support@quadstone.com)
 * Quadstone Ltd.      Tel: +44 131 220 4491
 * 16 Chester Street   Fax: +44 131 220 4492
 * Edinburgh, EH3 7RA, UK   WWW: http://www.paramics-online.com
 * ----- */

/* -----
 * API Example 4 - Vehicle Release.
 *
 * The aim of this example is to introduce some of those functions which
 * control the release of vehicles during a simulation. The example will
 * allow the user to set up an API control panel from which the release of
 * vehicles into the network can be controlled interactively.
 *
 * API Control Functions used:  api_setup(...)
 *                             api_coefficient_file(...)
 *                             api_coefficient_value(...)
 *                             zone_action(...)
 *
 * API CallBack functions used:  api_printf(...)
 *                             net_n_zones(...)
 *                             zone_vehicle_type_set(...)
 *                             zone_vehicle_destination_set(...)
 *                             zone_vehicle_aggression_set(...)
 *                             zone_vehicle_awareness_set(...)
 *                             zone_index(...)
 *                             timestep(...)
 * ----- */

#define QPV3_TYPES
#include <stdlib.h>
#include <stdio.h>
#include <string.h>
#include <math.h>

#include "programmer.h"

/* include our function definitions explicit to this example */
#include "plugin_p.h"

static int g_nZones;
static int **g_ReleaseRates;
static int g_ODRecords = 0;
static Bool g_Setup = FALSE;
int g_timerrecord = 0;
/*float g_divisor = 1.0;*/
char *g_ParamFile = "API_Example4";

/* Start control function calls */
/* -----
 * call api_setup once when the full network has been read into modeller

```

```

/* ----- */
void qpx_NET_postOpen(void)
{
    int max_zones = qpg_NET_zones() * qpg_NET_zones();
    int i;
    int j;

    /* first check that the number of zones supplied by the user via the
     * parameters file and the number provided by modeller match */
    if (g_nZones != (qpg_NET_zones()))
    {
        qps_GUI_printf("\nERROR: Discrepancy between user supplied number of\n"
            "      zones (%d), and the number supplied by\n"
            "      modeller (%d)", g_nZones, qpg_NET_zones());
        return;
    }

    /* how many possible OD records do we have? (netZones^2) so we must
     * check if the user has supplied a matrix value for all possible OD
     * records ,if the not warn the user that all OD records not specified will
     * be set to zero */
    if (g_ODRecords != max_zones)
    {
        /* a discrepancy is found */
        qps_GUI_printf("\nWARNING: Network requires %d OD records, the parameters "
            "file only holds %d,\n"
            "      OD records not defined in the parameters file will "
            "have target\n"
            "      release rates set to zero.\n\n",max_zones, g_ODRecords);
    }
    /*api_printf("\nParamics Programmer API: Vehicle Release\n");*/
    g_Setup = TRUE;
}

/* ----- */
/* This call allows the plugin to setup any required structures needed for
 * the API interface based on data provided in the parameters file.
 * ----- */
void api_coefficient_file(char *filename, int count)
{
    if (strcmp(filename,g_ParamFile ) == 0)
    {
        /* estimate how many OD records the user has supplied NOTE: all
         * coefficients supplied should be od records except the first */
        g_ODRecords = count - 1;
    }

    g_Setup = FALSE;
}

/* ----- */
/* This call is made for each of the parameters supplied in the plugin
 * parameter file and is used to store each of the users variables. In
 * this example we will use it to store the trip rates for each of our OD
 * pairs supplied in the parameters file. Note that these values will be
 * updated if the user changes a parameter via the GUI slider bar.

```

```

* ----- */
void qpx_GUI_parameterValue(char *filename,int index,char *label,float value)
{
    int from;
    int to;
    int max_release;
    int i;
    int j;
    /*api_printf("\nrunning api_coefficient_value function.....\n");
    api_printf("\ng_ParamFile= %s", g_ParamFile);
    api_printf("\nfilename= %s", filename);*/
    /* check the file name */
    if (strcmp(filename, g_ParamFile) == 0)
    {
        /* here we must assume that the first coefficient in the API Parameters
        * file is the number of zones in the network. We need to do this in
        * order to properly dimension our storage array before the trip
        * records can be read and stored */

        if ((strcmp(label, "Zones in network") == 0) && (index == 0))
        {
            /* the first line of the file with the correct label to identify
            * the number of zones in the network */
            g_nZones = value;

            /* as we now know the size of the matrix we need to build we can
            * allocate storage */
            if (g_ReleaseRates != NULL) free(g_ReleaseRates);
            g_ReleaseRates = malloc((g_nZones) * sizeof(int *));
            for (i = 0; i < (g_nZones); i++)
                g_ReleaseRates[i] = malloc((g_nZones) * sizeof(int));

            /* now clear all elements of our matrix prior to reading in the
            * values from our coefficient file */
            for (i = 0; i < (g_nZones); i++)
            {
                for(j = 0; j < (g_nZones); j++)
                    g_ReleaseRates[i][j] = 0;
            }
        }
        else if ((strcmp(label, "Zones in network") == 0) && (index != 0))
        {
            /* the label identifying the number of zones in the network has
            * been found but it is not the first coefficient in the
            * Parameters file :- there is a possibility that the user has
            * placed the coefficients in the wrong order, this will cause the
            * plugin to fail so warn the user */
            qps_GUI_printf("\nWARNING: Possible error in parameters file coefficient \n"
                           "          values ordering, please check you input data !");
            return;
        }
        else
        {
            /* store the trip record

            /* scan the label name to find the OD pair */

```

```

        sscanf(label, "Trips Zone %d to Zone %d", &from, &to);

        /*api_printf("\nfrom= %d\n", from);
        api_printf("\nto= %d\n", to);*/

        /* check for sensible zone numbers in the range 1 - g_nZones */
        if (((from < 1) || (to < 1)) || ((from > g_nZones) || (to > g_nZones)))
        {
            qps_GUI_printf("\nWarning: Invalid OD pair - coefficient %d in
parameters "
                        "file\n", index);
            return;
        }

        /* store trips to be released for the correct OD pair */
        g_ReleaseRates[from-1][to-1] = value;
    }
}

/*-----
function pp_api_coefficient_value
-----*/

/*static void pp_api_coefficient_value(char *filename,int index,char *label,float value)
{
    int from;
    int to;
    int max_release;
    int i;
    int j;
    /* check the file name */
    /*
        label = "Trips Zone 1 to Zone 2";
        sscanf(label, "Trips Zone %d to Zone %d", &from, &to);
        api_printf("\nlabel= %s\n", label);
        api_printf("\nfrom= %d\n", from);
        api_printf("\nto= %d\n", to);
        /* store trips to be released for the correct OD pair */
    /*
        g_ReleaseRates[from-1][to-1] = value;
        api_printf("\nvalue= %f\n", value);

}

/* -----
* This function sets all the variables needed for releasing a vehicle into
* our network.
* ----- */
static void pp_release_vehicle(int type, int dest, int orig)
{
    /* normal will be used as the distrution for our DVU's aggression and
    * awarness factors */
    int normal[9] = {1, 4, 11, 21, 26, 21, 11, 4, 1};
    int aggr;
    int awar;

```

```

int sum;
int new_sum;
/* maximum integer size */
int max_rand = 32767;
int i;

/*api_printf("\nrunning pp_release_vehicle....\n");*/
/* this callback function set the type of vehicle to be released from the
* zone */
qps_ZNE_vehicleType(type);
if(orig == 2){
    if(type == 2 || type == 16) qps_ZNE_vehicleLane(5);}
/* this callback function set the destination zone index of the vehicle
* about to be released */
qps_ZNE_vehicleDestination(dest);

/* calculate aggression and awareness factors */
aggr = (((float)rand()/(float)(max_rand)) *100.0);
awar = (((float)rand()/(float)(max_rand)) *100.0);

sum = 0;
for(i = 0; i < 9; i++)
{
    new_sum = sum + normal[i];

    if((aggr > sum) && (aggr <= new_sum))
    {
        qps_ZNE_vehicleAggression(i);
    }

    if((awar > sum) && (awar <= new_sum))
    {
        qps_ZNE_vehicleAwareness(i);
    }

    sum = new_sum;
}
}

/* -----
* This control function is called for each zone in the network for each
* time step, to determine if a vehicle should be released or not.
* ----- */
void qpx_ZNE_timeStep(ZONE* zone)
{
    int r = rand();
    float vehRand = 0;
    int max_rand = 32767;
    int max_release;
    int sum;
    int from_zone;
    int to_zone;
    int i;
    int j;
    int time=60;

```

```

        int timer;
/*      FILE * pFile;*/
        Bool released;

        double divisor[260] = {
0.84 ,0.99 ,1.16 ,0.91 ,1.01 ,0.98 ,0.98 ,0.92 ,0.91 ,0.99 ,
1.18 ,1.41 ,1.17 ,1.03 ,1.17 ,0.95 ,1.07 ,0.89 ,1.12 ,1.16 ,
1.1 ,1.18 ,0.89 ,1.18 ,0.97 ,1.04 ,1.22 ,1.13 ,1.02 ,0.92 ,
0.8 ,1.21 ,0.94 ,0.8 ,0.93 ,1.09 ,1.03 ,1.22 ,0.92 ,1.19 ,
0.96 ,0.92 ,0.87 ,1.06 ,1.16 ,0.83 ,0.88 ,1.11 ,1.15 ,0.91 ,
0.96 ,1.35 ,0.89 ,1.23 ,1 ,1.19 ,1 ,0.75 ,1.18 ,0.94 ,
1.31 ,1.33 ,1.06 ,1.32 ,1 ,0.85 ,0.88 ,1.04 ,0.86 ,1 ,
0.94 ,0.99 ,1.12 ,0.94 ,0.91 ,1.15 ,1.02 ,0.9 ,0.84 ,0.89 ,
1.03 ,0.83 ,0.93 ,1.01 ,1.17 ,0.88 ,1.11 ,0.87 ,0.95 ,0.96 ,
1.08 ,0.80 ,1.06 ,0.70 ,0.79 ,0.82 ,0.93 ,0.93 ,0.82 ,0.94 ,
1.08 ,0.88 ,0.92 ,1.32 ,0.86 ,1 ,0.98 ,0.97 ,0.82 ,1.03 ,
1.28 ,1.82 ,1 ,1.06 };

        for (i=0;i<260;i++)
        {
                if (divisor[i] == 0.0)
                        divisor[i] = 1.00;
        }

/*api_printf("\nrunning zone_action Function...\n");*/
/*-----
 *checking the simulation time is whole minute
 *-----*/
        if (((int)qpg_CFG_simulationTime() % time) == 0 && qpg_CFG_simulationTime()
- (float)floor((double)qpg_CFG_simulationTime())==0.0)
        {
                timer=(int)qpg_CFG_simulationTime()/time
((int)qpg_CFG_startTime()/time) + 15; /*345 */
                /*api_printf("\ntimer= %d\n", timer);*/

                g_timerrecord = g_timerrecord + 1;
                /*api_printf("\ng_timerrecord= %d\n", g_timerrecord);*/

                if (g_timerrecord == 1)
                {
                        /*api_printf("\n(int)simulation_time()= %d\n",
(int)simulation_time());*/
                        /*api_printf("\nsimulation_time()= %f\n", simulation_time() -
20700.0);

                        api_printf("\ntimer= %d\n", timer);
                        api_printf("\ndivisor[timer]= %f\n", divisor[timer]);*/

                        /*-----
 *restoring the OD demand matrix
 *-----*/
                        g_ReleaseRates[1][0] = 5594; /*zone 2 to zone 1 */
                        /*g_ReleaseRates[1][0] = 500; /*zone 2 to zone 1 */
                        g_ReleaseRates[1][2] = 0; /*zone 2 to zone 3 */
                        g_ReleaseRates[1][3] = 0; /*zone 2 to zone 4 */
                        /*g_ReleaseRates[1][5] = 370; /*zone 2 to zone 4 */
                        /*g_ReleaseRates[4][0] = 380; /*zone 3 to zone 1 */

```

```

        g_ReleaseRates[4][0] = 300; /*zone 5 to zone 1*/
        /*g_ReleaseRates[1][0] = 200; /*zone 2 to zone 1*/

        for (i=0; i<6; i++)
        {
            for (j=0; j<6; j++)
            {

                g_ReleaseRates[i][j] = g_ReleaseRates[i][j] /
divisor[timer];

                /*api_printf
("\ng_ReleaseRates[%d][%d]= %d\n", i, j, g_ReleaseRates[i][j]);*/
            }
        }

        } /*completing (g_timerrecord == 1) */

        } /*completing (((int)simulation_time() % time) == 0 && simulation_time() -
(float)floor((double)simulation_time())==0.0)*/

        else
        {
            g_timerrecord = 0;
        }

        from_zone = qpg_ZNE_index(zone) - 1;
        /*api_printf("from_zone= %d", from_zone);*/

        max_release = (int)(3600.00/qpg_CFG_timeStep());

        /* generate a random number between 0 and max_release */
        r = (int) (((float) r / (float) max_rand) * (float) max_release);

        /* here we loop through the release rates for the current zone (from_zone)
        * to each possible destination zone (to_zone), summing the total release rate
        * as we go, until the sum is greater than our random number (r). At that point
        * we instruct the current generating zone (from_zone) to prepare to release a
        * vehicle into the network.
        *
        * This will give the effect of releasing the vehicles randomly but
        * proportionally to their desired release rates */

        i = 0;
        to_zone = 0;
        released = FALSE;
        while ((i < (g_nZones)) && !released)
        {
            if(i == from_zone)
            {
                sum = 0;
                while (to_zone < (g_nZones) && !released)
                {
                    sum += g_ReleaseRates[from_zone][to_zone];
                    if (r < sum && (to_zone != from_zone))

```



```

    {
        /* here we use the index of the generating zone as as the
        * vehicle type to be generated, this is only to allow us
        * to distinguish between vehicles generated from each zone.
        * See the vehicles file in the example network for more
        * details */

        vehRand = (float)((float)rand() / (float) max_rand);
        //qps_GUI_printf("Random no. is %f\n",vehRand);
        if(vehRand<0.77 && vehRand >= 0){

            //pp_release_vehicle(from_zone +1, to_zone + 1);
            pp_release_vehicle(1, to_zone + 1, from_zone + 1);

        }
        else if(vehRand<0.94 && vehRand >= 0.77){
            pp_release_vehicle(2, to_zone + 1, from_zone + 1);
            //if(from_zone == 2)qps_ZNE_vehicleLane(5);
        }

        else if(vehRand<0.98 && vehRand >= 0.94){
            pp_release_vehicle(12, to_zone + 1, from_zone + 1);

        }

        else if(vehRand<=1.0 && vehRand >= 0.98){
            pp_release_vehicle(16, to_zone + 1, from_zone + 1);
            //if(from_zone == 2)qps_ZNE_vehicleLane(5);
        }

        released = TRUE;
    }
    to_zone++;
}
}
i++;
}
}

```

Curriculum Vita

JUNG-BEOM LEE

Education

- 2002-2008** Ph.D. in Civil and Environmental Engineering, Rutgers University, NJ
- 1999-2001** M.S. in Civil and Environmental Engineering, Dankook University, Korea
- 1993-1999** B.S. in Civil and Environmental Engineering, Dankook University, Korea
- 1993** Graduated from Whimoon High School, Korea

Work Experience

- 2003-2005** Graduate Assistant

Publications

Evaluation of Stochastic Approximation (SA) Algorithm-Based Parameter Optimization of Simulation Tools, *Jung-Beom Lee and Kaan Ozbay*, Advances in Information Sciences and Services, 2007.

Delay Estimation of Signalized Intersection Considering Acceleration and Deceleration, *Jung-Beom Lee and Dongnyeong Kim*, Journal of advanced Materials, 2004, pp. 193-208.